Quantification of Metal Loading by Tracer Injection and Synoptic Sampling, 1997–98

By Briant A. Kimball, Robert L. Runkel, Thomas E. Cleasby, and David A. Nimick

Chapter D6 of
Integrated Investigations of Environmental Effects of Historical Mining in the Basin and Boulder Mining Districts, Boulder River Watershed, Jefferson County, Montana
Edited by David A. Nimick, Stanley E. Church, and Susan E. Finger

Professional Paper 1652–D6

U.S. Department of the Interior
U.S. Geological Survey

Contents

Figures

Tables

METRIC CONVERSION FACTORS AND ABBREVIATIONS

Multiply	By	To obtain
foot (ft)	0.30481	meter (m)
cubic foot per second (ft^3/s)	28.317	liter per second (L/s)
pound (lb)	.45	kilogram (kg)

Temperature in degree Celsius (^oC) can be converted to temperature in degree Fahrenheit (^oF) by using the following equation:

$$^oF = 9/5^oC+32.$$

The following terms and abbreviations also are used in this report:

kilograms per day (kg/day)
milligram per liter (mg/L)
microgram per liter (μg/L)
millimoles per liter (mM/L)
milliliters per minute (mL/min)
milligram per second (mg/s)

Chapter D6
Quantification of Metal Loading by Tracer Injection and Synoptic Sampling, 1997–98

By Briant A. Kimball, Robert L. Runkel, Thomas E. Cleasby, and David A. Nimick

Abstract

Determination of the best sites for remediation of mine drainage requires an understanding of metal contributions from all sources in a watershed. A hydrologic framework to study metal loading in selected streams of the Boulder River watershed of Montana was established by a series of mass-loading studies of three impacted stream reaches. Each study used the tracer-dilution method in conjunction with synoptic sampling to determine the spatial distribution of discharge and concentration. Discharge and concentration data were then used to develop mass-loading profiles for the various metals of interest. Discharge and load profiles (1) identify the principal sources of load to the streams; (2) demonstrate the importance of unsampled, dispersed subsurface inflows; and (3) estimate the amount of attenuation. The two major sources of metal loading to the streams are the Crystal mine adit discharge in Uncle Sam Gulch and the Bullion mine adit in the Bullion Mine tributary. Other sources are small in comparison to these two. Along the 40,905-foot study reach of Cataract Creek, 21.2 kilograms per day of zinc were added to the stream. About 75 percent of this load came from Uncle Sam Gulch, a principal tributary. By comparison, the adit discharge from the Bullion mine accounted for 2.8 kilograms per day of zinc, which was only about 20 percent of the zinc load coming from the Crystal mine adit in Uncle Sam Gulch.

About 34 percent of the zinc load in Cataract Creek occurred as unsampled inflow, including part of the load from Uncle Sam Gulch. Along the study reach, about 34 percent of the zinc load was removed to the stream bed. Similar details are available for other metals in each of the three streams studied. This watershed approach provides a detailed snapshot of metal load for the watershed to support remediation decisions, and quantifies processes affecting metal transport.

Introduction

Land-management agencies in the Boulder River watershed of Montana are charged with the task of reclaiming abandoned mine lands. Numerous inactive mines contribute substantial metal loads and acidic waters to the streams that drain the Boulder River watershed. The affected streams are headwater systems that gain substantial amounts of water as they flow down valley. Sources of additional water range from well-defined tributary inflows to diffuse ground-water inflows that are not visible. The water quality associated with these sources also varies dramatically, from dilute mountain springs to metal-rich water emanating from mineralized areas. The challenge facing land-management agencies is thus one of source determination: For a given stream, what sources of water are most detrimental to water quality? This question is of paramount importance to land managers who must implement remedial actions subject to fiscal constraints.

The approach used in these studies to address the problem of source determination is based on two well-established techniques: the tracer-dilution method and synoptic sampling. The tracer-dilution method provides estimates of stream discharge that are in turn used to quantify the amount of water entering the stream through tributary and ground-water inflow. Synoptic sampling of instream and inflow chemistry provides a spatially detailed "snapshot" of stream-water quality. When used in unison, these techniques provide a description of the watershed that includes both discharge and concentration. Discharge and concentration data can then be used to determine the mass loading associated with various sources of water. Sources representing the greatest contributions in terms of mass loading can then be the target of remedial action.

Purpose and Scope

The purpose of this chapter is to describe the application of the combined tracer-dilution and synoptic-sampling method to selected stream reaches within the Boulder River watershed. Application of the method results in a set of mass-loading curves that illustrate the spatial distribution of the various inflow sources and the effects of the sources on instream water quality. The mass-loading curves are used to answer three basic questions. First, which sources have the greatest effect on stream-water quality in terms of the greatest contributions to constituent loads? Sources determined to be substantial in

terms of mass loading could be the subject of further study and candidates for remedial action. Second, are there substantial inflows that are primarily composed of diffuse ground-water inflow? Stream subreaches that are dominated by ground-water loading may not be amenable to remediation due to the lack of a well-defined surface-water inflow. Third, is there substantial instream attenuation of metal loads? Attenuation of metal loads by geochemical processes should be considered as part of the remedial design.

This chapter begins with a detailed account of the studies conducted on individual stream reaches within the watershed and the associated mass-loading curves. These studies were conducted over two field seasons (1997–98) during low flow. Despite the focus on the low-flow period, differences in the flow regimes arise as a result of yearly variability. The studies in Uncle Sam Gulch and the Bullion Mine tributary were conducted during a 2-week period in 1998.

Methods

The combined tracer-dilution and synoptic-sampling method has been applied to many streams in the Rocky Mountains (Bencala and McKnight, 1987; Kimball, Broshears, and others, 1994; Kimball, 1997; Kimball and others, 1999, 2001, 2002). The studies described herein were undertaken during low-flow conditions (generally August and September). Application of the method to low-flow conditions is an appropriate focus for two reasons. First, the mass-loading profile at low flow reflects the importance of metal sources that enter the stream on a continuous basis. Remedial actions that address the sources identified at low flow will, therefore, improve water quality during the entire year. Second, the pattern of metal loading at low flow indicates which sources contribute to high concentrations during the winter months when the most toxic conditions likely occur (Besser and Leib, 1999). During the winter months, the extent of dilution of mine drainage is less than during higher flow, and limits of toxicity are more likely to be exceeded (Besser and others, 2001). Although dissolved metal loads are greater during snowmelt runoff, true dissolved metal concentrations generally are lower (Nimick and Cleasby, this volume, Chapter D5) and the risk to aquatic life is not as great.

Tracer Injections and Stream Discharge

Quantifying discharge in mountain streams by the traditional velocity-area method[1] (Rantz and others, 1982) is compromised because of the roughness of the streambed and the variability caused by pools and riffles (Jarrett, 1992). Further, a substantial percentage of discharge may flow through porous areas of the streambed that make up the hyporheic zone (Zellweger and others, 1989). Measurement of discharge with the velocity-area method does not account for flow through the hyporheic zone[2], and discharge estimated by that method may result in an underestimate of metal loads (Zellweger and others, 1989; Kimball, 1997). Another limitation of the velocity-area method for the characterization of metal loads is the time and personnel requirements associated with each discharge measurement. In the studies described herein, numerous (about 30–50) instream samples were collected during a single day to characterize stream chemistry at steady state. Velocity-area discharge measurements made in conjunction with sample collection at a large number of sites are limiting, if not impossible.

The tracer-dilution method is an alternative means of estimating discharge (Kilpatrick and Cobb, 1985). The tracer-dilution method uses an inert tracer that is continuously injected into the stream at a constant rate and concentration. With sufficient time, all parts of the stream, including side pools and the hyporheic zone, will become saturated with the tracer. Instream concentrations at a specific distance downstream will become constant (Kimball, 1997). When the stream reaches this condition during a tracer-injection, it is at a "plateau concentration." Decreases in plateau concentration along the length of the stream reflect the dilution of tracer by additional water entering the channel from surface and ground-water inflows. This dilution allows for the calculation of discharge at each stream site. Application of the tracer-dilution method addresses both of the problems previously noted: (1) the tracer enters porous areas of the streambed such that flow through the hyporheic zone also is measured; and (2) collection of tracer samples when plateau concentrations are achieved provides the ability to obtain discharge estimates at numerous stream sites.

Successful implementation of the tracer-dilution method is dependent on two factors. First and foremost, the injected tracer must be transported through the stream reach in a conservative manner; concentrations of the tracer should be unaffected by biogeochemical reactions. Previous studies have documented the transport and chemistry of inorganic salt tracers (Bencala and others, 1990; Broshears and others, 1993; Zellweger, 1994). Because of the conservative behavior of chloride in most natural waters and the availability of inexpensive sodium chloride salt, NaCl was used in the studies described herein. A second important factor is the ability to maintain a constant rate of injection during the study. For the studies described here, tracer injections were controlled with precision metering pumps linked to a Campbell CR-10 data logger. Use of the data logger provides a means to maintain a constant injection rate as battery voltage decreases. Additional details on specific tracer injections are included in the "Subbasin Studies" section.

[1]Velocity-area discharge method. Physical measurement of discharge made by dividing a cross section of the flowing stream into at least 20 area increments and measuring velocity at the center of each increment. The sum gives the total discharge at that cross section.

[2]Hyporheic zone. That area of the streambed alluvium that contains at least 10 percent stream water as a result of exchange with the stream.

Kilpatrick and Cobb (1985) presented a simple mass-balance equation that considers the concentration and injection rate of the added tracer. Discharge at the first synoptic site downstream from the injection is given by:

$$Q_D = \frac{Q_{INJ} C_{INJ}}{C_D - C_0} \quad (1)$$

where Q_{INJ} = the injection rate,
C_{INJ} = the injectate concentration,
C_D = the tracer concentration at the plateau, and
C_0 = the naturally occurring concentration of the tracer upstream from the injection.

This equation is based on two assumptions: that (1) negligible inflow enters the stream between the injection site and the first synoptic site, and (2) the injection concentration is much greater than C_0. Discharge estimates at the remaining synoptic sites are given by:

$$Q_D = \frac{Q_U C_U - C_L}{C_D - C_L} \quad (2)$$

where C_L = tracer concentration in the inflow waters entering a specified subreach,
C_U = the plateau tracer concentration for the synoptic site immediately upstream, and
Q_U = the stream discharge for the synoptic site immediately upstream.

Inflow chloride concentrations in some subreaches represent well-defined surface inflows that are easily sampled. In other subreaches, inflow waters may be primarily diffuse ground-water inflows that are difficult or impossible to sample. These subreaches require estimation of the chloride inflow concentration, a process that can lead to uncertainty in discharge calculations. For the three studies described here, chloride values in subreaches that are dominated by unsampled ground-water inflow had to be estimated. The uniformity in surface-inflow chloride concentrations has a negligible effect on discharge estimates. Note that the problem of estimating chloride for systems with variable background concentrations may be avoided by conducting a pre-synoptic sampling of the stream (Kimball and others, 2001). At the start and end of the injection, samples generally are collected manually at intervals of 5 or 10 minutes at three to five sites, chosen from among the synoptic sampling sites, to define the arrival and departure of the tracer. During the plateau period, hourly samples are taken by automatic samplers at the same sites, which are called transport sites. These samples provide information for transport modeling and allow for resolving temporal effects from storms that could occur during synoptic sampling.

Synoptic Sampling and Analytical Methods

The spatial distribution of metal sources may be characterized by synoptic sampling. Under ideal conditions, samples at all of the sampling locations would be collected simultaneously, providing a description of stream-water quality at steady state. Personnel limitations generally preclude simultaneous sample collection, but the synoptic studies described in the following text provide an approximate means of describing steady-state conditions. This approximation is achieved by the collection of samples throughout a relatively short period (less than 8 hr) and by conducting the studies during low-flow conditions such that the effects of diurnal flow variation are minimized. By approximating steady-state conditions, synoptic sampling provides a spatially intensive "snapshot" of chemistry and discharge that is used to quantify instream loads.

During a synoptic study, samples are collected at several stream and inflow sites. Stream sites along the study reach are spaced such that they bracket the sampled inflows and areas of likely subsurface inflow. Subreaches that are bracketed by two adjacent stream sites are referred to as stream segments. The intent of this bracketing is to capture the changes in load that are attributable to visible surface inflow and (or) diffuse subsurface inflow within each segment. At this level of spatial detail, changes in stream chemistry and discharge between stream sampling sites reflect a net metal load for specific segments, although the loads cannot always be attributed to specific sources.

For each of the following studies, stream and inflow samples were collected at numerous predetermined locations, beginning at the downstream end of the study reach and ending upstream of the tracer-injection. This downstream-to-upstream sampling order was followed in order to avoid disturbing streambed materials. Inflow and stream sites that were considered well mixed were sampled by using grab techniques. Stream sites that were not well mixed were sampled by equal width integration[3] (Ward and Harr, 1990). Water temperature was measured on site and the collected samples were transported to a central location for further processing. Samples were processed at a central location to measure pH and specific conductance and to divide the sample into the following bottles: a raw (unfiltered) unacidified sample (RU), a raw acidified sample (RA), a filtered unacidified sample (FU), a filtered acidified sample (FA), and a ultrafiltered acidified sample (UFA).

Specific conductance and pH were determined from the RU sample within hours of sample collection. Filtration included tangential-flow filtration through 0.45-µm membranes (FU and FA samples) and ultrafiltration by using a 10,000-Dalton molecular weight membrane (UFA sample).

[3]Equal-width integration. Sample collected by moving a depth-integrating sampler, like a USGS DH-81, down and up at a constant rate at equal increments of width across a stream. Thus, those parts of the stream that have greater discharge will fill the bottle the most.

Metal concentrations for the RA, FA, and UFA samples were determined by inductively coupled plasma–atomic emission spectrometry (Lichte and others, 1987). Anion concentrations were determined from FU samples by using ion chromatography (Kimball and others, 1999). Ferrous iron was determined colorimetrically from the UFA samples (Kimball and others, 1992), and total alkalinity was determined by titration.

Use of two filter sizes provides for three different operationally defined concentrations for each metal. The unfiltered sample (RA) provides a measure of the total-recoverable metal concentration (dissolved + colloidal), and the ultrafiltrate concentration (UFA) is considered the dissolved metal concentration. The 0.45-µm concentration (FA) is used for comparison purposes. Colloidal metal concentrations are defined as the difference between the total-recoverable (RA) and the ultrafiltrate metal concentrations (UFA) for stream samples (Kimball and others, 1995).

Principal Components Analysis

An important objective of synoptic sampling is to recognize patterns or chemical characteristics that indicate the sources of mine drainage. Water-rock interactions with different mineral assemblages in source areas create distinct chemical signatures among the inflows. The signatures may produce groups of inflow samples that are distinguished by their similarities. Groups of stream samples may be linked to inflow groups, indicating which inflows influence stream chemistry. Distinctions among inflow groups also may lead to an understanding of differences in drainage from mined and nonmined areas.

Patterns in the chemistry, including the pH, of synoptic samples are displayed by using Principal Components Analysis (PCA). A principal component represents a transformed axis that is a linear combination of the original variables (Daultrey, 1976; Davis, 1986). The transformation to a new axis is not statistical, but is simply a rotation (in multi-dimensional space) that orients the data points so that we observe the greatest amount of difference (or variance) among them. The rotation does not change the relation of one sample to another; it only changes how we view the samples. For example, if the surface of a framed picture were given x, y, and z coordinates to represent its surface morphology, PCA would rotate the picture so that one would be looking at it straight on instead of at some angle. The x and y variables (height and width of the picture) are much greater than the depth (which would mostly be due to the frame). Conceptually, PCA rotates chemical data in a similar manner, and this helps one visualize the greatest distinctions among groups of samples. It also emphasizes distinct outlier samples. The first two principal components generally show enough of the variance in a data set to distinguish groups among the samples. Each sample is related to a principal component by its score on that component, which is the coordinate of the original data point on the new principal component axis.

PCA also can emphasize the physical and chemical processes that are responsible for the distinctions among groups of samples. Each chemical constituent has a correlation to the new principal components, called a loading in the jargon of PCA. These correlations can be expressed as arrows or vectors on a plot of sample scores. By combining the classification information of scores with the process information from loadings, a biplot is created. Biplots are used to present results of PCA for each mass-loading study.

Chemical reactions and mixing processes often result in linear relations among chemical constituents. To emphasize the linear relations among variables, the chemical concentration of each constituent, expressed in millimoles per liter, was log transformed. This improves correlations that may be related to stoichiometries of particular chemical reactions. It is the products of chemical reactions that end up as dissolved constituents in the stream and are sampled in a water-quality study. Mole ratios of those products provide mass-balance evidence of the water-rock reactions that may account for the observed chemistry. PCA calculations were carried out with the U.S. Geological Survey Statpac programs that include special scaling options to improve the biplot (Grundy and Miesch, 1987).

Constituent Loads

Given estimates of stream discharge and metal concentration, solute load at each stream site can be quantified as the simple product of discharge and concentration. This calculation leads to a longitudinal profile of the sampled instream load. Any change in load between a pair of stream sites accounts for the gain or loss of solute load for that segment. Gains in solute load imply the existence of a source for the solute that reaches the stream between the two stream sites. Instream load also can decrease within a stream segment, indicating a net loss of the solute as a result of chemical or biological processes. The sum of all the increases in load between sampling sites along the study reach produces cumulative instream load. At the end of the study reach, the cumulative instream load is an estimate of the total load of solute added to the stream; this estimate is likely a minimum estimate because it only measures the net loading between sites. Some of the load in that stream segment could be lost through attenuation within an individual stream segment.

The change in discharge between stream sites is used in a second approach to calculating loads. The change in discharge between two stream sites, multiplied by solute concentration of an inflow sample, provides an estimate of the inflow load for a stream segment. The sum of the inflow loads for all sampled inflows provides a longitudinal profile of the cumulative inflow load, which indicates how well the sampled inflows account for the load measured within the stream. The cumulative instream and cumulative inflow profiles are equivalent if the sampled inflows are representative of the inflows that enter the stream. This situation rarely occurs, however, because

inflows to streams include both surface and subsurface inflow. Greater subsurface concentrations would cause the profile of cumulative instream load to be more than the profile of cumulative inflow load.

Load profiles provide not only information to evaluate the location and magnitude of metal loading to the stream, but also help in understanding and quantifying watershed processes. The loading profile is a view from the stream; it accounts for the loads that actually reach the stream. A particular mine adit away from the stream may have a greater load at its adit, but if that load is attenuated before it reaches the stream, it is not accounted for within the load profile. Thus, inflow samples are obtained near the stream to represent the net delivery of metals to the stream from various sources. The three ways to account for loads from the watershed are based on instream and inflow loads. First, the sampled instream load provides information about the relative importance of metal sources in terms of which stream segments contribute the greatest loads. The level of detail from synoptic sampling allows individual increases, measured in each stream segment, to be viewed in the context of the whole watershed. Second, the difference between the cumulative instream and cumulative inflow loads provides information about the location of unsampled, or possible ground-water inflows. Third, the difference between the cumulative instream load and the sampled instream load provides information about the extent of attenuation of solutes. All this information is available on the scale of individual stream segments and the scale of the entire study reach.

Subbasin Studies

Complete chemical data for synoptic samples that were collected in each of the subbasin studies are presented in the database on CD-ROM. A description of sampling sites and summaries of chemical data are presented here for each subbasin. Locations of all the mines discussed in this chapter are in Martin (this volume, Chapter D3).

Cataract Creek Basin

Study Area and Experimental Design

The experimental design of the tracer-injection study in Cataract Creek is described in Cleasby and others (2000). The study reach started 3,000 ft upstream from Hoodoo Creek and ended at the confluence with the Boulder River (fig. 1); the total distance is more than 40,000 ft and was divided into 44 stream segments. Inflow samples were collected in 20 of the stream segments; 23 inflows were sampled in all. Downstream distance for each of the segments and inflows, along with site descriptions, are listed in table 1.

A sodium chloride tracer with a chloride concentration of 133,200 mg/L was injected at a rate of 435 mL/min. This provided a clear chloride signal that was elevated above background concentrations (fig. 2). Because the inflow chloride concentrations were low, but not constant, equation 2 was used to calculate discharge (fig. 2). The increase in discharge along the study reach was 12.5 ft^3/s. Discharge increased by 4.8 ft^3/s in those segments that had no inflow samples; this was 38 percent of the total increase in discharge, which was a considerable ground-water component to the increase in flow. The path of the creek generally follows the structural control of a major fault (O'Neill and others, this volume, Chapter D1, pl. 1), and the reach is predicted to be a gaining reach based on the lineament and fracture-density analysis of McDougal and others (this volume, Chapter D9).

Chemical Characterization of Synoptic Samples

Synoptic sampling of inflows provides a range of chemistry that affects the stream and provides a context for the changes in stream chemistry and solute loads. In a watershed affected by mine drainage that has outcrops of rocks with acid-neutralizing capacity, inflow chemistry can range from acidic and metal-rich to alkaline and essentially metal-free. Both kinds of inflow chemistries can affect the stream chemistry.

Stream water in Cataract Creek was a calcium bicarbonate type, reflecting the chemical weathering of bedrock in the watershed (Nimick and Cleasby, this volume, Chapter D5). The tracer overwhelmed baseline concentrations of sodium and chloride in the stream. The baseline concentrations of inflows, however, were approximately 3 mg/L sodium and 0.3 mg/L chloride. This baseline chloride concentration was about 10 times lower than the chloride concentration at the final stream sampling site (fig. 2). The alkalinity of Cataract Creek remained nearly constant along the entire reach (fig. 3). Concentration of the other major ions increased slightly downstream from Uncle Sam Gulch; changes in calcium and sulfate were the greatest (fig. 3). Calcium concentrations upstream from Uncle Sam Gulch averaged 12.4 mg/L, and 15.0 mg/L downstream; sulfate concentrations averaged 9.1 mg/L upstream and 16.8 mg/L downstream. The greater change in sulfate mostly represents the mine-drainage inputs from Uncle Sam Gulch.

Several metals occurred with measurable concentrations. Aluminum, copper, iron, manganese, and zinc concentrations were substantially above detection limits. Cadmium, nickel, and lead concentrations mostly were near limits of detection. Although no great variation occurred in major-ion concentrations or pH along the study reach, substantial differences did occur in metal concentrations upstream and downstream from Uncle Sam Gulch, with higher concentrations occurring downstream (fig. 4). Concentrations of aluminum, copper, and zinc that were less than the detection limits are not plotted; therefore, the lines are not all continuous. Average

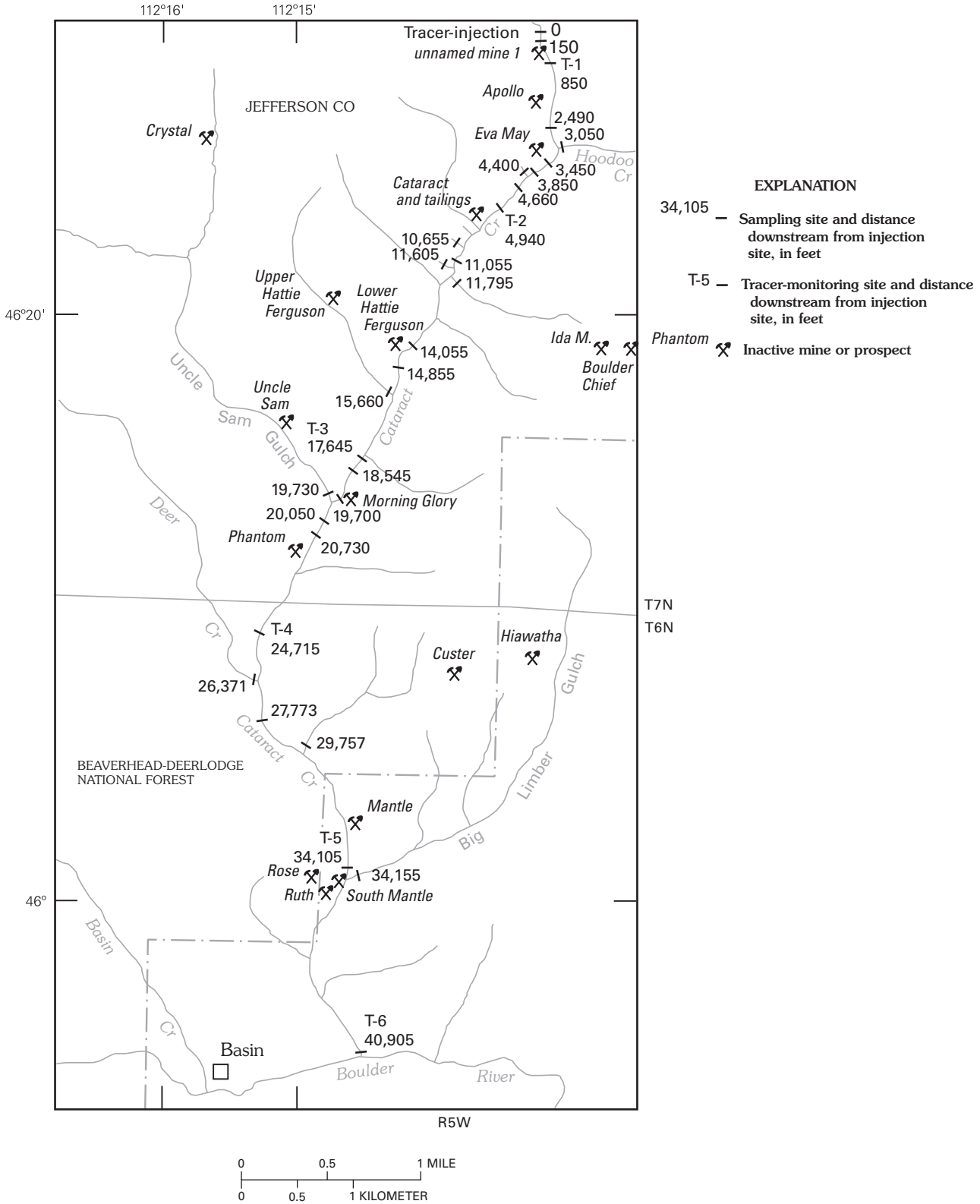

Figure 1. Location of study reach, selected inactive mines or prospects, and selected sampling sites, Cataract Creek drainage (modified from Cleasby and others, 2000).

Table 1. Segment number, distance along study reach, source, site description, and selected water-quality characteristics of water from synoptic sampling sites, Cataract Creek, August 13, 1997.

[Dist, distance, in feet along the study reach; source: S, stream; RBI, right-bank inflow; LBI, left-bank inflow; Q, discharge, in liters per second; T, temperature, in degrees Celsius; pH, in standard units; Ksc, specific conductance, in microsiemens per centimeter; Cl, chloride, in milligrams per liter]

Segment number	Dist	Source	Site description	Q	pH	Ksc	Cl
S01	150	S	First site below injection	117	7.71	110	8.28
T01	160	RBI	Right-bank inflow	4.0	7.62	70	< .1
S02	850	S	T1 transport site in canyon	121	7.85	108	8.26
S03	1,370	S	Above right-bank mine dump	124	7.82	106	8.08
T02	1,615	RBI	Right-bank inflow from mine dump	4.0	7.59	190	< .1
S04	1,690	S	Below mine dump at Apollo mine	130	7.87	107	7.72
T03	1,691	RBI	Right-bank inflow	0.1	7.81	175	< .1
S05	2,490	S	Above mine dump at Eva May mine	130	7.83	107	7.74
T04	3,050	LBI	Hoodoo Creek on left bank	40.0	7.75	106	< .1
S06	3,450	S	Below Hoodoo Creek	170	7.82	106	5.99
S07	3,850	S	Above Eva May mine tailings	174	7.83	105	5.85
T05	4,400	RBI	Eva May tailings inflow	8.0	7.48	100	< .1
S08	4,660	S	Adjacent to Eva May tailings pile	182	7.83	106	5.61
S09	4,940	S	T2 transport site below Eva May mine	185	7.73	107	5.52
T06	4,941	RBI	From pipe under road	2.0	7.71	92	< .1
S10	5,940	S	Below curve with overbank tailings	187	7.74	108	5.46
S11	6,800	S	Along bend	189	7.74	107	5.42
S12	7,900	S	Below old cabin	191	7.80	108	5.37
S13	8,700	S	Below mine dump, at Cataract mine tailings	193	7.71	108	5.31
T07	8,820	RBI	Below Cataract mine dump	5.0	7.26	65	< .1
S14	9,220	S	Adjacent to Cataract mine tailings	198	7.66	108	5.20
T08	9,225	RBI	Cataract mine tailings with iron stains	3.5	7.20	88	< .1
S15	10,380	S	End of large flood plain	205	7.52	110	5.02
T09	10,655	RBI	Right-bank inflow	10.0	7.51	57	< .1
S16	11,055	S	Adjacent to ponded water on right bank	215	7.38	109	4.81
T10	11,605	RBI	Inflow with iron stains	4.5	6.61	130	< .1
T11	11,795	LBI	Boulder Chief and Ida M. mines	4.5	7.57	122	< .1
S17	12,115	S	Above large clear-cut area	224	7.68	109	4.63
T12	12,120	LBI	Left-bank inflow	7.0	7.63	143	< .1
S18	13,255	S	Above Lower Hattie Ferguson mine	231	7.77	111	4.49
S19	14,055	S	Below Lower Hattie Ferguson mine	236	7.82	113	4.42
S20	14,855	S	Above left-bank inflow	239	7.81	113	4.37
T13	14,860	LBI	Left-bank inflow	3.0	7.89	84	< .1
S21	15,655	S	Below Upper Hattie Ferguson mine	242	7.44	112	4.31
T14	15,660	RBI	Upper Hattie Ferguson mine	4.0	7.59	116	< .1
T15	15,845	RBI	Right-bank inflow	4.0	7.45	135	< .1
S22	16,845	S	Below inflows	250	7.81	113	4.19
S23	17,645	S	T3 transport site below logging-road ford	261	7.72	114	4.05
S24	18,545	S	Above biological sampling site	270	7.80	116	3.93
S25	19,245	S	Above Morning Glory mine	276	7.64	116	3.85
S26	19,700	S	Below Morning Glory mine	276	7.83	116	3.92
T16	19,730	RBI	Uncle Sam Gulch	50.0	7.32	134	< .1
S27	20,050	S	Below Uncle Sam Gulch	326	7.63	119	3.30
S28	20,730	S	Below cabin and tailings pile on right bank	336	7.81	118	3.22
S29	21,130	S	Check for reaction below Uncle Sam Gulch	336	7.61	118	3.22
T17	21,315	LBI	Waste-rock piles on both banks	2.0	8.10	409	< .1
S30	21,715	S	Along cascades below small mine dumps	338	7.83	118	3.21
S31	22,315	S	Above rock wall	338	7.80	118	3.21

Table 1. Segment number, distance along study reach, source, site description, and selected water-quality characteristics of water from synoptic sampling sites, Cataract Creek, August 13, 1997.—Continued

Segment number	Dist	Source	Site description	Q	pH	Ksc	Cl
T18	22,565	LBI	Left-bank inflow	0.1	7.77	222	< .1
T19	22,715	LBI	Left-bank inflow	0.1	7.19	220	< .1
S32	22,915	S	Below small inflow	338	7.65	120	3.21
S33	23,715	S	At old lean-to	342	7.74	123	3.18
T20	24,495	RBI	Draining oxbows	3.0	7.20	279	< .1
S34	24,715	S	T4 transport site above canyon	345	7.65	123	3.16
S35	25,215	S	Above start of canyon	349	7.70	124	3.13
S36	26,335	S	Above Deer Creek	349		126	3.13

Segment number	Dist	Source	Site description	Q	T	pH	Ksc	Cl
T21	26,370	RB	Deer Creek	11.0	11.5	8.14	188	<.1
S37	26,590	S	Below Deer Creek	360	13.5	7.88	126	3.05
S38	26,970	S	Below large concrete bridge	361	13.5	8.01	126	3.04
S39	27,775	S	Below second wooden bridge	364	13.5	8.23	126	3.02
T22	29,760	LB	Left-bank inflow	13.0	11.5	8.48	500	<.1
S40	29,970	S	Below old cabin on right bank	377	13.5	7.40	126	2.99
S41	31,470	S	Along cascade reach	382	13.5	7.82	128	2.96
S42	32,970	S	Wide section of canyon	387	13.5		128	2.93
S43	34,105	S	T5 transport site above Big Limber Gulch	394	13.5	7.84	128	2.89
T23	34,155	LB	Big Limber Creek	36.0	14.5	8.00	280	<.1
S44	34,355	S	Below Big Limber Creek	430	14.0	7.84	130	2.79
S45	40,905	S	T6 transport site Cataract Creek at mouth	472	14.8	7.83	131	2.59

concentrations of total-recoverable aluminum increased from less than 50 to about 80 µg/L at S27 (fig. 4*A*). All of the filtered copper concentrations were less than detection, and only a few sites downstream from Uncle Sam Gulch had total-recoverable concentrations greater than detection (fig. 4*B*). Copper concentrations of Uncle Sam Gulch and Big Limber Gulch were greater than 100 µg/L. Total-recoverable concentrations of iron decreased from 300 to 249 µg/L (fig. 4*C*). Filtered and total-recoverable zinc concentrations were near detection limits from the injection site to the area of the Eva May mine tailings (S08). Downstream from S08, zinc concentrations were measurable all the way to S26, upstream from Uncle Sam Gulch. Downstream from Uncle Sam Gulch, filtered zinc concentration increased an average of 34 to 461 µg/L (fig. 4*D*). Concentrations of total manganese increased from an average of 12 to 75 µg/L at S27, and had a pattern similar to that of zinc. Concentrations of cadmium, lead, and nickel were too low to observe patterns.

Nimick and Cleasby (this volume, Chapter D5) indicate those parts of Cataract Creek where metal concentrations exceeded instream aquatic life standards for acute and chronic toxicity. The tracer-study results are comparable to their findings.

The importance of the iron and aluminum colloids is seen by their impact on other metals. Total-recoverable copper concentrations were substantially higher downstream from Uncle Sam Gulch, most likely because copper was sorbed to the iron colloids (fig. 4*B*). Total-recoverable zinc concentrations increased from near the detection limit to an average of 461 µg/L downstream from Uncle Sam Gulch, and about 14 percent of that total-recoverable zinc was transported in the colloidal phase (fig. 4*D*). The presence of copper and zinc in the colloidal material could have effects on the chronic toxicity of the stream (Clements, 1994; Besser and others, 2001). The colloidal concentrations contribute to the high concentrations of copper and zinc in the bed sediments downstream from Uncle Sam Gulch (Church and others, this volume, Chapter D8).

On the basis of principal components analysis (Kimball and others, 2001), differences in chemical composition among inflows along Cataract Creek distinguish five groups among the synoptic samples (fig. 5). Three of these groups represent both stream and inflow samples, and two include only inflows. The combination of stream and inflow samples in a group may explain two conditions. First, for stream samples collected upstream of mine-drainage inflows, the chemical character of the stream samples should resemble

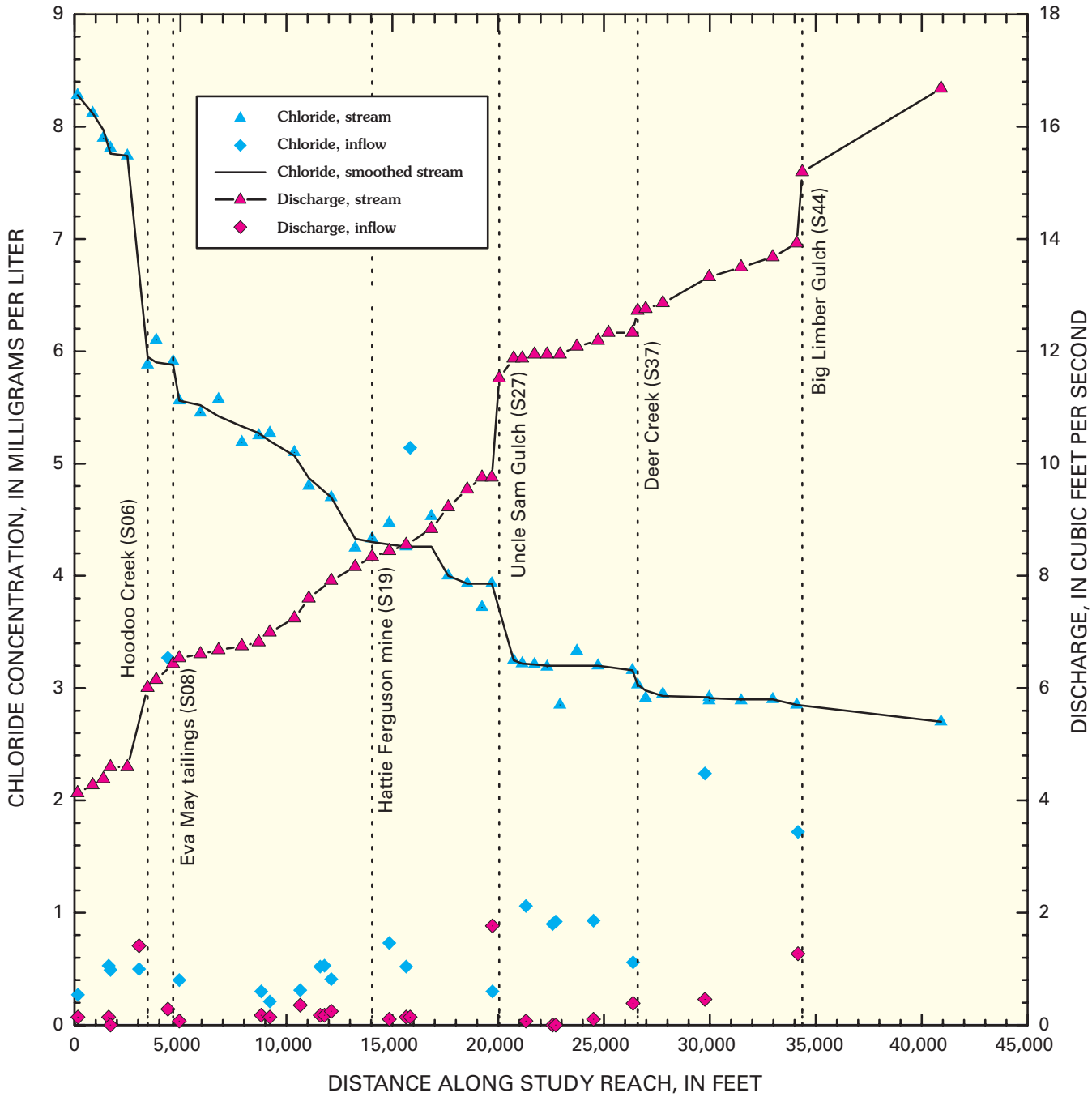

Figure 2. Injected chloride concentration and calculated discharge, Cataract Creek, August 1997. Numbers are segment numbers, table 1.

inflows that drain the same unaltered bedrock in the catchment. Second, where an inflow dramatically changes the character of the stream water, that inflow may determine the character of stream samples for some distance downstream until additional inflows or instream chemical reactions cause further change.

The vectors indicate the chemical differences among groups of samples (fig. 5). For example, samples that plot to the upper left are higher in metals, while samples that plot to the upper right have higher concentrations of the alkaline-earth metals and sulfate. Group 1 represents samples somewhat affected by mining, and includes samples upstream from Hoodoo Creek and inflow T08 (table 2). Group 2 includes most stream sites upstream from Uncle Sam Gulch and most of the inflows along that reach. These samples plot in the direction of slightly greater metal concentrations than group 1, and several of these inflows are draining areas that include tailings. Group 2 represents inflows and stream sites upstream from Uncle Sam Gulch that have higher concentrations of alkaline-earth metals and sulfate. Group 3 represents the

Table 2. Average composition of groups from principal components analysis of synoptic samples, Cataract Creek, August 1997.

[pH, in standard units; all concentrations in milligrams per liter]

Solute	Group 1 Limited effects of mining, upstream from Hoodoo Creek	Group 2 Stream samples upstream from Uncle Sam Gulch	Group 3 Stream samples downstream from Uncle Sam Gulch	Group 4 Inflows affected by alkaline-earth weathering	Group 5 Inflows from Big Limber Gulch area
Number of samples	13	24	20	9	2
pH	7.70	7.63	7.76	7.64	8.29
Sulfate	10.8	12.7	13.3	29.9	38.3
Calcium	12.5	13.7	14.6	33.4	48.3
Magnesium	2.43	2.68	2.92	5.74	9.46
Aluminum	.040	.043	.039	.025	.001
Cadmium	.003	.005	.003	.005	.001
Copper	.019	.021	.022	.028	.003
Iron	.222	.248	.311	.086	.004
Manganese	.033	.047	.062	.145	.031
Nickel	.003	.004	.003	.001	.001
Lead	.002	.003	.002	.001	.001
Strontium	.095	.118	.105	.233	.370
Zinc	.154	.243	.234	.173	.001

change in composition downstream from Uncle Sam Gulch. The sample from Uncle Sam Gulch, T16, was the only inflow sample in group 3. It is grouped with the downstream samples because it has a great influence on the chemistry of those stream samples. Stream samples in group 3 plot between the stream samples of group 2 and inflow T16; this indicates the change that resulted from the inflow of Uncle Sam Gulch. The vectors around T16 indicate that it is mostly a shift in cadmium, copper, manganese, and zinc. Groups 4 and 5 include only inflow samples, representing higher concentrations of alkaline-earth metals and sulfate, but not contributing metals.

Load Profiles

A summary of the net change in load for each segment is listed in table 3, along with a summary of calculations for the whole study reach. Cumulative instream loads provide the best estimate of the total loading for an element in a study reach. The cumulative instream load for the selected constituents in table 3 varies considerably. Sulfate load was the greatest, more than 720 kg/day, while copper load was only 2 kg/day. Among the metals, zinc had the greatest cumulative load, with 17 kg/day. The details of this loading are illustrated in load profiles and bar charts showing summaries of surface inflow, unsampled inflow, and net losses for individual stream segments (figs. 6–11).

There are differences among the profiles of metal and sulfate loading along the study reach of Cataract Creek. The two extreme profiles were those of sulfate (fig. 6) and zinc (fig. 7). The profile of sulfate shows loading in many stream segments all along the study reach. The resulting profile is a broad gradual increase in the cumulative instream load, punctuated by the tributary inflows at Hoodoo Creek (S06), Uncle Sam Gulch (S27), and Big Limber Gulch (S44). The most plausible cause of this profile is the contribution from weathering reactions throughout the watershed. Sulfate most likely has a mineralogical residence in sulfide minerals associated with alteration in the watershed. However, it is most likely more widespread than the metals associated with ore deposits.

At the other extreme, zinc loading was dominated by a large loading in one stream segment, the inflow of Uncle Sam Gulch (fig. 7). There were a few other, much smaller loads from stream segments, but none compares with the loading from Uncle Sam Gulch. This pattern results from the adit drainage of the Crystal mine into Uncle Sam Gulch (Nimick and Cleasby, this volume, Chapter D5).

These two patterns of sulfate and zinc load profiles represent different mixtures of weathering processes and mine drainage in the watershed. Profiles of other metals have some differences from these two that mostly result from the conservative or reactive behavior of the metals once they have been added to the stream. Manganese loading was similar to that of zinc, and the load from the segment containing Uncle Sam Gulch (S27) dominated the profile (fig. 8). Downstream from Uncle Sam Gulch, the manganese load decreased slightly, but no transfer of manganese to the colloidal phase took place. Instead, manganese was lost to the streambed, probably through sorption to streambed materials. A similar pattern was observed for manganese in Little Cottonwood Creek, Utah, where the pH was comparable to that of Cataract Creek (Kimball and others, 2001).

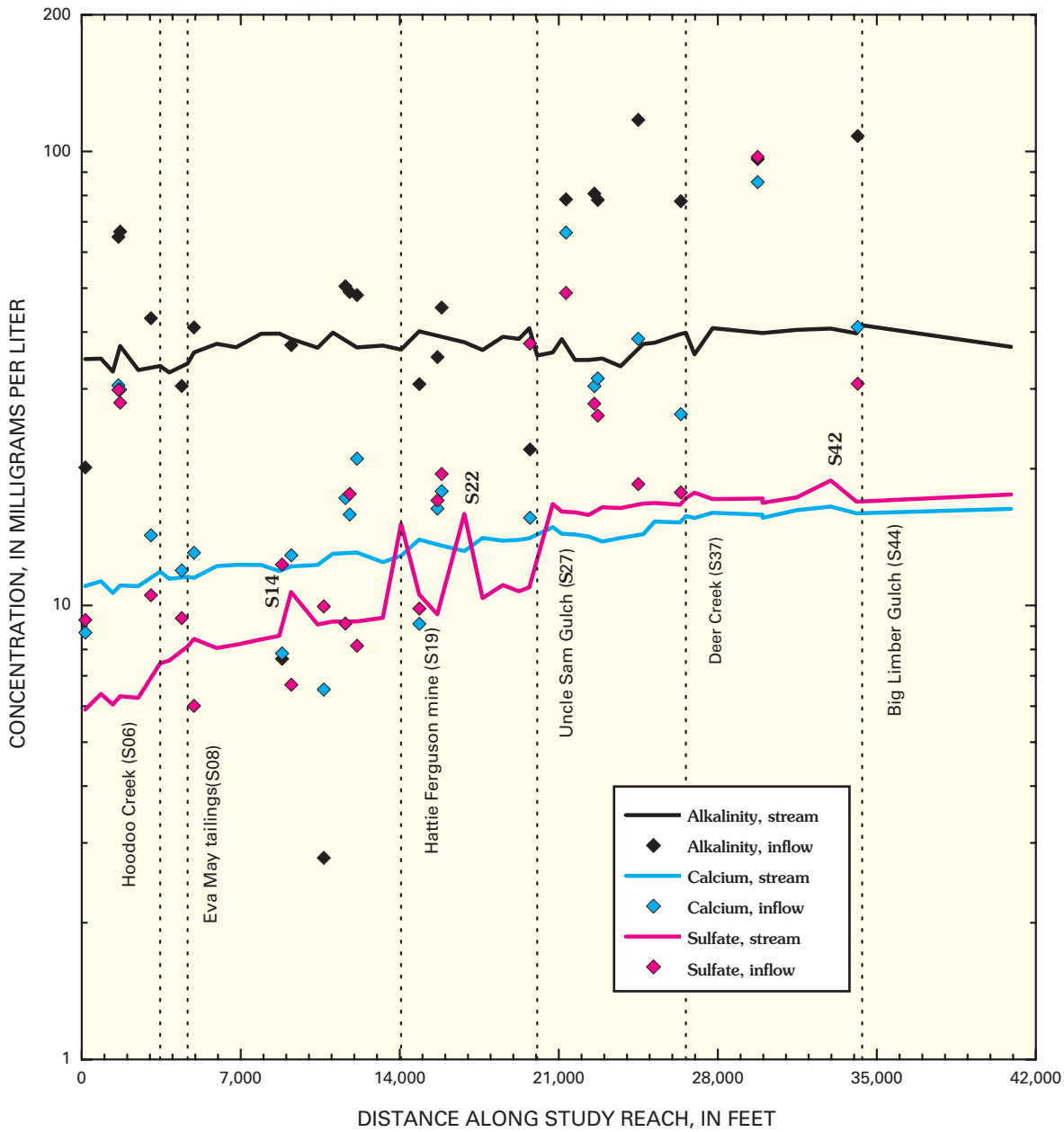

Figure 3. Variation of alkalinity, calcium, and sulfate concentrations with distance, Cataract Creek, August 1997.

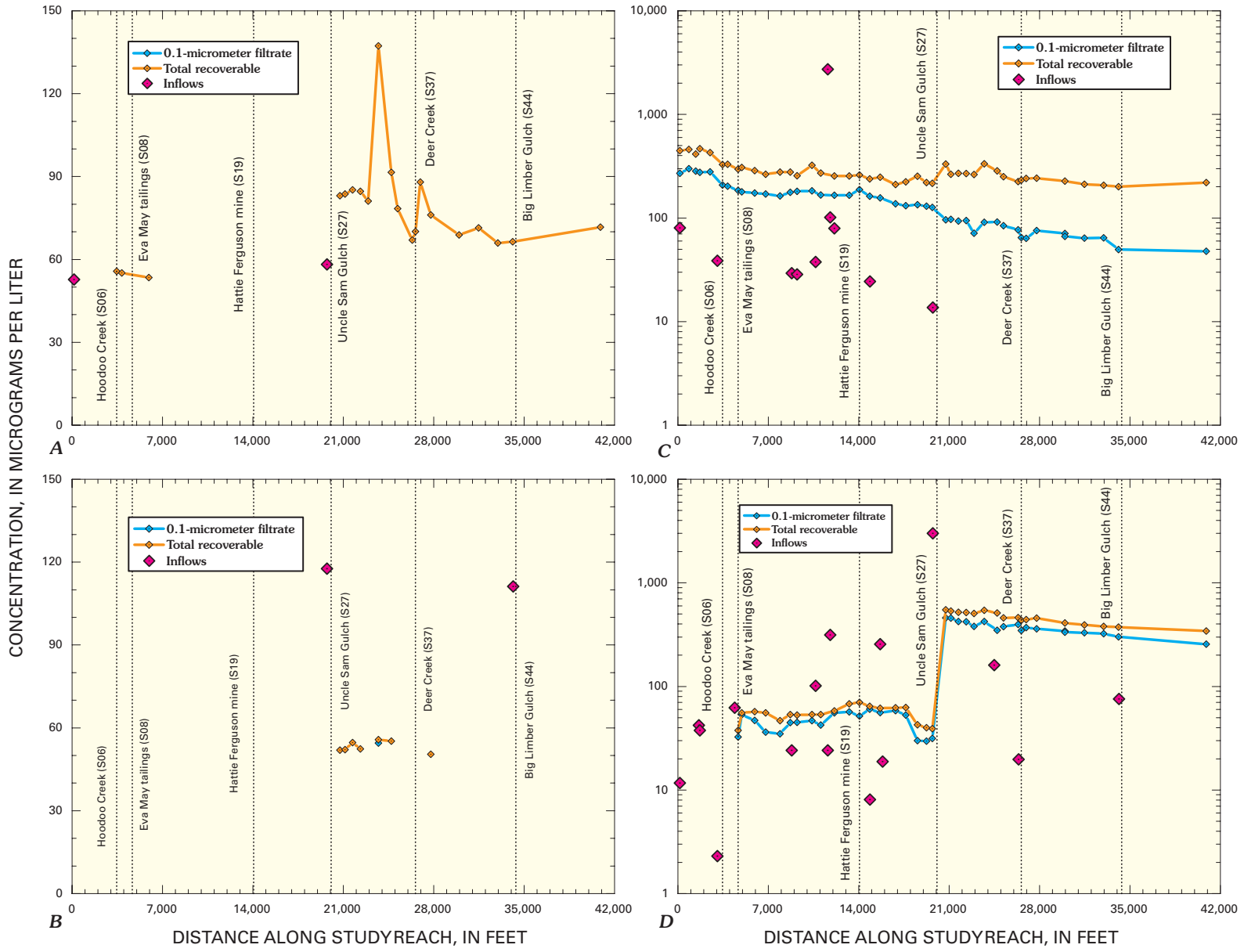

Figure 4. Variation of *A*, aluminum; *B*, copper; *C*, iron; and *D*, zinc concentrations with distance, Cataract Creek, August 1997.

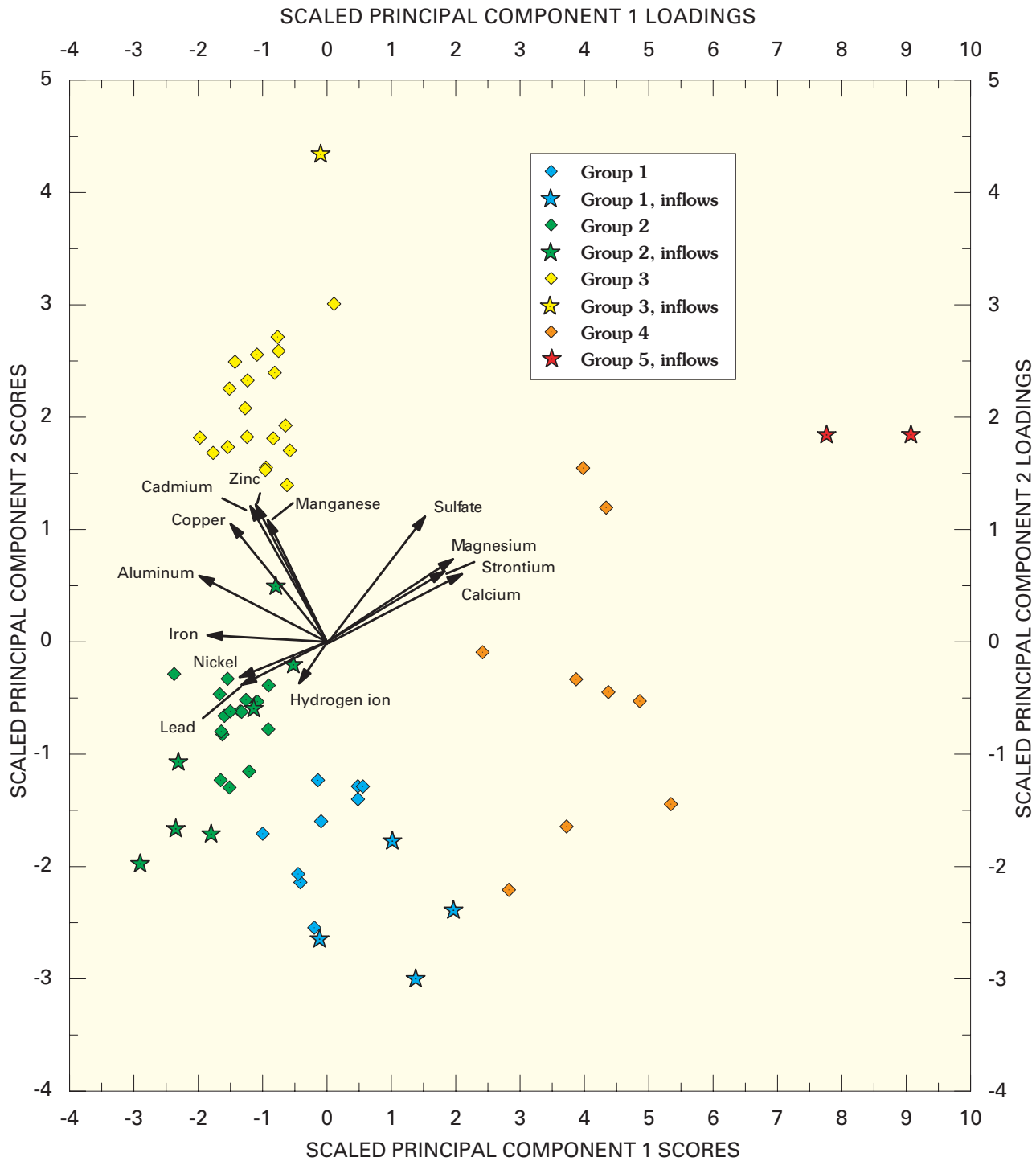

Figure 5. Biplot of principal component scores for synoptic samples and loadings for chemical constituents, Cataract Creek, August 1997.

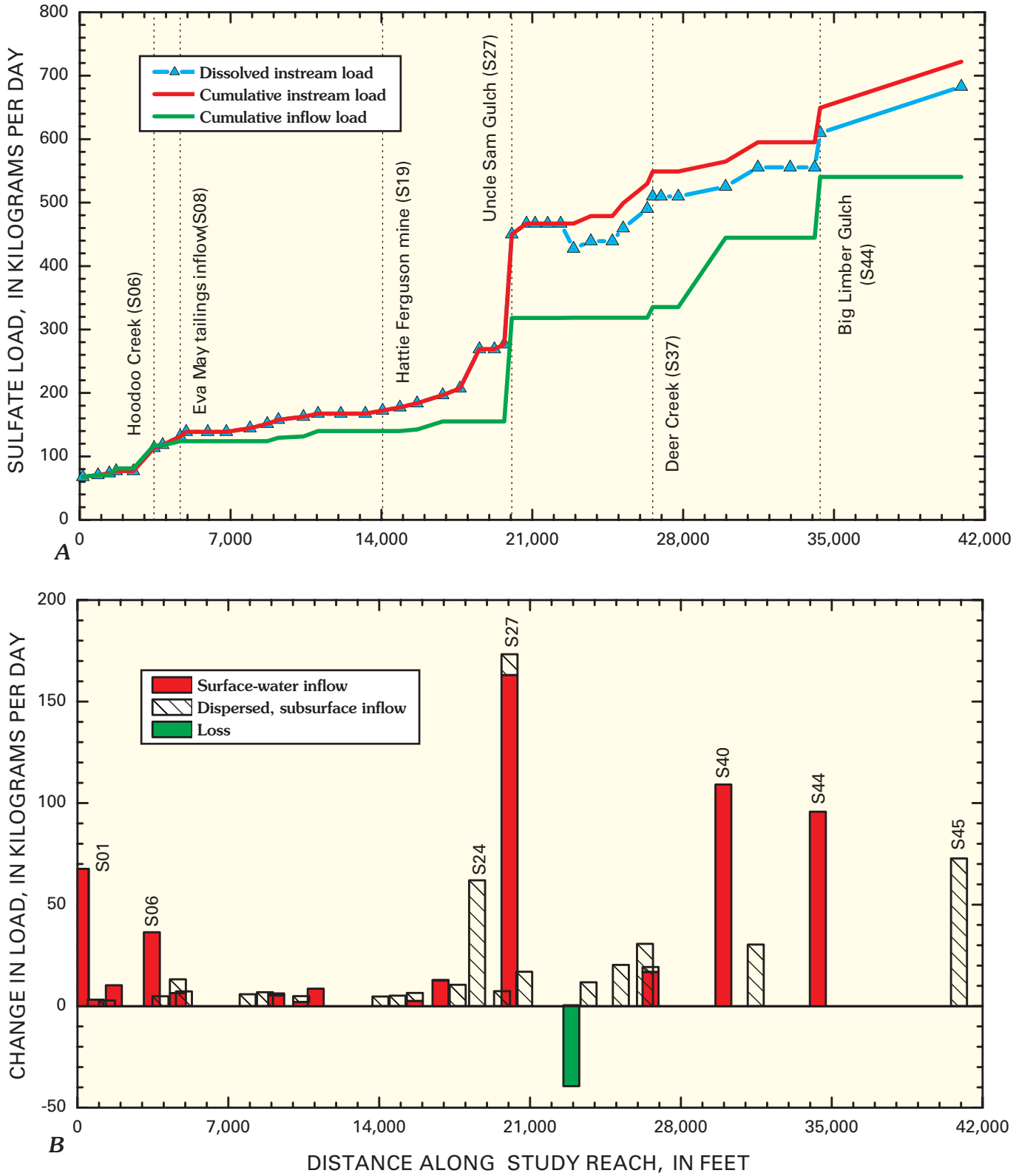

Figure 6. Variation of *A*, sulfate load with distance, and *B*, changes in load for individual stream segments, Cataract Creek, August 1997.

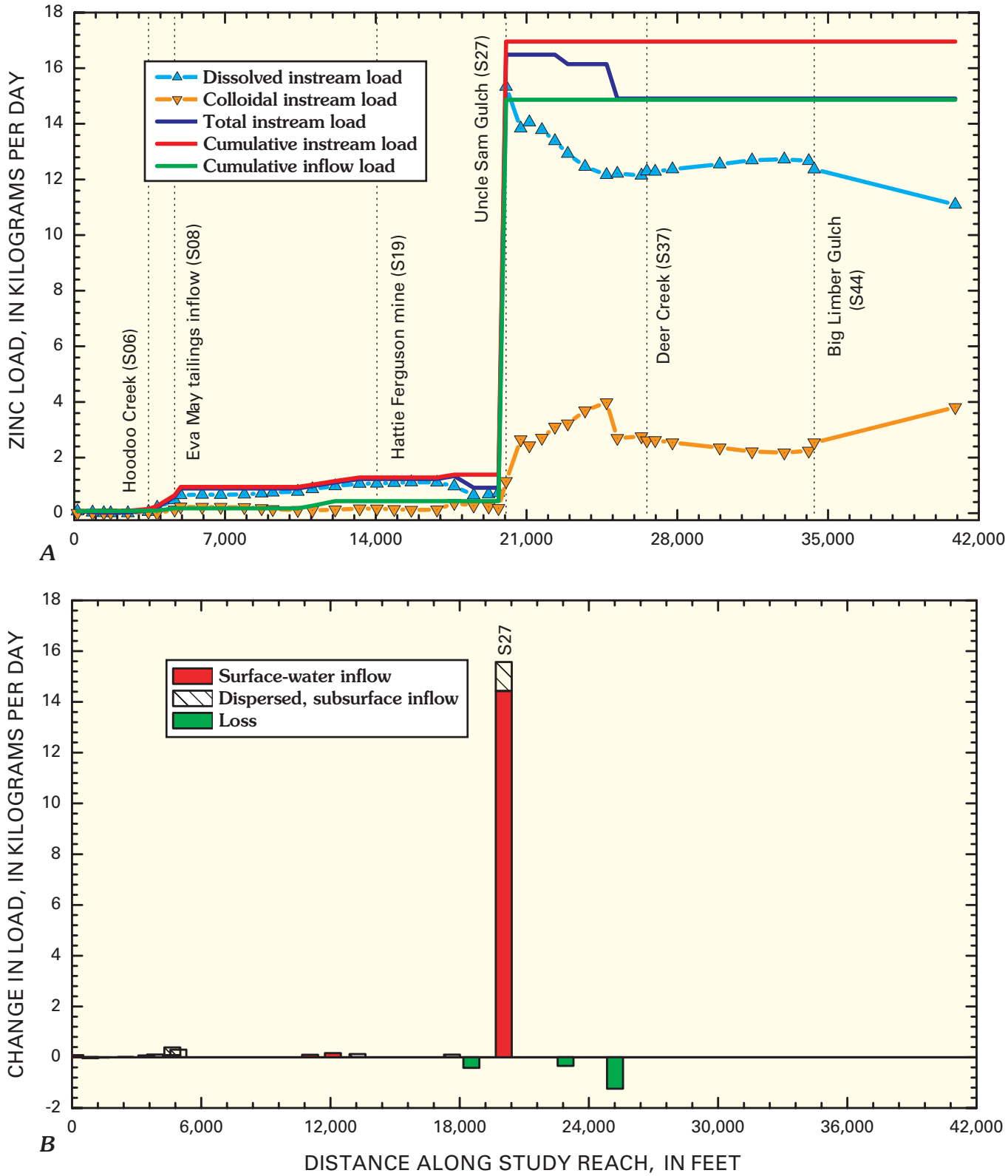

Figure 7. Variation of *A*, zinc load with distance, and *B*, changes in load for individual stream segments, Cataract Creek, August 1997.

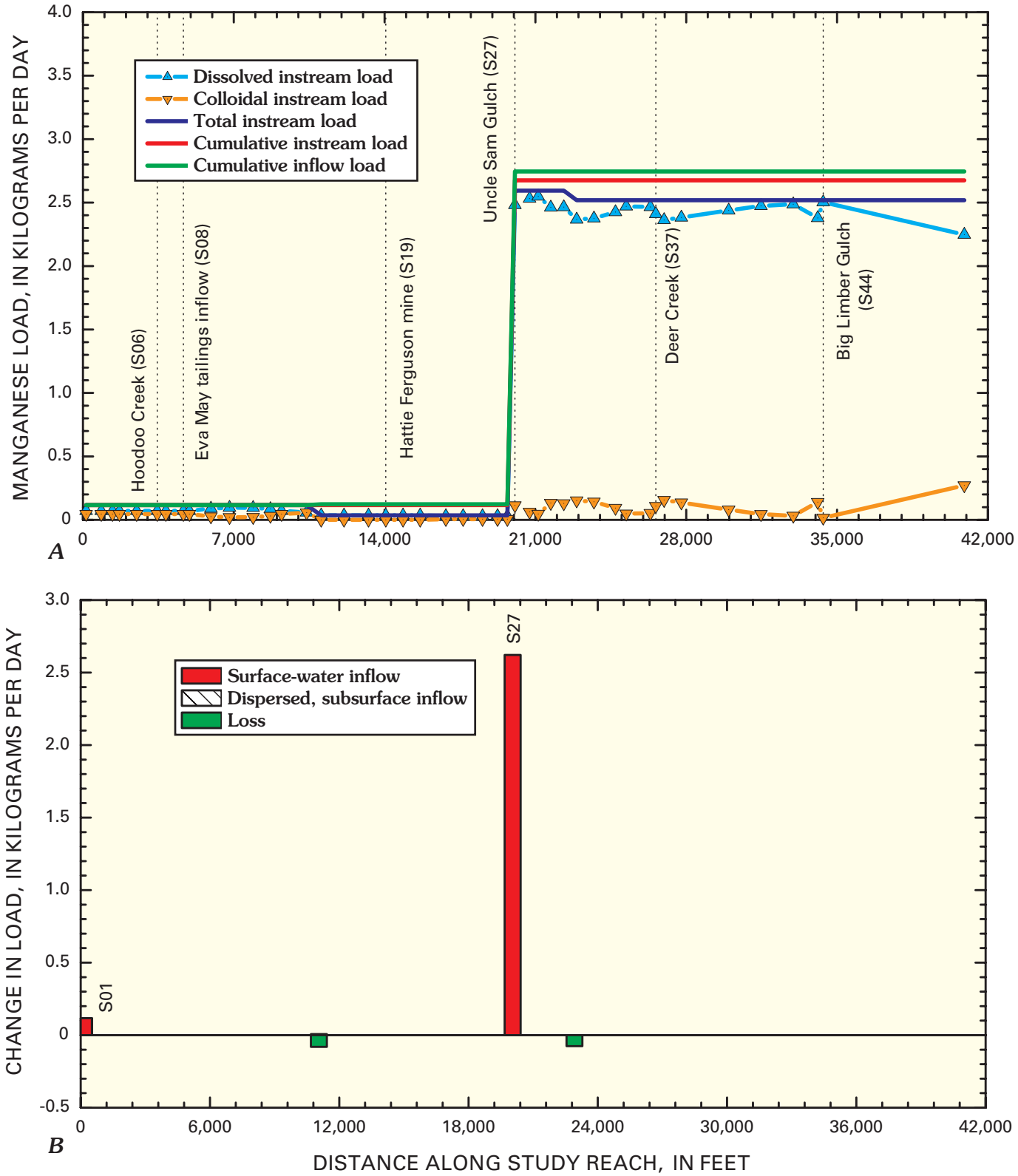

Figure 8. Variation of *A*, manganese load with distance, and *B*, changes in load for individual stream segments, Cataract Creek, August 1997.

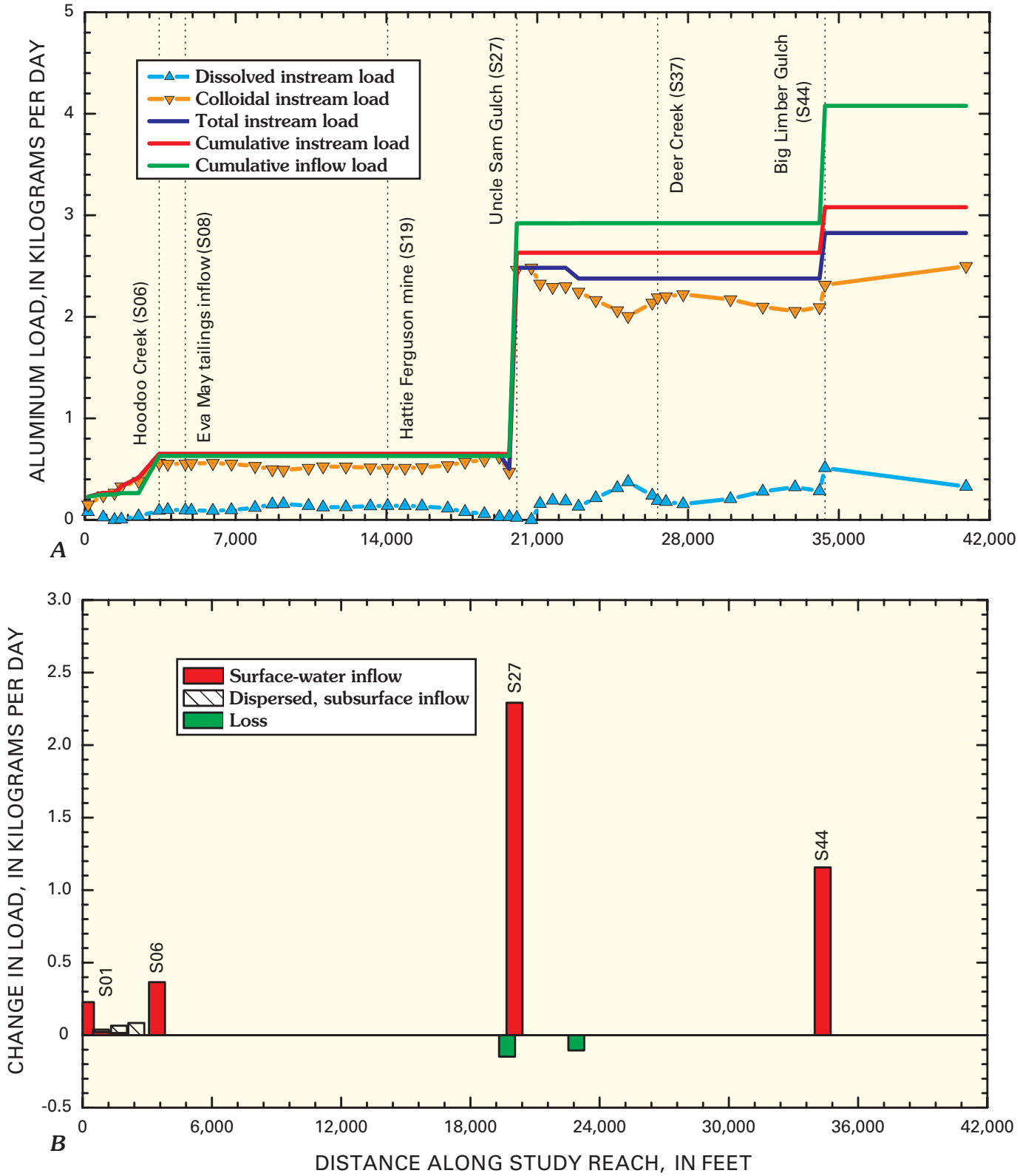

Figure 9. Variation of *A*, aluminum load with distance, and *B*, changes in load for individual stream segments, Cataract Creek, August 1997.

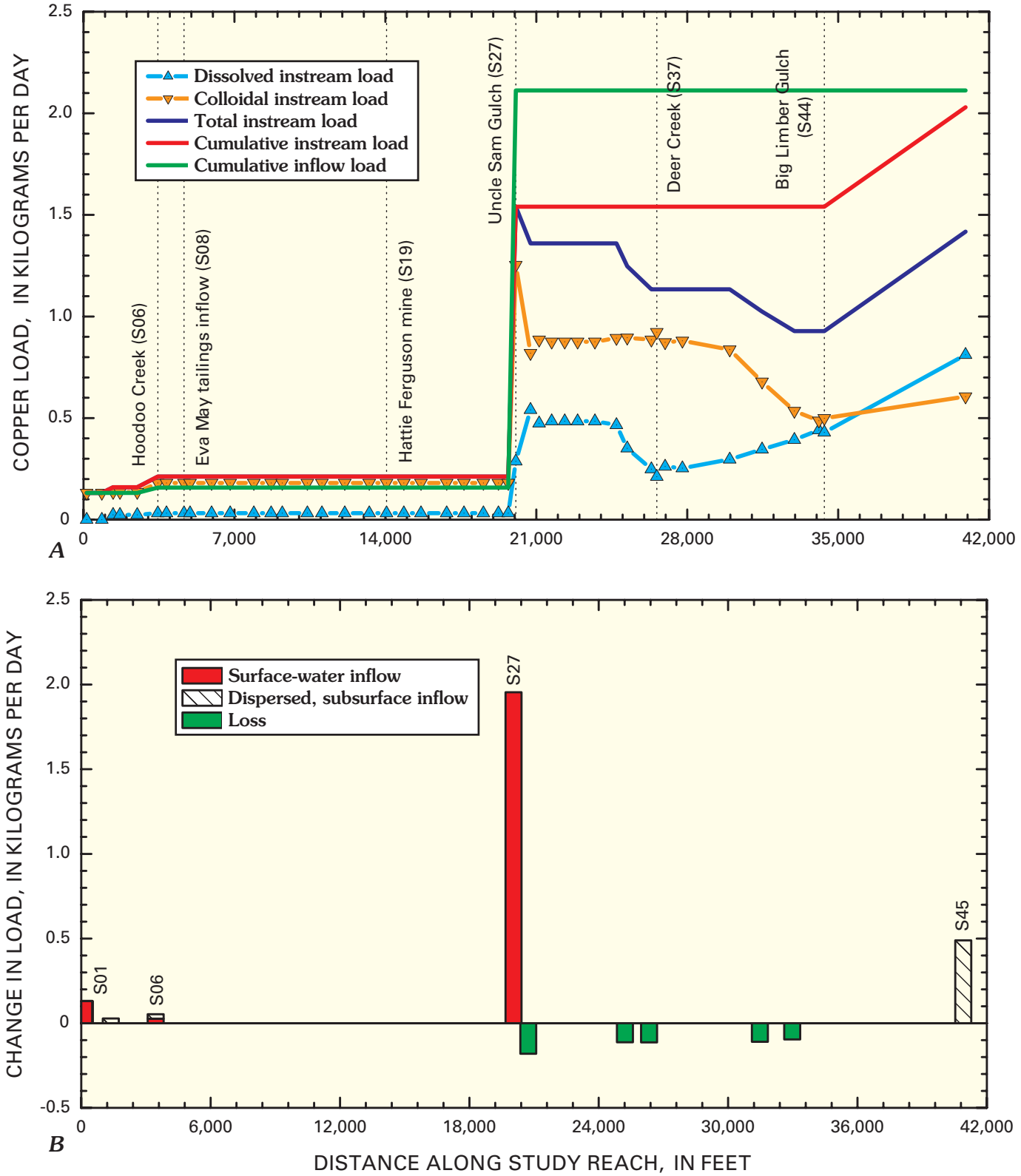

Figure 10. Variation of *A*, copper load with distance, and *B*, changes in load for individual stream segments, Cataract Creek, August 1997.

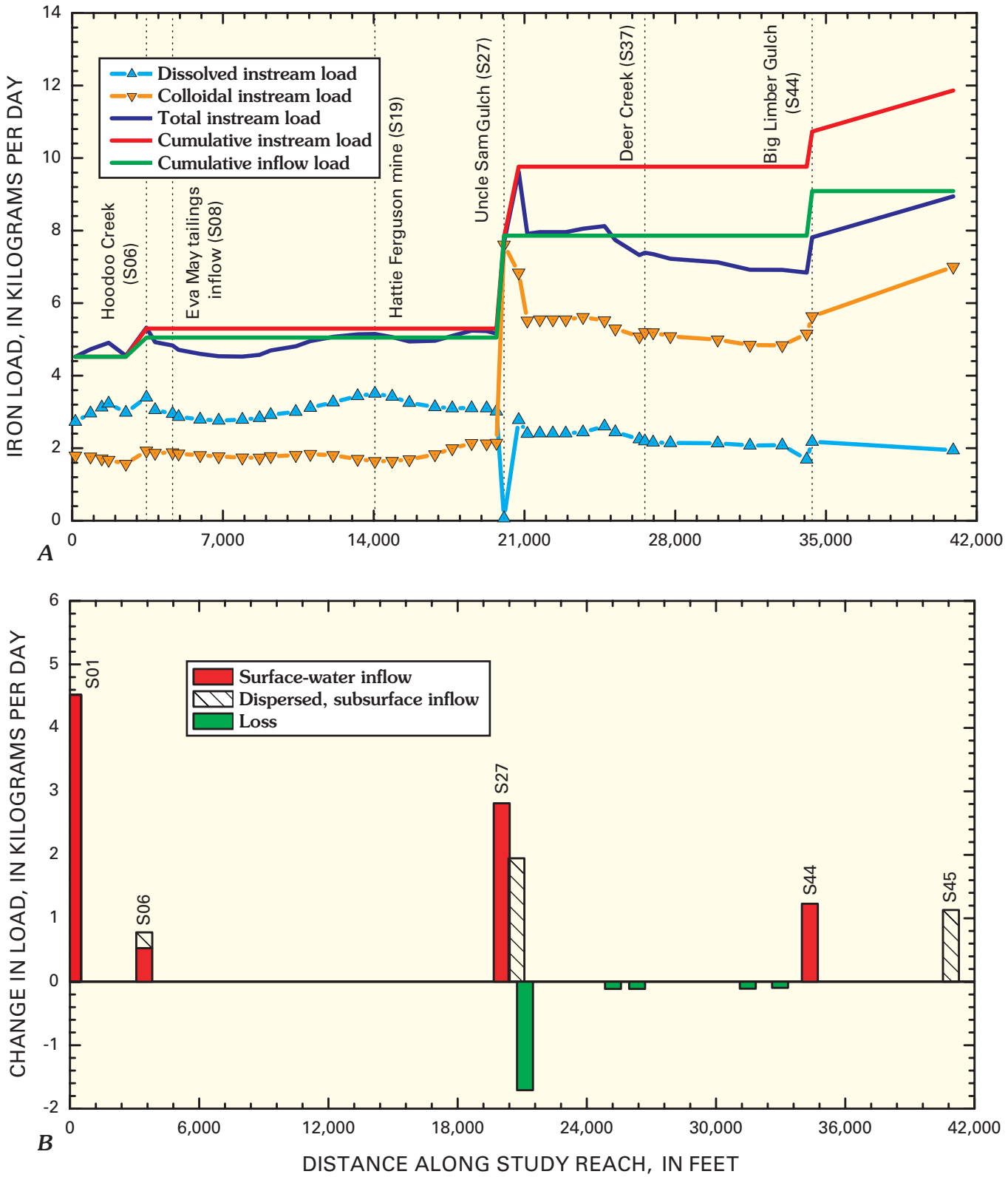

Figure 11. Variation of *A*, iron load with distance, and *B*, changes in load for individual stream segments, Cataract Creek, August 1997.

Loading profiles of aluminum, copper, and iron were mixtures between the sulfate and zinc profiles. Substantial loads of aluminum entered the stream at Uncle Sam Gulch (S27) and segment S44 (fig. 9*A*). Most of the aluminum that entered the stream at Uncle Sam Gulch was transported downstream as colloidal aluminum (figs. 4*A*, 9*A*). Copper loading mostly occurred at Uncle Sam Gulch (segment S27; fig. 10). Downstream from there, the copper was mostly present as colloidal copper, but there appeared to be some transformation between dissolved and colloidal phases in response to downstream inflows. There was a loss of copper load to the streambed between Uncle Sam Gulch and Big Limber Gulch, which, in part, was due to loss in the iron colloids.

The iron profile (fig. 11*A*) indicates a relatively small increase in load from Uncle Sam Gulch (segment S27); the greatest loading was from upstream sources (segment S01). Because iron is reactive in mine-drainage settings, there very likely was attenuation of iron concentrations as water traveled from sources at adits or seeps to the stream (Kimball, Broshears, and others, 1994). Unsampled inflow of iron occurred in segment S28, downstream from Uncle Sam Gulch. This corresponds to unsampled inflow of sulfate (fig. 6*B*), and could indicate weathering of pyrite in tailings piles along the stream in that area. Because most of the iron load was colloidal, losses such as that downstream from segment S28 very likely involved the transformation of dissolved to colloidal iron and then settling of aggregated colloids and (or) entrapment in the algae covering streambed cobbles, as indicated by Church, Unruh, and others (this volume, Chapter D8).

Locations of Major Loading

The cumulative instream load listed in table 3 is the best estimate of the total metal loading along the study reach. Although differences are seen among metal loading profiles, their similarities identify the locations where most of the metal loading occurs. Locations of the major contributions to Cataract Creek are indicated in table 3 by color shading. There were five locations where most of the loading occurred. The greatest loading occurred with the inflow of Uncle Sam Gulch (S27). This inflow accounted for 64 percent of the aluminum load, 66 percent of the copper load, 21 percent of the iron load, 96 percent of the manganese load, 92 percent of the zinc load, and 24 percent of the sulfate load (table 3). Iron (38 percent) and manganese (4 percent) loads were important at the beginning of the study reach (segment S01). The other constituents were also present (table 3). The Eva May tailings (segment S08) contributed to the load of zinc (2 percent). The inflow of Big Limber Gulch (segment S44) accounted for aluminum (14 percent), iron (8 percent), and sulfate (8 percent). Mines and mineralized rock in that drainage could account for these loads (O'Neill and others, this volume, pl. 1; McCafferty and others, this volume). Finally, loads of copper (24 percent), iron (10 percent), and sulfate (10 percent) increased in the large segment represented by the sample at the mouth of Cataract Creek (S45). Little is known about possible sources in this segment.

Unsampled Inflow

The principal locations of unsampled inflow include Uncle Sam Gulch (S17), segment S28 downstream from Uncle Sam Gulch, and segment S45 between Big Limber Gulch and the mouth of Cataract Creek. The unsampled inflow from Uncle Sam Gulch consisted of sulfate (fig. 6*B*) and zinc (fig. 7*B*). Downstream from Uncle Sam Gulch, a substantial tailings pile lies along Cataract Creek in segment S28, and this could be the source of iron and sulfate loading to the stream in that segment. Little is known about the last stream segment, S45, where there was unsampled inflow of copper, iron, and sulfate because there was no access to the stream along that reach.

Attenuation of Load

Along the length of the study reach, substantial attenuation only occurred for copper (30 percent) and iron (25 percent, table 3); most of the constituents were transported to the Boulder River once they entered Cataract Creek. Attenuation of copper and iron occurred downstream from Uncle Sam Gulch (figs. 10*B* and 11*B*), after the load had greatly increased. This was likely a result of the loss of colloidal iron to the streambed through settling of aggregated colloids or through entrapment by algae on the streambed cobbles.

Uncle Sam Gulch Subbasin

Results of the tracer-injection study in Cataract Creek indicated that Uncle Sam Gulch was the principal source of metal loading to the stream. A tracer-injection study was done during low-flow conditions in late August 1998 to investigate the source of metals and the patterns of metal loading.

Study Area and Experimental Design

The study reach began upstream from the Crystal mine, near the headwaters of the stream, and continued to the mouth of Uncle Sam Gulch, where the stream discharges into lower Cataract Creek (fig. 12). Synoptic sampling sites defined 36 stream segments. Stream segment numbers are listed in table 4, but the detailed descriptions of these sites are found in the database (Rich and others, this volume, Chapter G). Fourteen inflows were sampled in 13 of these segments.

A sodium chloride solution of 161,200 mg/L chloride was injected at a rate of 92 mL/min for a 48.7-hour period starting at 16:50 MDT on August 27, 1998. During the course of the injection, difficulties with the pumps complicated the interpretation of the chloride profile downstream from the injection.

Table 3. Change in load for individual stream segments and summary of load calculations, Cataract Creek, August 1997.

[Distance, in feet along the study reach; Al, aluminum; Cu, copper; Fe, iron; Mn; manganese; Zn, zinc; SO_4, sulfate; all values of load are in kilograms per day; percentages are percent of cumulative instream load; color of cell indicates rank of load: red, first; orange, second; yellow, third; green, fourth; blue, fifth; negative values of load indicated in red type with parentheses]

Segment number	Site descriptions	Distance	Al	Cu	Fe	Mn	Zn	SO_4
S01	First site below injection	150	0.227	0.131	4.52	0.116	0.078	67.6
S02	T1 transport site in canyon	850	0.038				(0.038)	3.09
S03	Above right-bank mine dump	1,370		0.028			(0.016)	2.80
S04	Below mine dump at Apollo mine	1,690	0.066					3.53
S05	Above mine dump at Eva May mine	2,490	0.084				0.007	
S06	Below Hoodoo Creek	3,450	0.234	0.053	0.778		0.068	36.3
S07	Above Eva May mine tailings	3,850					0.107	4.87
S08	Adjacent to Eva May tailings pile	4,660					0.386	13.2
S09	T2 transport site below Eva May mine	4,940					0.299	7.25
S10	Below curve with overbank tailings	5,940						
S11	Along bend	6,800						
S12	Below old cabin	7,900						5.89
S13	Below mine dump, at Cataract mine tailings	8,700						6.85
S14	Adjacent to Cataract mine tailings	9,220						6.27
S15	End of large flood plain	10,380						4.92
S16	Adjacent to ponded water on right bank	11,055				(0.081)	0.083	4.82
S17	Above large clear-cut area	12,115					0.132	
S18	Above Lower Hattie Ferguson mine	13,255					0.127	
S19	Below Lower Hattie Ferguson mine	14,055						4.78
S20	Above left-bank inflow	14,855						5.14
S21	Below Upper Hattie Ferguson mine	15,655						6.51
S22	Below inflows, checking water inflow	16,845						12.9
S23	T3 transport site below logging-road	17,645					0.103	10.5
S24	Above biological sampling site	18,545					(0.418)	62.0
S25	Above Morning Glory mine	19,245						
S26	Above Uncle Sam Gulch, below Morning Glory mine	19,700	(0.149)					7.39
S27	Below Uncle Sam Gulch	20,050	1.98	1.33	2.52	2.56	15.6	173
S28	Below cabin and tailings pile on right bank	20,730		(0.180)	1.95			17.0
S29	Check for reaction below Uncle Sam Gulch	21,130			(1.71)			
S30	Along cascades below small mine dump	21,715						
S31	Above rock wall	22,315						
S32	Below small inflow	22,915	(0.105)			(0.076)	(0.342)	(39.4)
S33	At old lean-to	23,715						11.8
S34	T4 transport site above canyon	24,715						
S35	Above start of canyon	25,215		(0.113)			(1.24)	20.3
S36	Above Deer Creek	26,335		(0.113)				30.7
S37	Below Deer Creek	26,590						19.3
S38	Below large concrete bridge	26,970						
S39	Below second wooden bridge	27,775						
S40	Below old cabin on right bank	29,970						15.6
S41	Along cascade reach	31,470		(0.110)				30.4
S42	Wide section of canyon	32,970		(0.096)				
S43	T5 transport site above Big Limber Gulch	34,105						
S44	Below Big Limber Gulch	34,355	0.448		0.971			54.3
S45	Cataract Creek at mouth	40,905		0.489	1.13			72.7
	Cumulative instream load		3.08	2.03	11.9	2.68	17.0	722
	Cumulative inflow load		4.08	2.11	9.09	2.75	14.9	540
	Percent inflow		132	104	77	103	88	75
	Unsampled inflow		< 0	< 0	2.77	< 0	2.09	182
	Percent unsampled		< 1	< 1	23	< 1	12	25
	Attenuation		0.254	0.612	2.92	0.157	2.05	39.4
	Percent attenuation		8	30	25	6	12	5

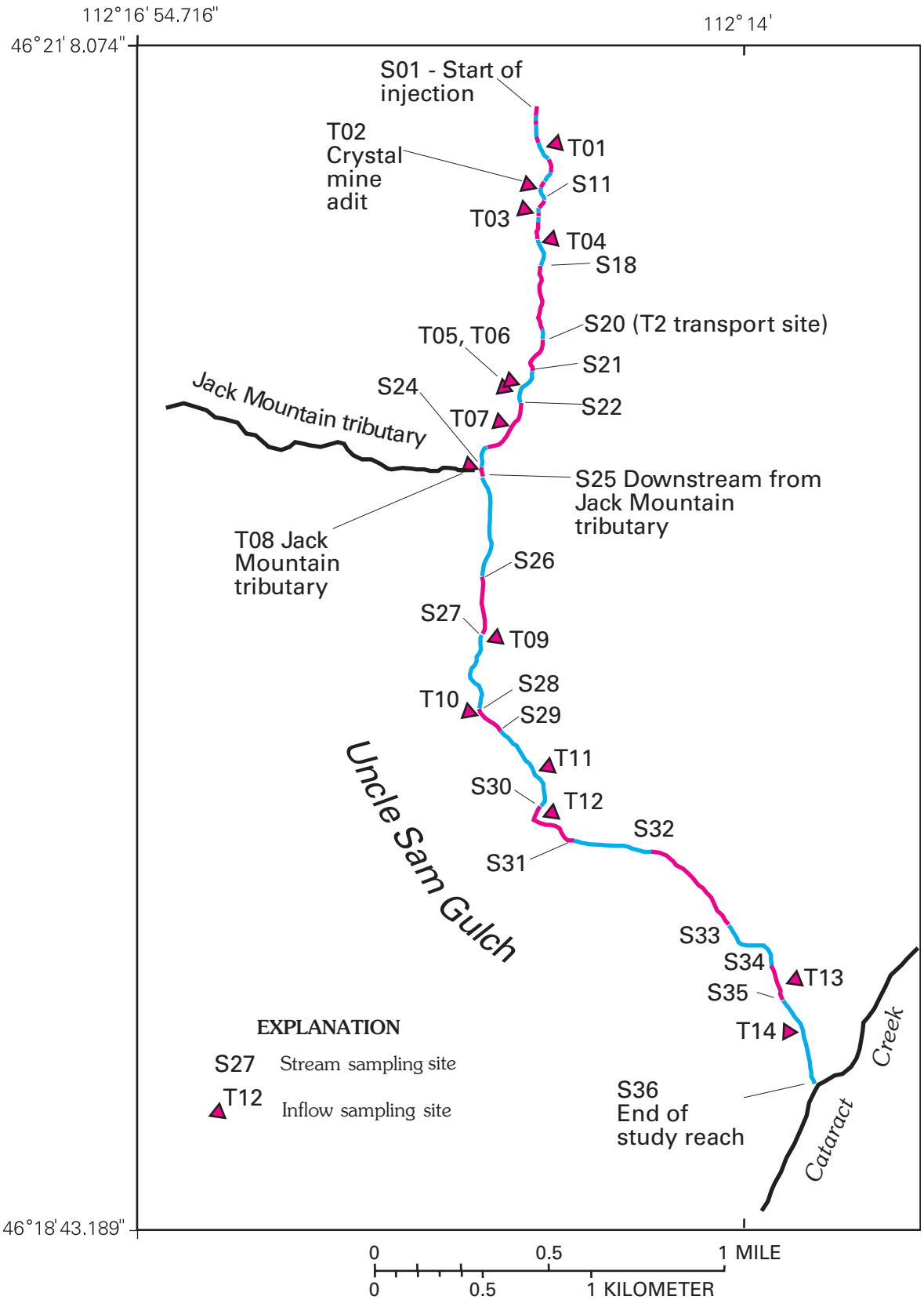

Figure 12. Location of stream segments (indicated by alternating colors) and inflows for synoptic sampling, Uncle Sam Gulch, August 1998.

Table 4. Segment number, source, distance along study reach, site description, and field data for water from synoptic sampling sites, Uncle Sam Gulch, August 29, 1998.

[Dist, distance, in feet along the study reach; source: S, stream; LBI, left bank inflow, RBI, right bank inflow; pH, in standard units; Ksc, specific conductance, in microsiemens per centimeter; Q, discharge, in liters per second; Cl, chloride, in milligrams per liter]

Segment number	Dist	Source	Description	Site identifier	pH	Ksc	Q	Cl
S01	0	S	Upstream from injection	SAM0	7.18	45	0.07	4.00
S02	278	S	First site below injection	SAM278	7.26	45	0.07	4.29
S03	305	S	Stream site, no description	SAM305	7.45	220	0.09	50.1
S04	592	S	Channel converges	SAM592	7.47	1,045	0.10	279
S05	702	S	Below several small tailings piles	SAM702	7.43	2,340	0.27	650
S06	780	S	T1 transport site	SAM780	7.24	2,210	0.28	606
T01	792	LBI	Left bank tributary from old prospect	SAM792	7.04	78	0.03	3.94
S07	957	S	At steep waste rock pile	SAM957	7.29	1,838	0.31	509
S08	1,152	S	Below deep cuts eroding banks	SAM1152	7.29	1,535	0.28	390
S09	1,314	S	At toe of waste rock pile	SAM1314	7.13	1,356	0.37	345
S10	1,399	S	Above Crystal adit discharge	SAM1399	7.05	1,302	0.43	325
T02	1,413	RBI	Right bank Crystal adit inflow	SAM1413	3.21	1,164	2.27	4.84
S11	1,461	S	Below Crystal mine adit	SAM1461	3.27	1,195	2.70	50.7
S12	1,560	S	Below Crystal waste rock pile	SAM1560	3.25	1,204	2.71	54.6
S13	1,661	S	At edge of treatment pond	SAM1661	3.23	1,210	2.71	51.6
S14	1,764	S	At treatment pond pipe	SAM1764	3.20	1,195	2.74	53.7
T03	1,829	RBI	Right bank inflow from waste rock	SAM1829	2.83	1,563	0.04	7.50
S15	1,866	S	Below obvious mining disturbance	SAM1866	3.19	1,205	2.77	54.4
S16	2,026	S	Below mining disturbance (2)	SAM2026	3.17	1,189	2.81	52.4
S17	2,273	S	Below mining disturbance (3)	SAM2273	3.14	1,182	2.89	51.2
T04	2,286	LBI	Left bank tributary, low conductance	SAM2286	7.26	56	0.25	3.41
S18	2,727	S	Below left bank inflow	SAM2727	3.22	1,065	3.14	40.9
S19	3,170	S	Stream near road	SAM3170	3.30	878	3.90	25.0
S20	3,777	S	T2 transport site—edge of clear cut	SAM3777	3.32	774	4.48	20.0
S21	4,365	S	Stream at lower conductance	SAM4365	3.44	732	4.71	20.2
T05	4,650	RBI	Right bank tributary	SAM4650	6.97	80	0.19	5.40
T06	4,763	RBI	Right bank seep with iron precipitate	SAM4763	6.71	123	0.37	6.66
S22	4,915	S	At boggy area along right bank	SAM4915	3.48	686	5.28	21.3
T07	5,264	RBI	Right bank tributary near road	SAM5264	6.83	139	0.47	6.80
S23	5,830	S	T3 transport site	SAM5830	3.53	642	5.75	24.1
S24	6,068	S	Upstream from Jack Mountain tributary	SAM6068	3.58	621	5.65	22.1
T08	6,088	RBI	Jack Mountain tributary (right bank)	SAM6088	7.17	63	10.12	4.21
S25	6,213	S	Below Jack Mountain tributary	SAM6213	4.81	243	15.76	10.1
S26	7,417	S	At heavy vegetation, low gradient	SAM7417	4.91	229	17.14	10.5
S27	8,270	S	At small clearing near road	SAM8270	5.13	222	17.41	9.86
T09	8,374	LBI	Left bank inflow from marshy area	SAM8374	6.95	116	1.22	4.85
S28	9,200	S	T4-Upstream from old cabin	SAM9200	6.62	211	18.63	5.05
T10	9,400	RBI	Right bank tributary by cabin	SAM9400	7.61	91	1.60	6.22
S29	9,588	S	Near road below cabin inflow	SAM9588	6.74	201	20.23	8.34
T11	10,289	LBI	Left bank tributary	SAM10289	7.24	147	0.77	5.56
S30	10,856	S	Split in stream	SAM10856	7.14	194	20.99	8.00
T12	11,006	LBI	Left bank tributary	SAM11006	7.50	114	3.43	5.82
S31	11,724	S	Stream below dilution inflow	SAM11724	6.89	183	24.42	7.54
S32	12,795	S	Below tailings	SAM12795	7.28	181	25.51	7.38
S33	14,540	S	T5 transport site—upstream end of culvert	SAM14540	7.29	177	26.42	7.37
S34	15,314	S	Below power line crossing	SAM15314	7.32	176	27.08	7.22
T13	15,671	LBI	Left bank tributary	SAM15671	7.84	165	5.58	5.44
S35	15,971	S	Below tributary near road	SAM15971	7.36	184	32.65	6.93
T14	16,471	RBI	Right bank tributary draining wet area	SAM16471	7.74	217	4.14	0.94
S36	17,095	S	Uncle Sam at mouth	SAM17095	6.62	180	36.80	6.79

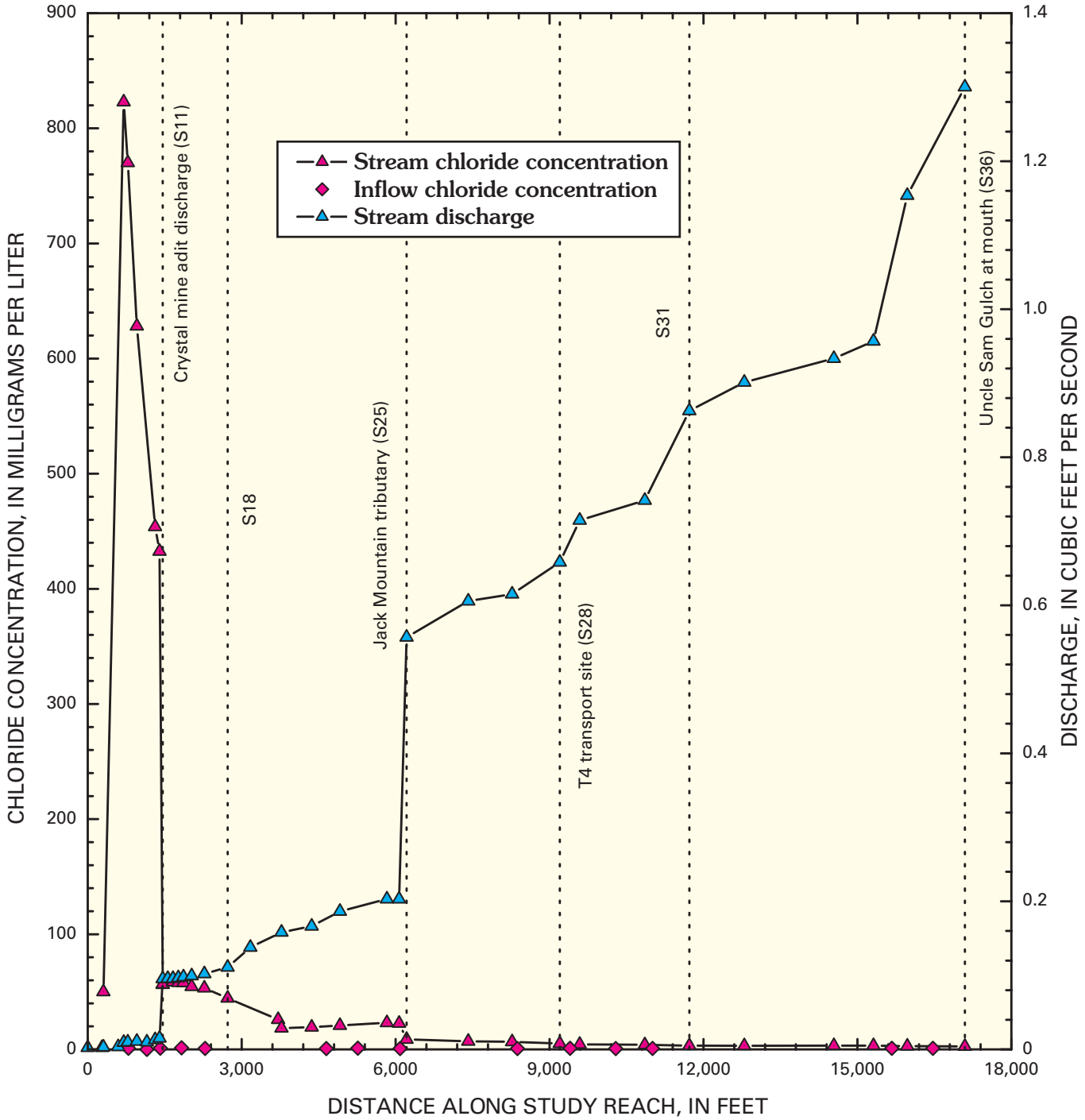

Figure 13. Variation of chloride concentration and calculated discharge with distance, Uncle Sam Gulch, August 1998.

Although the decrease of chloride concentration appeared to be systematic, a "wave" of chloride moved through the study reach during the synoptic sampling, indicated by the increase of chloride at the first few sampling sites (fig. 13). Because of these complications, chloride and sulfate ratios around inflows, along with velocity-area discharge measurements, were used to calculate the increase of flow due to individual inflows. The resulting calculated discharge ranged from 0.004 to 1.3 ft^3/s (fig. 13). Most of this increase was from Jack Mountain tributary (T8). Discharge increased only 0.07 ft^3/s in those segments that had no sampled inflow, only 10 percent of the total increase, and so the explicit amount of ground-water inflow was small.

Chemical Characterization of Synoptic Samples

Changes in stream-water chemistry along Uncle Sam Gulch were distinct and occurred over short distances in response to acidic and neutral inflows. The abrupt changes of pH along the study reach indicate where the changes occurred (fig. 14). Upstream from the Crystal mine, pH was greater than 7.0, sulfate concentration was less than 25 mg/L, and metal concentrations were relatively low (fig. 15). With the addition of the adit drainage (T2), and the spring from the mine waste-rock pile (T3), pH dropped substantially, to less than 3.5, and sulfate increased to greater than 550 mg/L. Metal concentrations increased to greater than 10,000 µg/L aluminum, 10,000 µg/L copper, 40,000 µg/L iron, and 60,000 µg/L zinc (fig. 15). Baseline sediment chemistry also indicates the impact from mining (Church, Unruh, and others, this volume, figs. 4–10). Inflow from Jack Mountain tributary increased the pH to 4.81 in segment S25, and pH continued to increase to 5.13 by the end of segment S27. Farther downstream, after additional neutral inflows at T9 and T10, the pH increased to 6.74 at segment S29. Within the reach of increasing pH, from segment S25 to S27, dissolved concentrations of the metals decreased and colloidal concentrations increased. Iron colloids, however, started forming upstream from the inflow of Jack Mountain tributary; the total-recoverable iron was greater than the two filtered concentrations (fig. 15*C*). At the higher pH there was a steady formation of aluminum and iron colloids as water moved downstream (fig. 15*A*, *C*). As the colloids formed, dissolved copper concentrations decreased and most of the copper became associated with the colloidal phase (fig. 15*B*). Concentrations of dissolved zinc exceeded chronic water-quality criteria at all sites downstream from the Crystal mine adit, as noted by Nimick and Cleasby (this volume, Chapter D5).

Table 5. Average chemical composition of groups from principal components analysis of synoptic samples, Uncle Sam Gulch, August 1998.

[LD, less than detection limit; all values in milligrams per liter, except pH, which is in standard units]

Number of samples or solute	Group 1 Stream from S1 to S3, upstream from acid inflows	Group 1 Unaffected inflows	Group 2 Stream site S4, unaffected by acid inflows	Group 2 Inflows unaffected by mining	Group 3 Stream from S5 to S10, affected bull-dozed area	Group 4 Stream from S11 to S18, affected by Crystal mine adit	Group 4 Most acidic inflow, including Crystal mine adit	Group 5 Stream between S19 and S24	Group 6 Stream between S25 and S31	Group 7 Stream between S32 and S36
Number of samples	3	2	1	10	6	6	2	6	7	5
pH	7.30	7.15	7.47	7.26	7.24	3.21	3.02	3.44	6.03	7.17
Calcium	5.44	9.29	9.84	17.3	23.6	54.3	62.0	35.2	17.6	18.2
Magnesium	.957	1.47	1.67	3.18	3.84	15.5	19.7	9.43	4.24	4.07
Sulfate	6.11	9.31	10.0	15.9	10.1	507	706	293	78.4	53.1
Aluminum	.121	.032	.045	.017	.037	12.4	17.3	7.86	1.83	.683
Cadmium	.002	.002	.003	.004	.006	.771	.891	.453	.119	.072
Copper	.007	.008	.015	.027	.023	12.4	15.6	7.36	1.93	.731
Iron	1.11	.242	.499	.139	.232	36.0	43.0	10.5	1.03	.284
Manganese	.067	.069	.084	.409	.075	11.9	16.4	7.19	1.87	.949
Nickel	.001	LD	.001	LD	.001	.054	.065	.030	.008	.006
Lead	.009	LD	.001	LD	.001	.243	.134	.188	.042	.001
Strontium	.066	.070	.121	.131	.271	.267	.270	.212	.126	.134
Zinc	.047	.085	.121	.157	.232	56.7	71.4	33.7	8.92	5.60

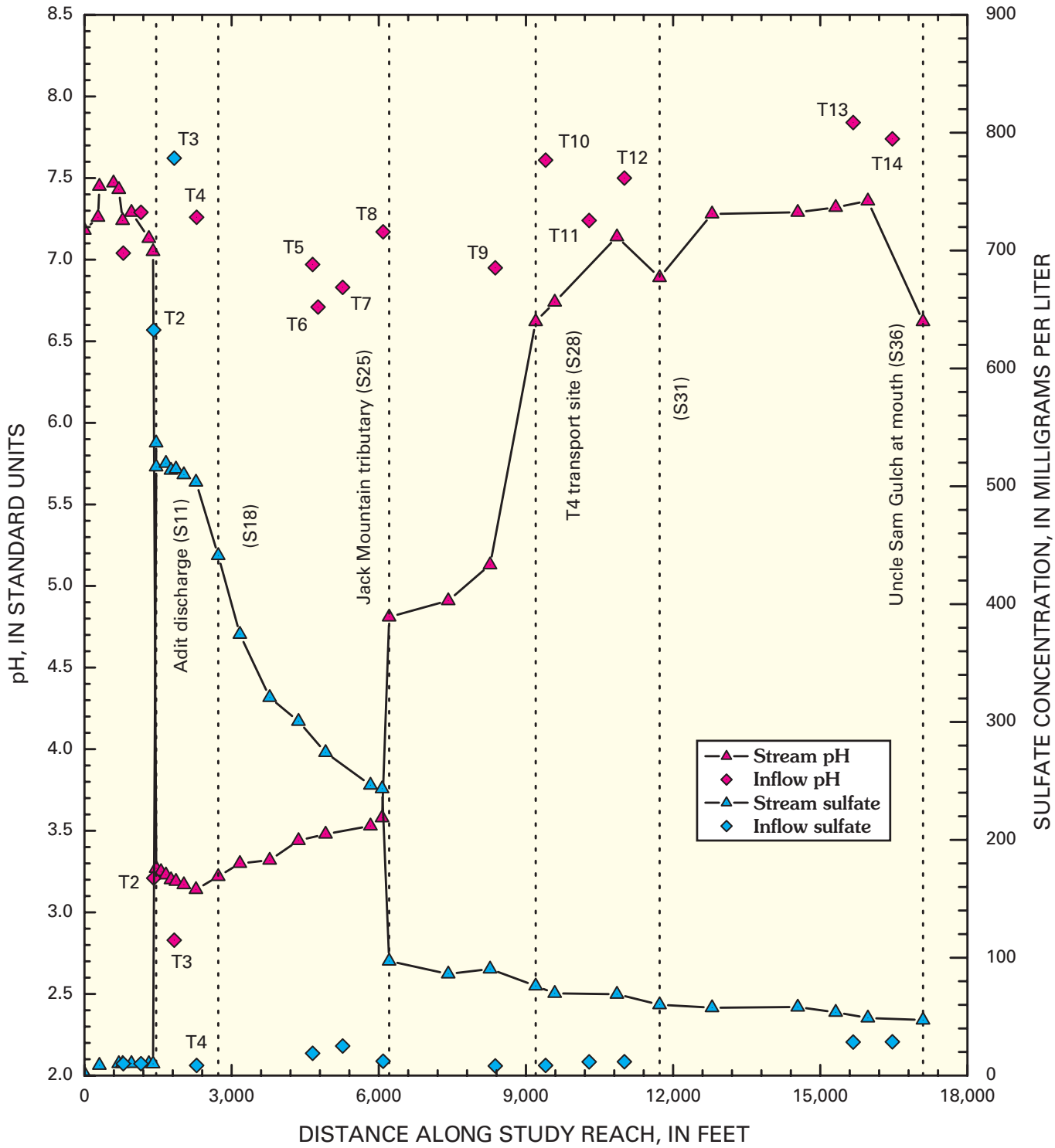

Figure 14. Variation of pH and sulfate with distance, Uncle Sam Gulch, August 1998.

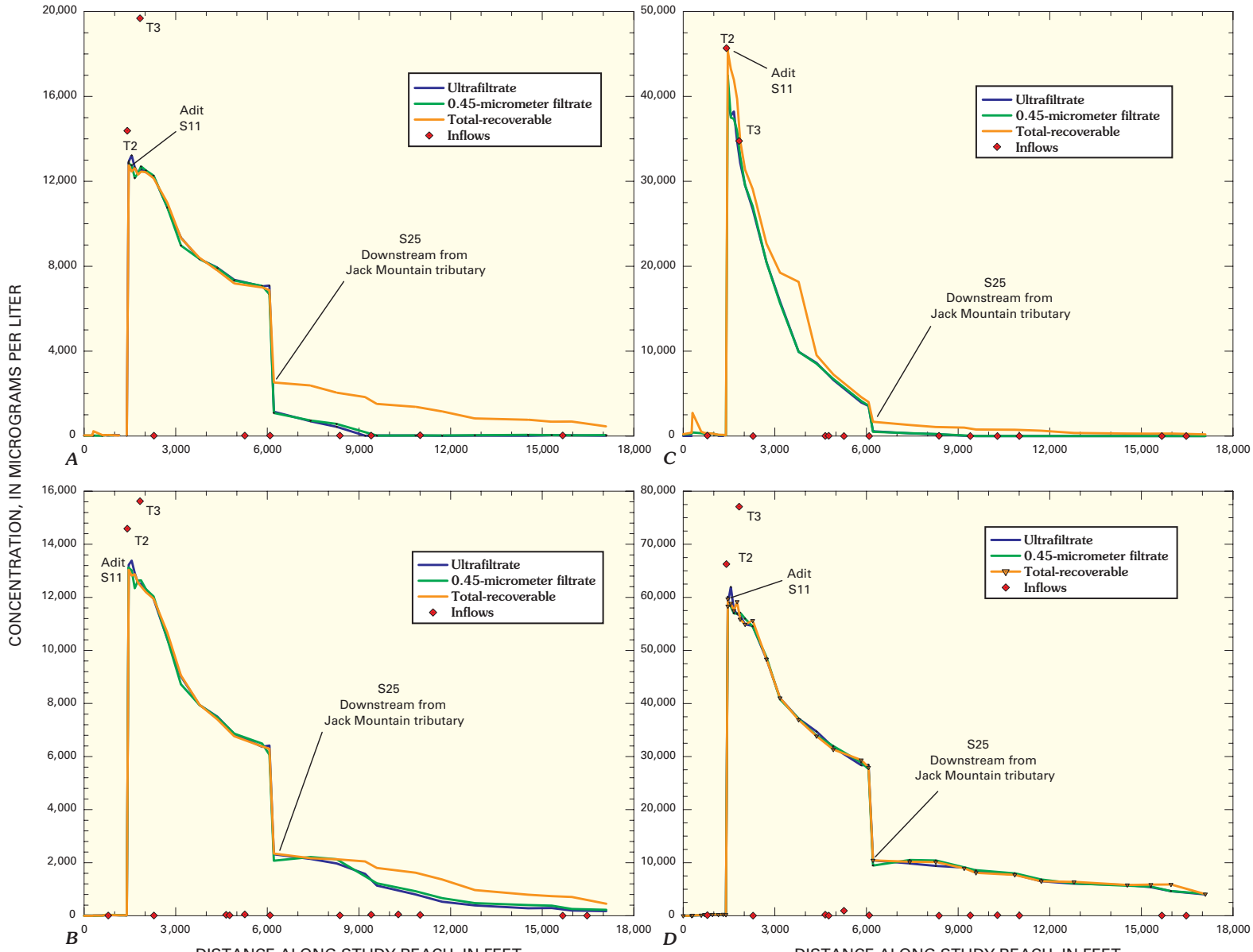

Figure 15. Variation of *A*, aluminum, *B*, copper, *C*, iron, and *D*, zinc concentrations with distance, Uncle Sam Gulch, August 1998.

These substantial changes in stream chemistry and the variability of inflows resulted in a classification of seven groups of samples by PCA (fig. 16). Six of the groups represent variations in stream-water chemistry, with associated inflows, and one represents inflows unaffected by mining or alteration (table 5). The biplot provides a reasonable interpretation of the chemical variation among synoptic samples from Uncle Sam Gulch. Two sets of stream sites (groups 1 and 3) are unaffected by discharge from the Crystal mine adit and plot to the right on the biplot (fig. 16). All the vectors indicate increasing concentrations to the right; the vectors for metals from the mine are very similar and so they are only identified as a group. Samples to the left of the biplot are opposite all the vectors, and have the lowest concentrations. Group 1 contains two inflow samples (T01 and T04) that resulted from the same weathering reactions that produced the stream-water chemistry upstream from segment S04. An extensive amount of disturbance resulted from bulldozing of soil up the mountain on the right bank of the stream. Inflow water that drained the disturbed area contributed high calcium, sulfate, and some zinc (group 3). With the inflow of adit discharge and water from the waste-rock pile (inflows T02 and T03), the chemistry shifted to reflect the acidic, metal-rich character of those inflows (group 4), far to the right of the biplot. Variations among stream samples in groups 5, 6, and 7 represent dilution by the non-mining inflows as water moved downstream. With greater dilution, the chemical character of the stream water becomes increasingly more like the inflows of group 2; samples plot progressively to the left downstream. Thus, in groups 5, 6, and 7 segment numbers increase from right to left, indicating a sequential dilution. The large jump from group 5 to 6 results from the inflow of Jack Mountain tributary (T08), which is one of the group 2 inflows (fig. 16).

Load Profiles

Colloids were responsible for much of the metal transport in Uncle Sam Gulch (fig. 15). Load profiles reflect dynamic changes between dissolved and colloidal phases along the study reach (figs. 17–25). A summary of load calculations for each solute is listed in table 6. A distinction is evident between the loading profile of strontium and those of the other metals. Although the Crystal mine adit in stream segment S11 contributed a substantial load of strontium, it was not the largest loading among the stream segments (fig. 17). Similar to the strontium profile in Cataract Creek, the profile in Uncle Sam Gulch most likely represents weathering from non-mined sources. However, all the metals and sulfate had similar loading profiles in segment S01. Downstream from the Crystal mine adit, however, individual profiles of metal loading differed because of the conservative or reactive nature of the different metals.

The pattern of strontium loading indicated more segments contributing to the load than most other constituents (fig. 17; table 6). Although drainage from the Crystal mine adit in segment S11 contributes a substantial strontium load, other segments were equally important. Unlike the sulfate loading in Cataract Creek, sulfate loading in Uncle Sam Gulch was derived substantially from one source, the Crystal mine adit in segment S11 (fig. 18). Other locations of sulfate loading throughout the watershed were minor (fig. 18*B*). A small amount of unsampled inflow occurred in segments S19, S20, and S26, but most of the sulfate loading was accounted for by the sampled inflows. One similarity between profiles of sulfate and strontium was the increase in load in the last two stream segments of the study reach (segments S35 and S36). The source of these loads may be a large fault that intersects the stream in segment S35 (O'Neill and others, this volume, pl. 1). Some of the metal loads also increased in segment S35, near the end of the study reach.

Downstream from the inflow of the Crystal mine adit, cadmium, manganese, nickel, and zinc were mostly conservative. These metals had fewer sources than strontium and sulfate. The principal source of cadmium load was the inflow from the Crystal mine adit (fig. 19). At segment S35, near the confluence with Cataract Creek, there was a substantial increase in cadmium load, which was all in the colloidal phase. Profiles of manganese (fig. 20) and zinc (fig. 21) load were similar to that of cadmium. The principal source of loading for both metals was inflow from the Crystal mine adit (T02, segment S11). Manganese load increased slightly with the inflow of Jack Mountain tributary. Manganese load decreased downstream from segment S30, but zinc load did not. Zinc had unsampled inflow at segment S19 and segment S26, one segment downstream from Jack Mountain tributary. The instream load of both metals was substantial at the confluence with Cataract Creek, which is consistent with the contribution of Uncle Sam Gulch on the loads in Cataract Creek (figs. 7 and 8).

Other metals were reactive downstream from the Crystal mine adit (S11). Iron was the most reactive (fig. 22); aluminum (fig. 23), copper (fig. 24), and lead (fig. 25) were reactive downstream from the inflow of Jack Mountain tributary (S25). The adit of the Crystal mine was essentially the only measurable source of iron load along the study reach; however, sources downstream from the adit could have been masked by a net negative change in iron load within individual stream segments due to loss from the water column (fig. 22). Downstream from the adit inflow the profile of iron load differed from profiles of the other solutes because of a continuous decrease in total iron load. Upstream from Jack Mountain tributary, the iron load was mostly in the dissolved phase and decreased by about 80 percent from segment S11 to segment S24. Downstream from Jack Mountain tributary, there was essentially a complete transformation of iron from the dissolved to the colloidal phase, and the colloidal phase was dominant all the way to the confluence with Cataract Creek. Downstream from Jack Mountain tributary, ferrihydrite is probably the iron phase being precipitated at the higher pH (Bigham and Nordstrom, 2000). Loss of iron load along the

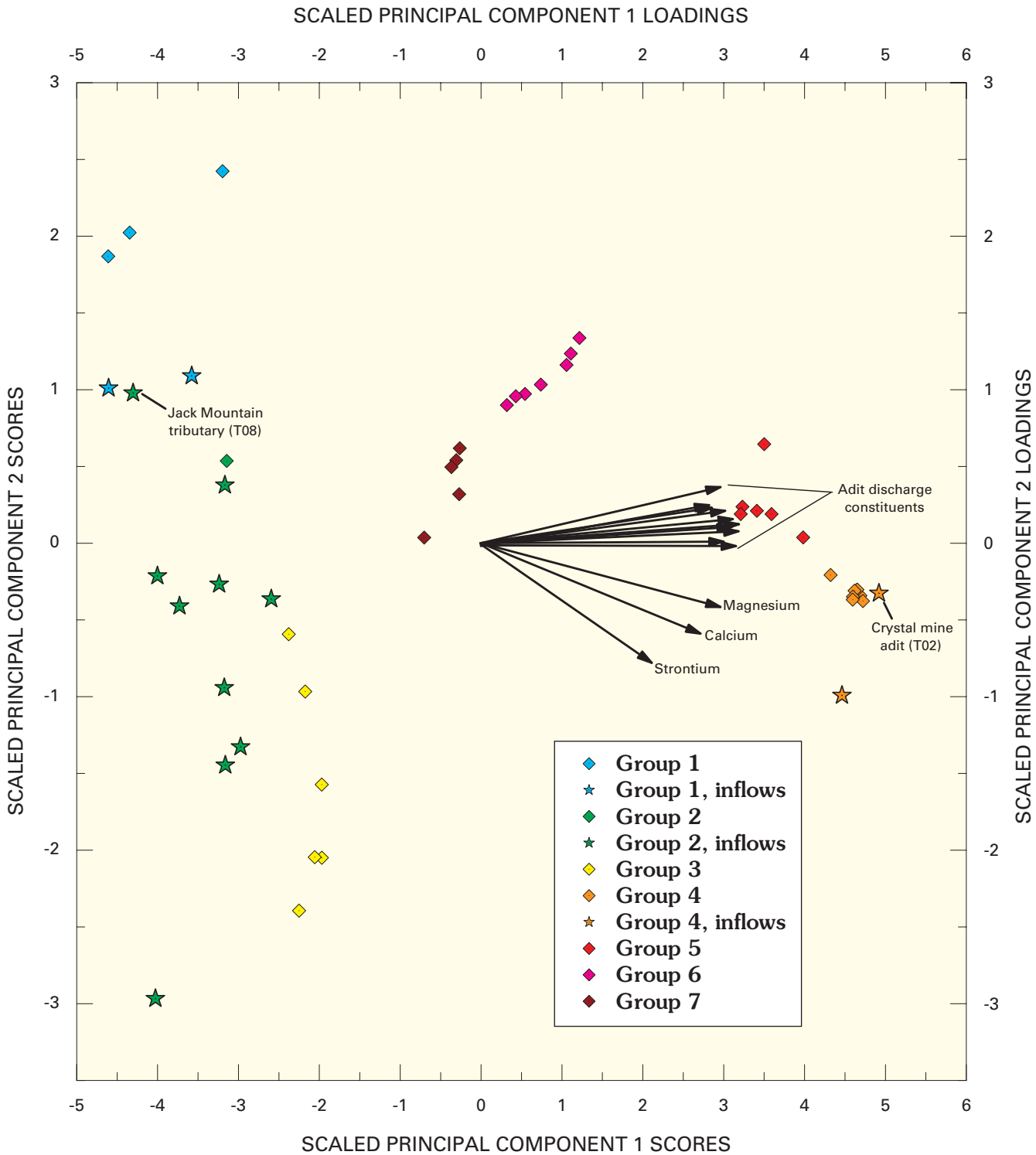

Figure 16. Biplot of principal component scores for synoptic samples and loadings for chemical constituents, Uncle Sam Gulch, August 1998.

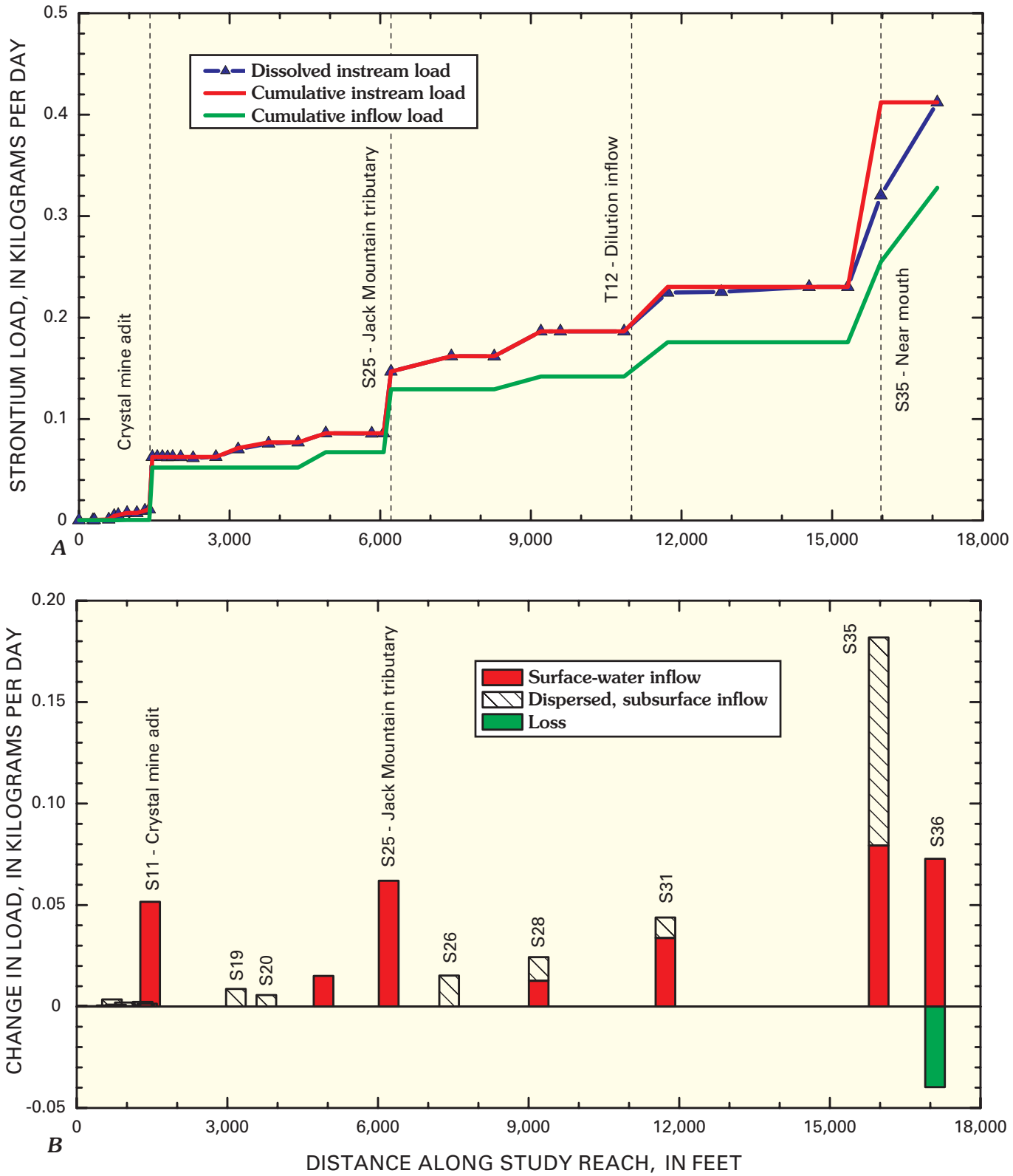

Figure 17. Variation of *A*, strontium load with distance, and *B*, changes in load for individual stream segments, Uncle Sam Gulch, August 1998.

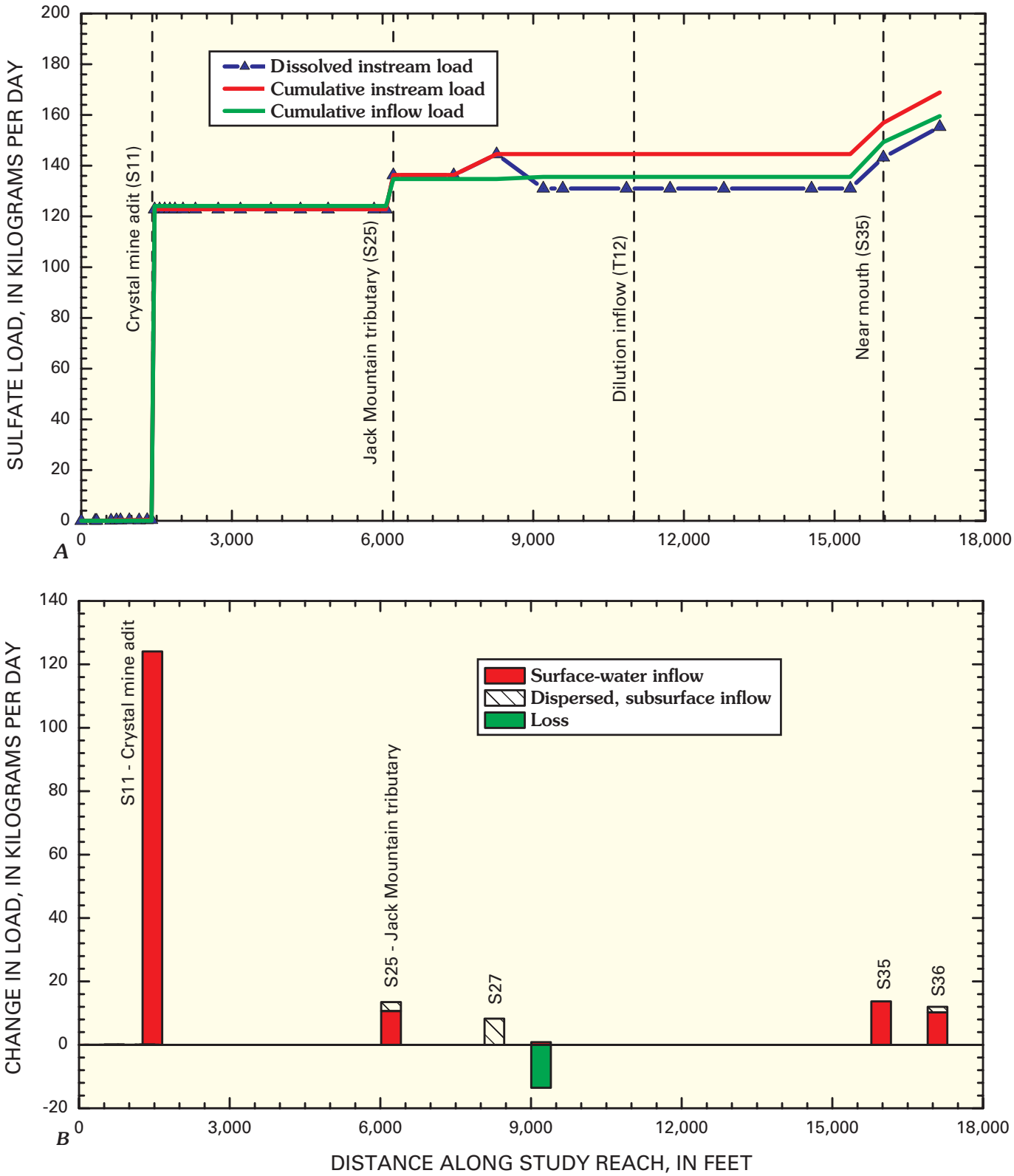

Figure 18. Variation of *A*, sulfate load with distance, and *B*, changes in load for individual stream segments, Uncle Sam Gulch, August 1998.

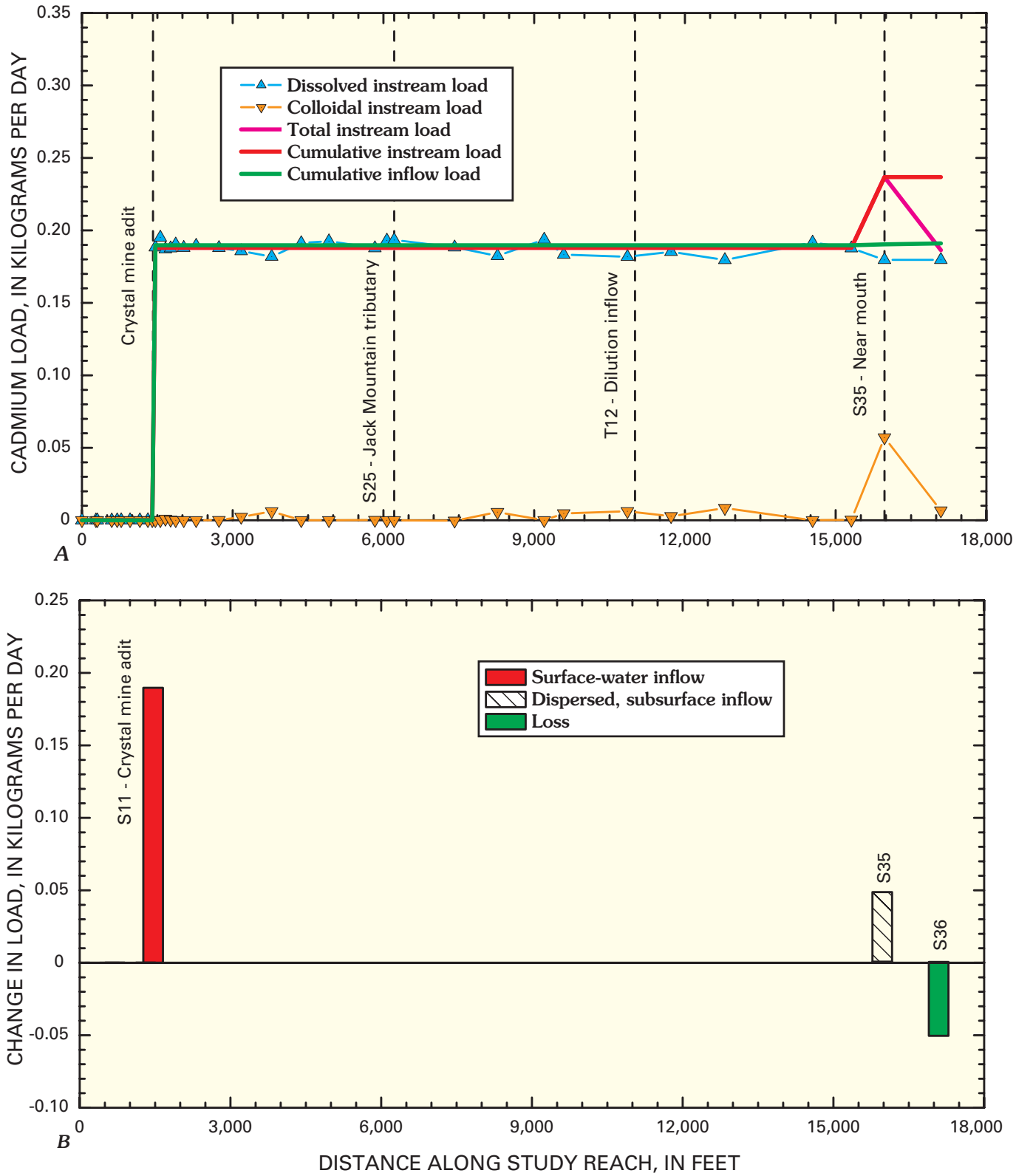

Figure 19. Variation of *A*, cadmium load with distance, and *B*, changes in load for individual stream segments, Uncle Sam Gulch, August 1998.

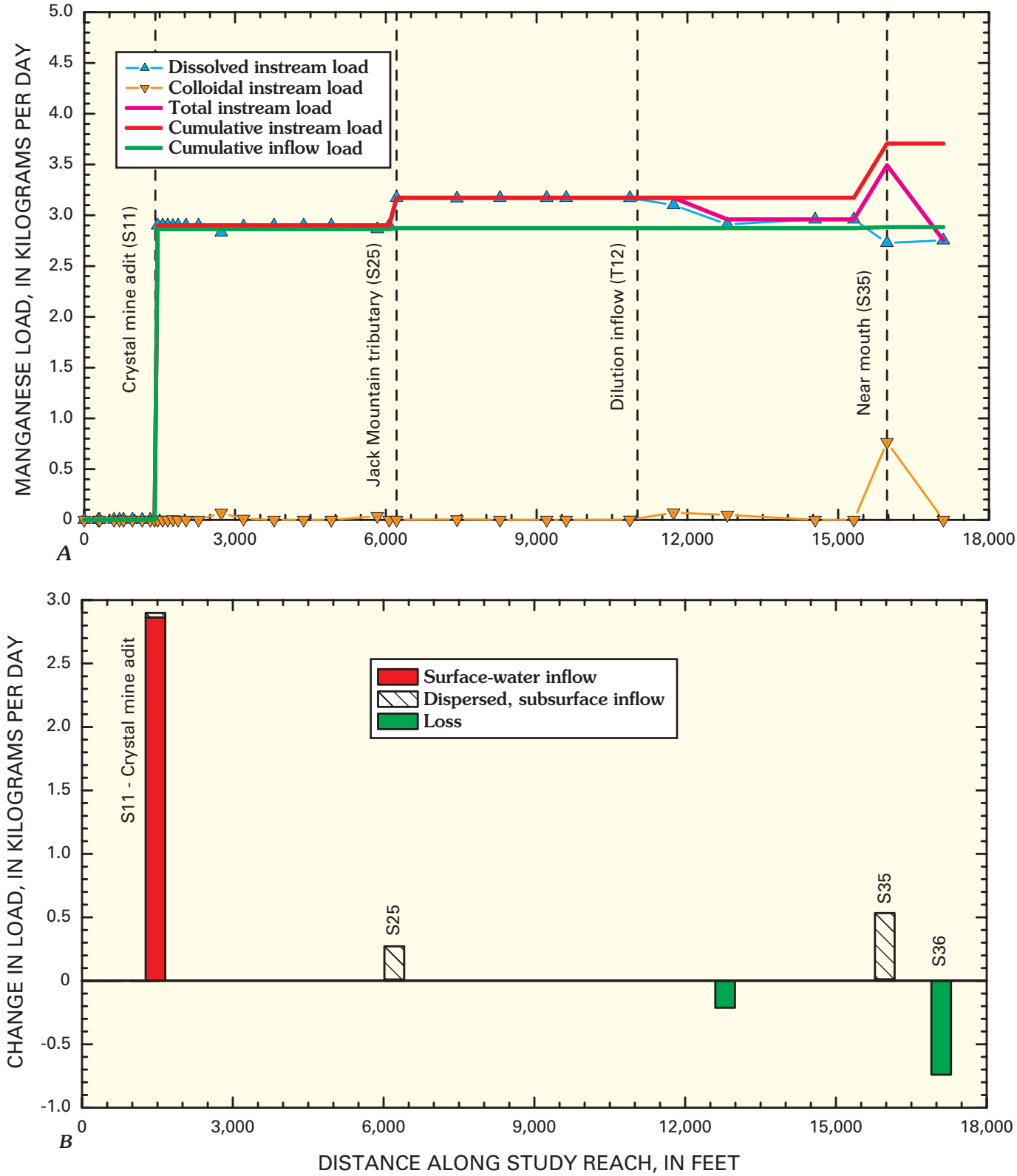

Figure 20. Variation of *A*, manganese load with distance, and *B*, changes in load for individual stream segments, Uncle Sam Gulch, August 1998.

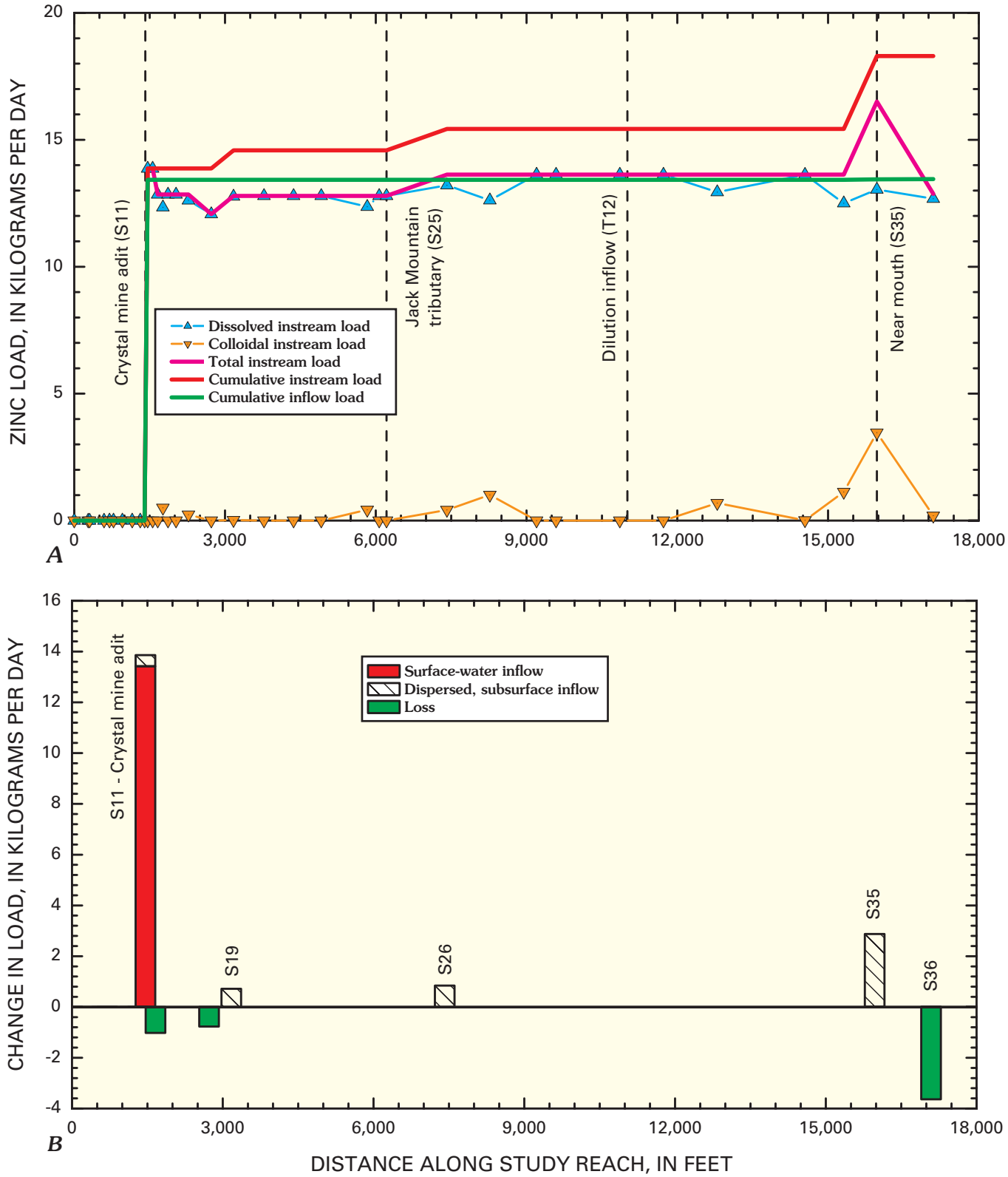

Figure 21. Variation of *A*, zinc load with distance, and *B*, changes in load for individual stream segments, Uncle Sam Gulch, August 1998.

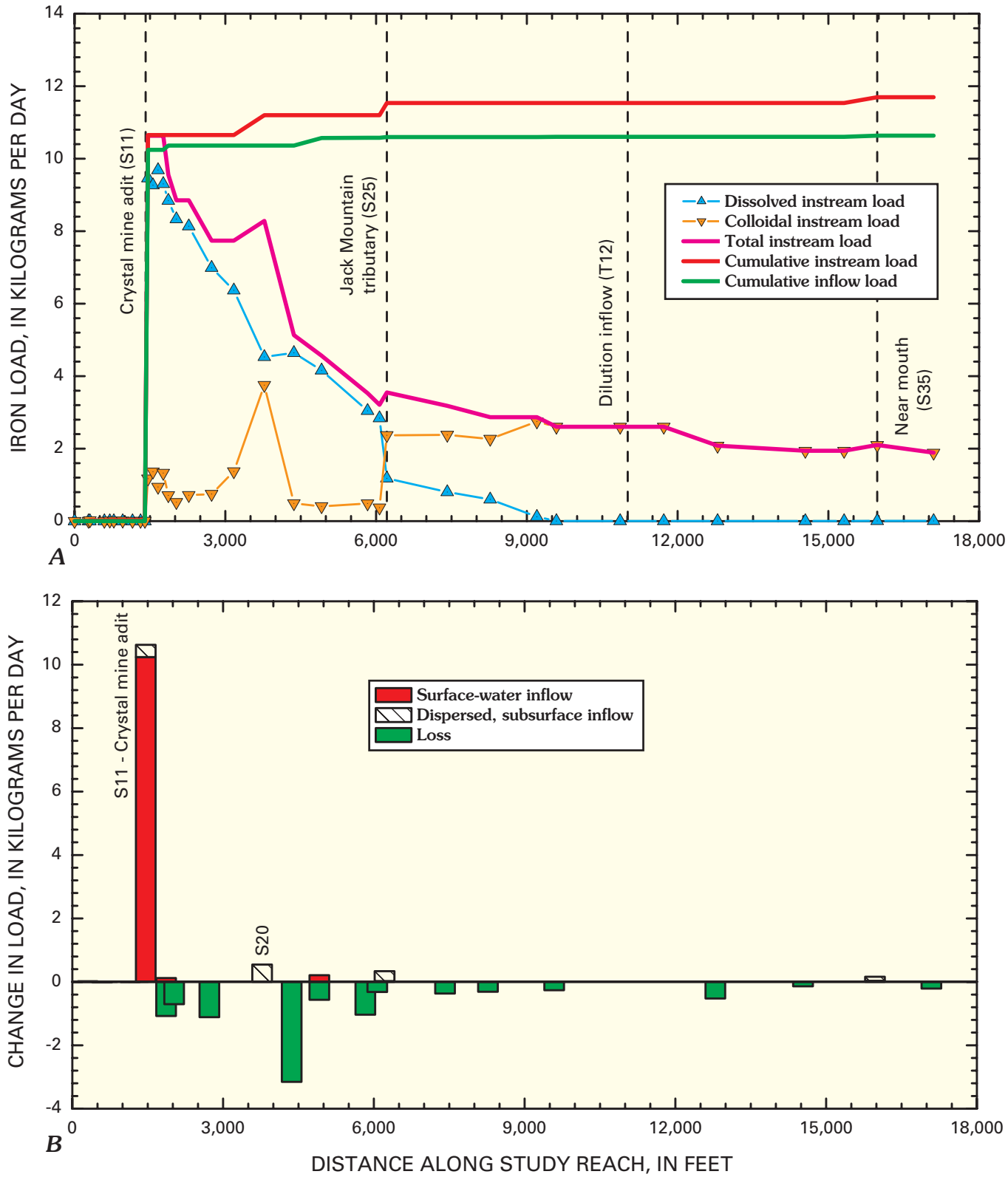

Figure 22. Variation of *A*, iron load with distance, and *B*, changes in load for individual stream segments, Uncle Sam Gulch, August 1998.

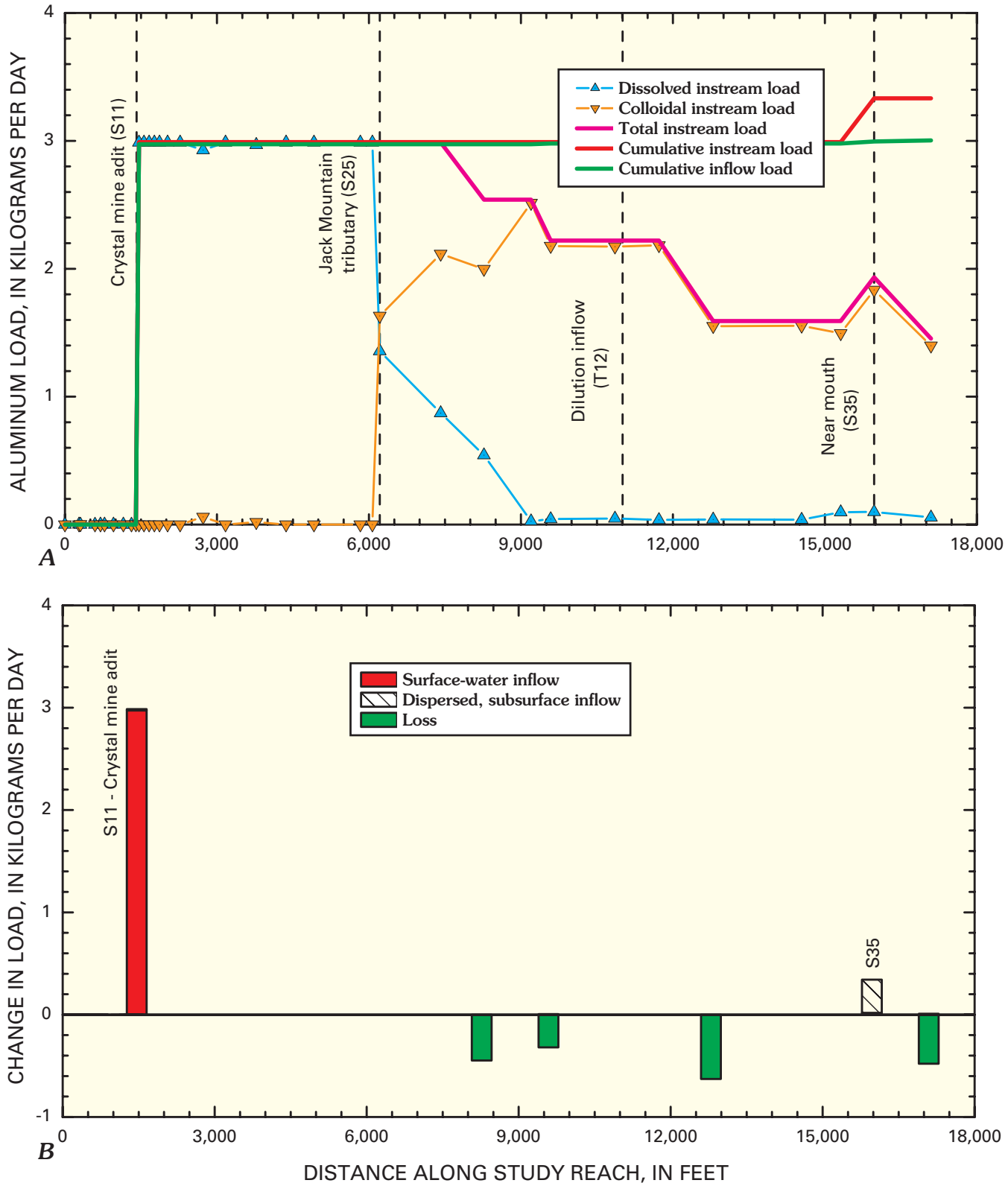

Figure 23. Variation of *A*, aluminum load with distance, and *B*, changes in load for individual stream segments, Uncle Sam Gulch, August 1998.

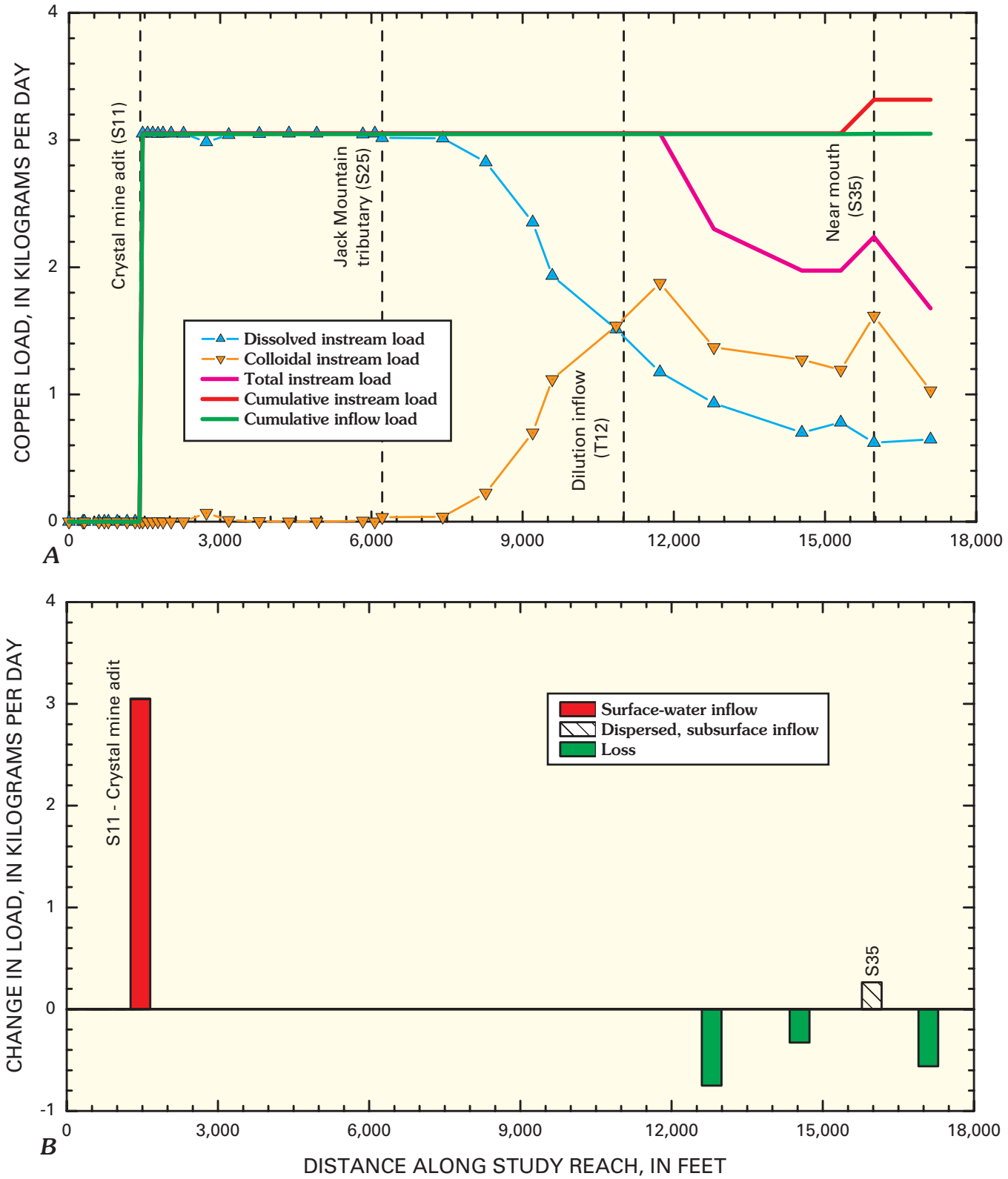

Figure 24. Variation of *A*, copper load with distance, and *B*, changes in load for individual stream segments, Uncle Sam Gulch, August 1998.

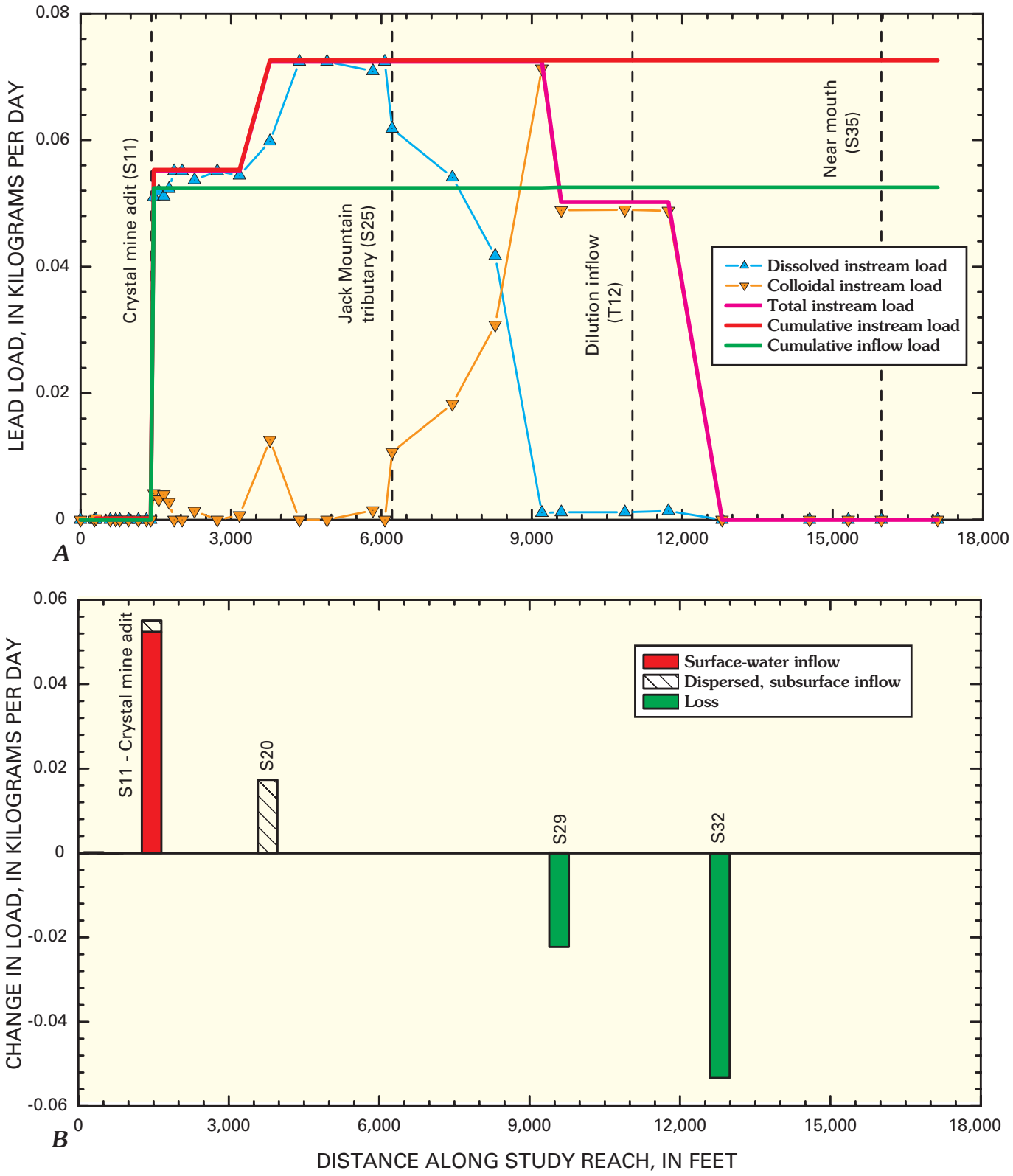

Figure 25. Variation of *A*, lead load with distance, and *B*, changes in load for individual stream segments, Uncle Sam Gulch, August 1998.

Table 6. Change in load for individual stream segments and summary of load calculations for selected solutes, Uncle Sam Gulch, August 1998.

[Distance, in meters along the study reach; Al, aluminum; Cu, copper; Fe, iron; Pb, lead; Mn, manganese; Sr, strontium; Zn, zinc; SO_4, sulfate; cumulative instream load, cumulative inflow load, unsampled load, and attenuation in kilograms per day; numbers in red with parentheses indicate a loss of load; color of cell indicates the segments with the greatest load: red, largest load; orange, second largest; yellow; third; green, fourth; blue, fifth]

Segment number	Distance	Al	Cu	Fe	Pb	Mn	Sr	Zn	SO_4
S01	0	0.000	0.000	0.001	0.000	0.000	0.000	0.000	0.010
S02	278	.000	(.000)	.001		.000		(.000)	.039
S03	305	.001	.000	.019	.000	.001	.000	.001	.019
S04	592	(.001)	.000	(.017)	(.000)	(.000)	.001	.000	.019
S05	702	.001	.001	.004	.000	.002	.003	.004	.151
S06	780						.001		
S07	957		(.000)				.002	.001	.026
S08	1,152	(.000)	(.000)	(.004)		(.001)		(.001)	(.030)
S09	1,314	(.001)	.000	.001		.000	.002	.003	.081
S10	1,399	.001					.001	(.001)	.043
S11	1,461	2.99	3.05	10.6	.055	2.90	.052	13.9	122
S12	1,560								
S13	1,661							(1.02)	
S14	1,764								
S15	1,866			(1.08)					
S16	2,026			(.702)					
S17	2,273								
S18	2,727			(1.11)				(.772)	
S19	3,170						.009	.715	
S20	3,777			0.547	.017		.006		
S21	4,365			(3.15)					
S22	4,915			(.567)			.009		
S23	5,830			(1.03)					
S24	6,068			(.320)					
S25	6,213			.337		.272	.061		13.5
S26	7,417			(.368)			.015	.841	
S27	8,270	(.447)		(.313)					8.25
S28	9,200						.024		(13.6)
S29	9,588	(.320)		(.263)	(.022)				
S30	10,856								
S31	11,724						.044		
S32	12,795	(.629)	(.751)	(.524)	(.053)	(.212)			
S33	14,540		(.327)	(.140)					
S34	15,314								
S35	15,971	.342	.265	0.160		2.87	.182	2.87	12.3
S36	17,095	(.479)	(.561)	(.212)		(.740)	(.040)	(3.63)	12.0
Cumulative instream load		3.33	3.32	11.7	.073	3.71	.412	18.3	169
Cumulative inflow load		3.00	3.05	10.6	.053	2.88	.328	13.5	160
Percent inflow load		90	92	91	72	78	80	74	94
Unsampled inflow		.329	.268	1.06	.020	.823	.084	4.85	9.33
Percent unsampled inflow		10	8	9	28	22	20	26	6
Attenuation		1.88	1.64	9.81	.073	.953	.000	5.43	13.6
Percent attenuation		56	49	84	100	26	0	30	8

study reach is consistent with the relatively small contribution of iron load from Uncle Sam Gulch to Cataract Creek (fig. 11).

Most of the aluminum load also entered the stream in the adit discharge of the Crystal mine (fig. 23). One additional increase was measurable in segment S35, and it was unsampled inflow for aluminum as it was for other metals. Higher pH downstream from Jack Mountain tributary caused a complete change in aluminum load from the dissolved to the colloidal phase. Unlike the transformation of iron, this change in aluminum phase occurred along the next 2,000 ft of stream. The colloidal aluminum load subsequently decreased downstream to about half the amount present before the transformation.

Copper loading resembled that of aluminum; the major source was the adit inflow from the Crystal mine, and load decreased substantially downstream from Jack Mountain tributary (fig. 24). For copper, the decrease in load was not as abrupt as for iron. Instead, there was a gradual transformation from dissolved to colloidal copper after sorption to iron and perhaps aluminum colloids between segments S25 and S29. The percentage of total-recoverable copper that is in the colloidal form increased systematically with pH, in a manner very similar to a sorption isotherm (Smith, 1999). The increase in copper load at segment S35 was an increase in colloidal, rather than dissolved, copper. The unsampled inflow of copper likely occurred as dissolved copper that was sorbed to iron colloids during the time of transport through the stream segment.

The loading profile of lead differed from those of the other metals because some of the loading occurred downstream from the inflow from the Crystal mine adit (segment S20), and not just from the adit inflow (fig. 25). The greatest increase occurred in segment S20, from unsampled inflow. Downstream from Jack Mountain tributary, the lead load decreased, but in a pattern more like copper indicating gradual sorption rather than precipitation. In stream segment S32, essentially the entire lead load was gone from the water column, possibly due to the increase of instream pH in this segment. The loss of lead is consistent with the increase of lead concentration in the bed sediments (Church and others, this volume, fig. 5).

Locations of Major Loading

Inflow from the Crystal mine adit at segment S11 dominated the loading of all the constituents except strontium (table 6). Loading from the adit accounted for more than 90 percent of the aluminum, copper, and iron; more than 70 percent of the lead, manganese, zinc, and sulfate; but only 13 percent of the strontium load. Segment S35, which was almost to the mouth of Uncle Sam Gulch, was the next most substantial source for loads for several constituents. This is the location of a major fault and several veins that have not been mined (O'Neill and others, this volume, pl. 1). Segment S20 was a source for 23 percent of the lead load. The inflow of Jack Mountain tributary, accounted for by segment S25, was a source for iron, manganese, strontium, and sulfate.

Unsampled Inflow

Unsampled inflow was less than 30 percent for all the constituents. The greatest amount of unsampled inflow was for lead (28 percent), manganese (22 percent), and strontium (20 percent). For lead (fig. 25*B*), the unsampled inflow occurred in segment S20 (fig. 25*B*). The source of this loading is unknown, but likely is associated with ground water from the Crystal mine or the waste-rock pile. Unsampled inflow for manganese (fig. 20*B*) occurred in segments S25 and S35, and for strontium (fig. 17*B*) it mostly occurred in segment S35, but there were several segments with a small amount of unsampled inflow. The small amount of unsampled inflow for zinc and sulfate reflects a general lack of widespread alteration of rocks in the watershed.

Attenuation of Load

Most of the attenuation of metals in Uncle Sam Gulch occurred downstream from Jack Mountain tributary. About 50 percent of the aluminum (fig. 23*A*) and copper (fig 24*A*), more than 80 percent of the iron (fig. 22*A*), and all of the lead (fig. 25*A*) that entered Uncle Sam Gulch were removed from the water column by the end of the study reach (table 6). This metal attenuation resulted in the accumulation of colloidal floc on the streambed. In the Animas River watershed, Church and others (1997) quantified a large increase in the load of colloidal floc that was transported, or flushed, by high flows during snowmelt runoff. About 30 percent of the manganese and zinc loads were removed (table 6), but only 8 percent of the sulfate load and less than 1 percent of the strontium load were removed.

The attenuation of iron started immediately downstream from the adit inflow (fig. 22). The geochemical behavior of iron makes its loading profile different from that of other metals. The profile indicates that only segment S11 was a major source of loading; the net gain for all but three other segments was negative or near zero. This does not mean, however, that there were no contributions from other stream segments. Because the transformation of dissolved to colloidal iron occurred rapidly with respect to transport of the metals in the stream (Kimball, Broshears, and others, 1994), most of the colloidal iron can be lost through aggregation, settling, and filtering through the streambed within the same stream segment where it enters (Grundl and Delwiche, 1993; Packman and others, 2000). Thus, there could have been contributions or iron load in other stream segments, but if the iron entering the stream is rapidly transformed to colloidal iron and removed from the water column, there is no accounting of that mass loading at this stream-segment scale.

Load profiles help to quantify the mass transfer of chemical reactions in the stream. Changes in load indicate the timing and mechanisms of precipitation and sorption reactions in the context of stream transport (Kimball, Bencala, and Broshears, 1994). The dominant reactions affecting metals downstream from Jack Mountain tributary were the formation of iron and

aluminum colloids. At the low pH upstream from Jack Mountain tributary, Desborough and others (2000) determined that the iron precipitate was schwertmannite. Bigham and Nordstrom (2000) discussed the steps in the formation of schwertmannite, and the final step is represented as:

$$8Fe^{3+}+SO_4^{-2}+14H_2O=Fe_8O_8(OH)_6(SO_4)+22H^+ \quad (3)$$

Downstream from Jack Mountain tributary, at a higher pH, the precipitate was ferrihydrite:

$$Fe^{3+}+3OH^-=Fe(OH)_{3,s} \quad (4)$$

The change may be due to a more positive surface charge on the iron colloid at low pH, favoring anion sorption. Attenuation of aluminum, on the other hand, begins with a transformation from dissolved to colloidal aluminum, probably through the formation of polynuclear aluminum complexes at low temperature (Baes and Mesmer, 1976):

$$xAl^{3+}+yH_2O\Leftrightarrow Al_x(OH)_y^{(3x-y)+}+H^+ \quad (5)$$

Downstream from the inflow of Jack Mountain tributary where the pH increased above 5.5, this transformation begins (fig. 24). As the complex grows it becomes too large to pass through the 10,000 Dalton filter and can be considered colloidal. A crystalline mineral phase, like gibbsite ($Al(OH)_{3,s}$), would occur with aging on the streambed.

Loads of dissolved iron and dissolved aluminum were transformed from the dissolved to the colloidal phase in segments S25 through S28, downstream from Jack Mountain tributary (fig. 26). In each successive stream segment the total load was constant; before the loss of any load, only the portion of the colloidal phase increased. By adding in the amount of the colloidal phases lost to the streambed, the mass balance was still constant. After transport to segment S28, both aluminum and iron were completely transformed to the colloidal phase. Once the colloidal iron was present, dissolved copper started to change to colloidal copper, most likely from sorption to the iron solids. Often it is not possible to distinguish if copper is removed by sorption or coprecipitation (Fulghum and others, 1988), but these data clearly point toward sorption, rather than coprecipitation, as the mechanism of copper removal, because copper was transformed only after the iron colloid had formed. At segment S30, the dissolved and colloidal copper loads were nearly equal, and by segment S32 there was a loss of copper load to the streambed. By accounting for the dissolved, colloidal, and lost copper loads, the total copper remained constant and the mass balance indicates that the mass transfer between phases occurred in the water column.

Comparison of copper mass transfer (figs. 24 and 26) clearly indicates that the transformation of copper from the dissolved to the colloidal phase occurred after the formation of the aluminum and iron colloids. The moles of copper sorbed were less than one tenth of the moles of aluminum or iron formed, but this was a substantial quantity of mass transfer. Webster and others (1998) have shown that a high sulfate percentage in iron hydroxides increases the sorption capacity of the iron phase; schwertmannite has a higher sulfate percentage. This profile and timing strongly indicate that the process for copper removal is sorption rather than coprecipitation, according to a general reaction, using ferrihydrite:

$$Cu^{2+}+2H^+\equiv Fe(OH)_{3,s}\Leftrightarrow 2H^++Cu^{2+}\equiv Fe(OH)_{3,s} \quad (6)$$

where ≡ indicates bonding to a solid surface. Runkel and others (1999) have simulated sorption of copper to iron colloids in a mine-drainage stream, showing that it is a reversible reaction.

Bullion Mine Tributary Subbasin

Mine drainage that affects a small tributary of Jack Creek, called the Bullion Mine tributary in this report, originates from the same ore body that was mined at the Crystal mine in Uncle Sam Gulch (fig. 12). The adit of the Bullion mine discharges to the Bullion Mine tributary where it is a small stream, and the impact of the mine drainage is substantial. A mass-loading study was done during low-flow conditions in early September 1998 to investigate the source of metals and the patterns of metal loading.

Study Area and Experimental Design

Stream samples defined 33 segments and bracketed a total of 11 inflows along the study reach (fig. 27). Site numbers and descriptions of stream and inflow sites are listed in table 7 for reference; detailed field and chemical data for these sites are in the database (Rich and others, this volume). A sodium chloride solution, with 79,040 mg/L chloride, was injected into the Bullion Mine tributary at a rate of 0.0017 L/s for 36 hours, starting at 10:00 MDT on August 30, 1998. Chloride concentration decreased systematically downstream from the injection, indicating those stream segments that contributed water to the stream (fig. 28). Calculated discharge ranged from 0.12 to 0.80 ft^3/s (fig. 28). The largest inflow was Jack Creek (site T11) with a calculated discharge of 0.52 ft^3/s. Jack Creek represented 65 percent of the total streamflow. Stream segments that had sampled inflows accounted for 88 percent of the total increase in streamflow, and discharge increased 0.20 ft^3/s in those segments that had no sampled inflow. This indicates that a minimum of 12 percent of the total increase in streamflow was unsampled inflow, on the basis of tracer information.

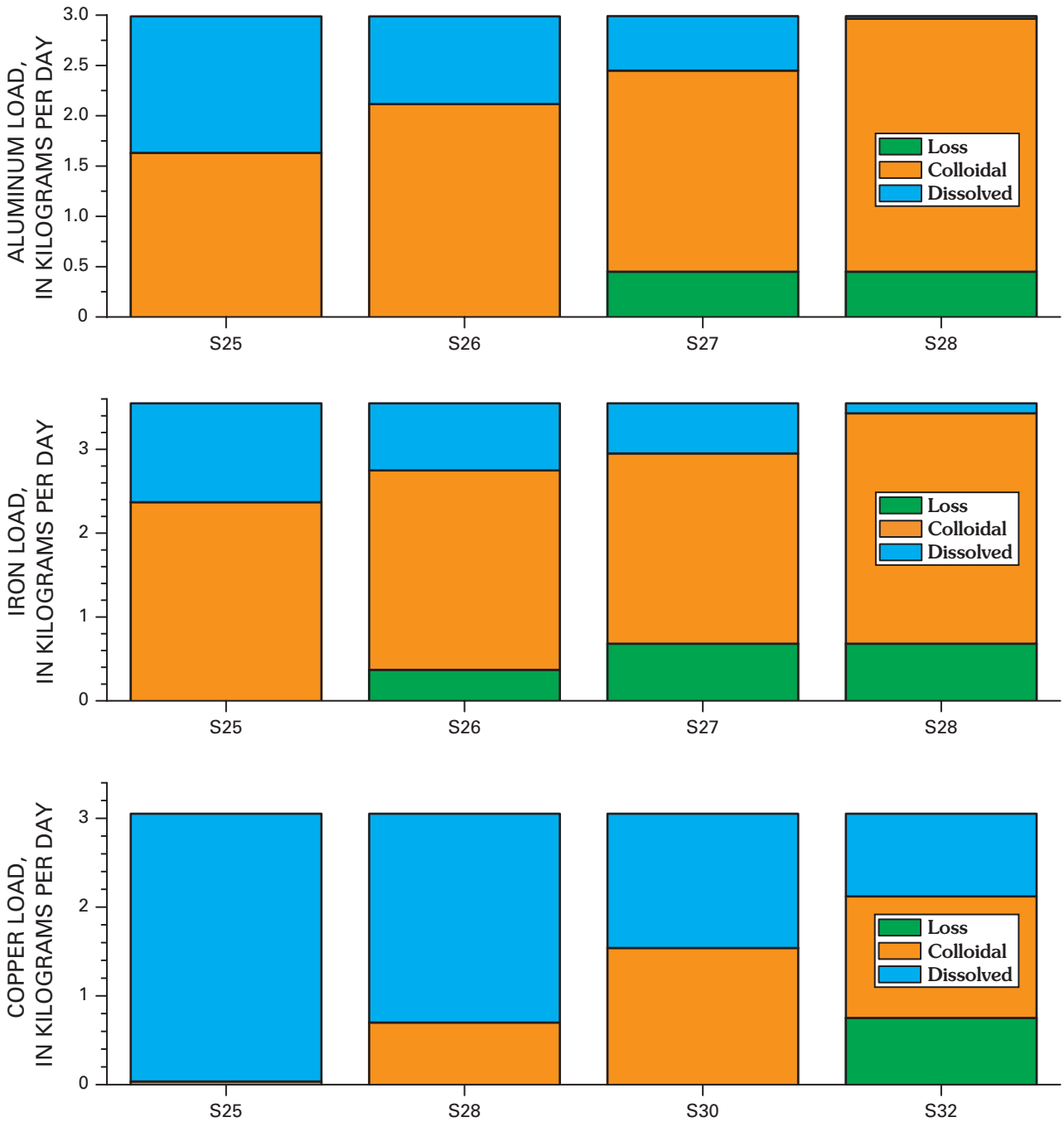

Figure 26. Mass transfer of metals between dissolved and colloidal phases, Uncle Sam Gulch, August 1998.

Table 7. Segment number, distance along study reach, source, site description, site number, and field and chemical data for water from synoptic sampling sites, Bullion Mine tributary, September 1, 1998.

[Dist, distance, in feet along the study reach; source: S, stream; LBI, left bank inflow; RBI, right bank inflow; pH, in standard units; Ksc, specific conductance, in microsiemens per centimeter; Q, discharge, in liters per second; Cl, chloride, in milligrams per liter]

Segment number	Dist	Source	Description	Site Number	pH	Ksc	Q	Cl
S01	0	S	Above injection site	Bull0	6.82	67	3.3	0.28
S02	150	S	Below injection site	Bull150	7.07	171	3.3	33.5
S03	235	S	T1 transport site below injection	Bull235	7.08	168	3.3	31.8
S04	296	S	At start of mining disturbance	Bull296	6.89	167	3.3	32.0
S05	341	S	Above acidic inflows	Bull341	6.88	169	3.4	31.1
T01	346	LBI	Left bank inflow from mine	Bull346	2.78	1,827	0.17	2.94
T02	359	LBI	Second acid inflow	Bull355	2.83	1,829	0.35	3.46
S06	383	S	Below acidic inflows—log jam	Bull383	3.61	419	3.9	26.9
S07	437	S	Stream below acidic inflows	Bull437	3.55	439	3.9	26.5
S08	485	S	Below rock dam in small pond	Bull485	3.63	443	4.0	26.2
S09	540	S	At pine over creek	Bull540	3.60	448	4.0	26.1
T03	582	LBI	Left bank inflow	Bull582	3.52	1,185	0.20	1.54
S10	627	S	Below high conductance inflow	Bull627	3.52	473	4.2	24.5
S11	726	S	Upstream from bedrock control	Bull726	3.58	418	4.2	24.8
T04	733	LBI	Left bank near end of tailings	Bull733	4.61	532	0.02	0.73
S12	793	S	Downstream of log at meander	Bull793	3.52	478	4.2	24.2
S13	856	S	At large boulder control	Bull856	3.56	477	4.2	23.4
S14	945	S	Stream	Bull945	3.52	476	4.3	23.3
S15	1,025	S	Above breached settling dam	Bull1025	3.56	476	4.4	22.4
S16	1,109	S	At breached dam	Bull1109	3.58	478	4.5	23.2
S17	1,197	S	At convergence of stream channels	Bull1197	3.63	475	4.5	22.7
S18	1,264	S	Stream	Bull1264	3.75	468	4.5	22.4
S19	1,404	S	At meander bend	Bull1404	3.71	471	4.5	22.1
S20	1,522	S	At log jam	Bull1522	3.66	458	4.6	21.9
T05	1,554	RBI	Right bank tributary	Bull1554	6.72	81	0.00	0.26
S21	1,672	S	Pool upstream from log jam	Bull1672	3.73	454	4.6	21.3
S22	1,808	S	Upstream from rock falls	Bull1808	3.68	456	4.7	21.3
T06	1,874	LBI	First high pH left bank inflow	Bull1874	6.79	190	0.00	0.41
S23	1,990	S	Below high pH inflow	Bull1990	3.73	450	4.7	20.9
T07	1,992	LBI	Second high pH left bank inflow	Bull1992	6.83	129	0.45	0.27
S24	2,155	S	T2 transport site	Bull2155	3.85	413	5.2	18.8
T08	2,157	LBI	Left bank tributary	Bull2157	6.40	162	0.37	0.36
T09	2,191	RBI	Right bank tributary	Bull2191	6.50	67	0.37	0.20
S25	2,278	S	At narrow point in canyon	Bull2278	4.14	360	5.9	16.5
S26	2,585	S	Stream	Bull2585	4.11	357	5.9	16.7
S27	2,951	S	Stream	Bull2951	4.39	349	6.1	16.3
S28	3,457	S	Downstream from steep gradient	Bull3457	4.20	348	6.1	16.2
S29	3,958	S	Stream	Bull3958	4.32	338	6.3	15.3
S30	4,729	S	Stream	Bull4729	4.34	319	6.6	14.9
T10	5,245	LBI	Left bank inflow	Bull5245	6.33	54	0.32	0.20
S31	5,338	S	T3 transport site—near mouth	Bull5338	4.64	310	6.9	13.9
T11	5,339	RBI	Jack Creek	Bull5339	6.77		15	0.22
S32	5,454	S	Jack Creek below Bullion Mine tributary	Bull5454	6.60	152	22	4.17
S33	6,019	S	Jack Creek above tailings impoundment	Bull6019	6.70	151	23	4.00

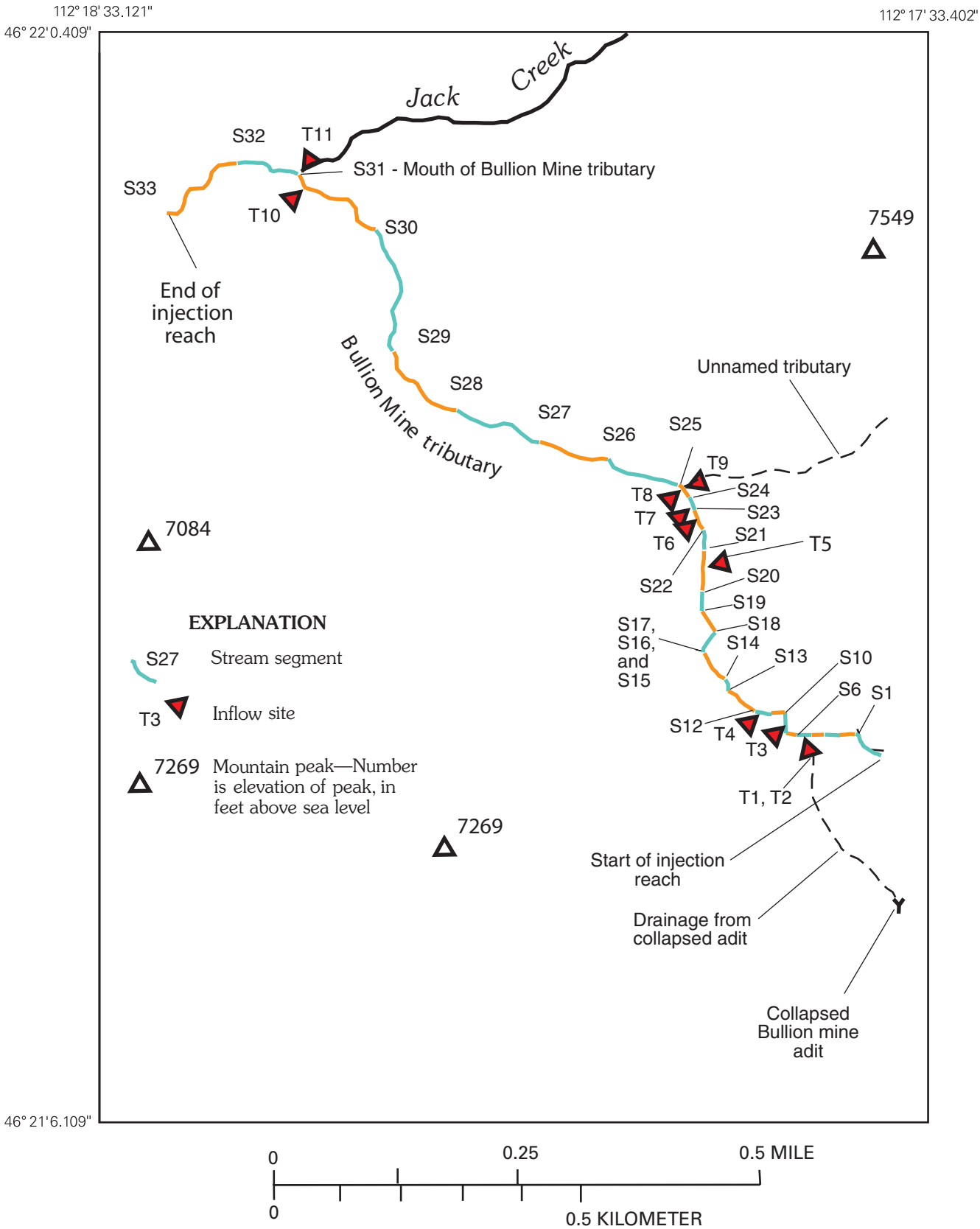

Figure 27. Location of stream segments (indicated by alternating colors) and inflows for synoptic sampling, Bullion Mine tributary, September 1998.

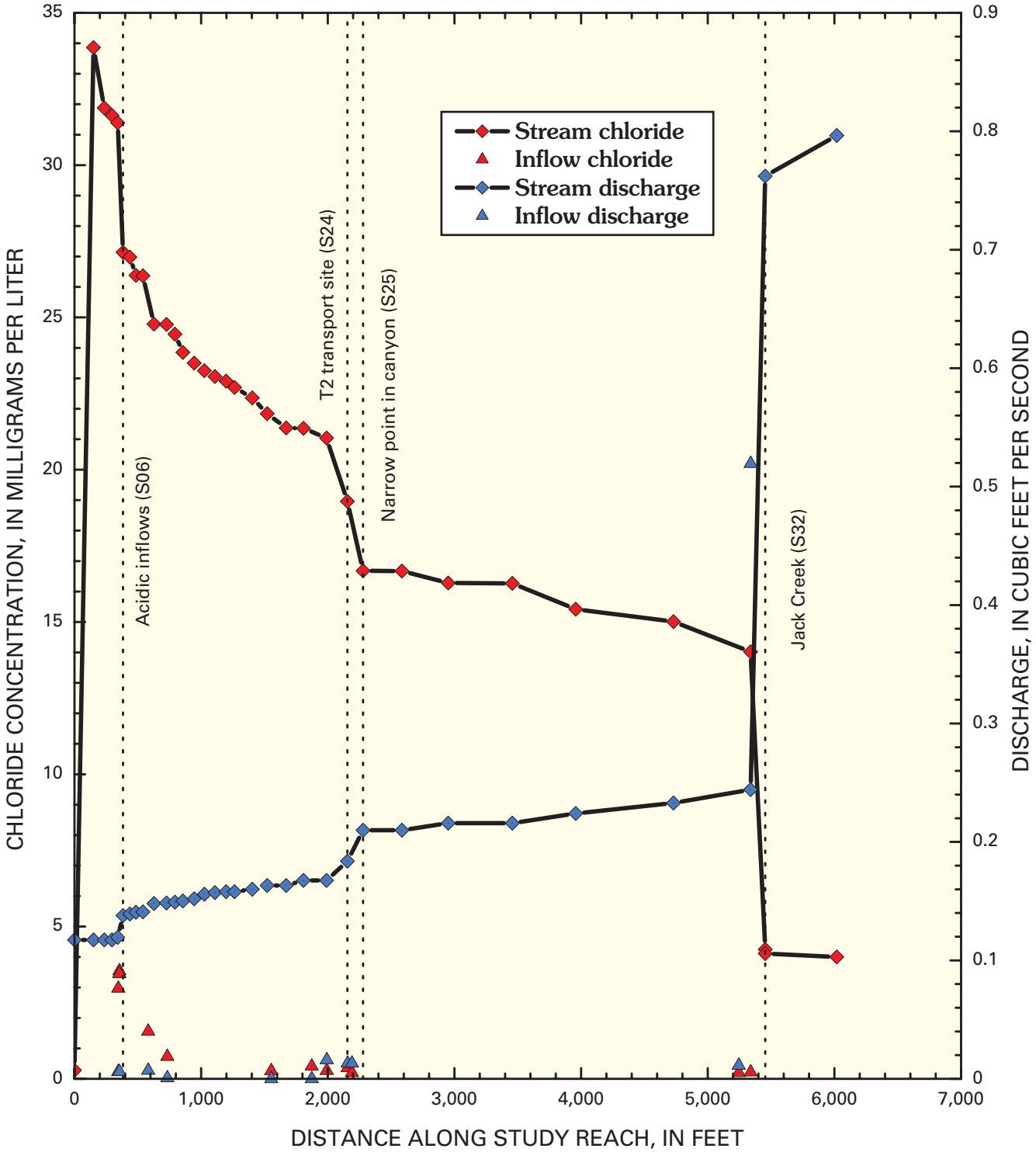

Figure 28. Variation of chloride concentration and calculated discharge with distance along the study reach, Bullion Mine tributary, September 1998.

Chemical Characterization of Synoptic Samples

The impact of inflows from the Bullion mine adit was evident from the variation of pH along the study reach in the Bullion Mine tributary (fig. 29). Three acidic inflows (T01, T02, and T03) caused a large decrease in pH (Metesh and others, 1994). Within this same area of the stream are old mill tailings that may affect the stream chemistry, along with the drainage from the collapsed adit (Fey and others, 2000). Near-neutral pH inflows at T05 through T09 only raised the pH slightly. Downstream from the confluence with Jack Creek, the pH returned to neutral, as indicated by Nimick and Cleasby (this volume, fig. 2). Changes in dissolved and colloidal metal concentrations occurred at the same locations as the changes in pH (fig. 30). The greatest increase in concentration for each of the metals was at segment S06, downstream from inflows T01 and T02. Both the filtered concentrations and the total-recoverable concentrations of aluminum, copper, and zinc increased (fig. 30*A*, *C*, *D*), indicating that these metals were present as truly dissolved metals at this low pH. The concentration decreased at segment S25 owing to inflows. At this point, there were small differences between filtered and total-recoverable concentrations, indicating colloidal concentrations. Concentrations of these metals remained nearly constant until the inflow of Jack Creek, where concentration decreased substantially (segment S32), and aluminum and copper were transformed to colloidal concentrations. Only a small part of the zinc was transformed to the colloidal form. Nimick and Cleasby (this volume) have noted where concentrations of zinc exceeded water-quality criteria at sites downstream from the Bullion mine adit inflows.

Most of the iron occurred as colloidal solids (fig. 30*B*), as indicated by the large difference between the total-recoverable and the ultrafiltrate concentrations. At site S06, downstream from the first acidic inflow, the colloidal iron concentration was 11 mg/L and the dissolved concentration was 5 mg/L. From that point on downstream, the water was noticeably cloudy due to colloidal solids (fig. 31), which were most likely schwertmannite due to the low pH of the stream. Downstream from the inflow of Jack Creek, iron concentrations were lower, but a greater percentage of the total-recoverable iron occurred as colloidal iron.

The difference between iron and the other metals resulted from the low pH of the Bullion Mine tributary (fig. 29). At S06, the pH was 3.61, which was sufficiently high for iron precipitation, but too low for the precipitation of aluminum (Nordstrom and Ball, 1986; Bigham and Nordstrom, 2000). This pH also was too low for any substantial sorption of copper or zinc to the iron colloids (Smith, 1999). Downstream from Jack Creek, at segment S32, the pH increased to 6.60, causing substantial formation of aluminum colloids and sorption of copper (fig. 30*A*, *C*), but the pH was not high enough for sorption of zinc (fig. 30*D*). At this higher pH, however, a clear distinction existed between unfiltered and 0.45-µm filtered concentrations of aluminum, copper, and zinc. This indicates a continuum of colloid sizes, and that the 0.45-µm membrane was not effective in separating the colloidal and dissolved concentrations, as observed in many other streams affected by acid mine drainage (Kimball and others, 1992; Kimball and others, 1995).

Clear chemical distinctions among stream and inflow samples were distinguished by principal components analysis into seven groups (table 8). Inflows were part of four different groups. The most dilute inflows were grouped with the stream samples that were upstream from any mining influence. All these samples represent the results of weathering catchment bedrock that is unaffected by alteration or mining (group 1). One of these inflows was Jack Creek (T10), which drains a much larger area than the Bullion Mine tributary but results in this same dilute chemical composition as the most upstream samples in the Bullion Mine tributary (table 8). A second set of inflows (group 7) differed from the dilute inflows because they had higher calcium and sulfate concentrations, possibly reflecting some effects of mine waste or a change in the mineralogy that they drain. A third group of inflows (group 6) includes the acidic inflows that had such a strong effect on the stream.

Three groups of stream samples occurred downstream from the acidic inflows. Group 2 was immediately downstream from T01 and T02, and reflects the change to acidic, metal-rich stream water. In the biplot (fig. 32), this group generally lies along a line between inflows T01 and T02 and the dilute samples of group 1. Downstream from inflow T03 a change occurred in the stream-water chemistry to higher concentrations of calcium and sulfate, and group 3 plots to the upper right of group 2 in the direction of inflow T03 (group 3). Downstream from inflows T08 and T09, a change to a higher pH occurred, and concentrations of several metals decreased (group 4). Segments S32 and S33 (group 5), downstream from Jack Creek, were quite different because of the dilution by Jack Creek and the instream chemical reactions that occurred in the mixing zone. Thus, changes in stream chemistry were quite systematic in response to the inflows. Details of these changes among groups will be illustrated by profiles of metal loading.

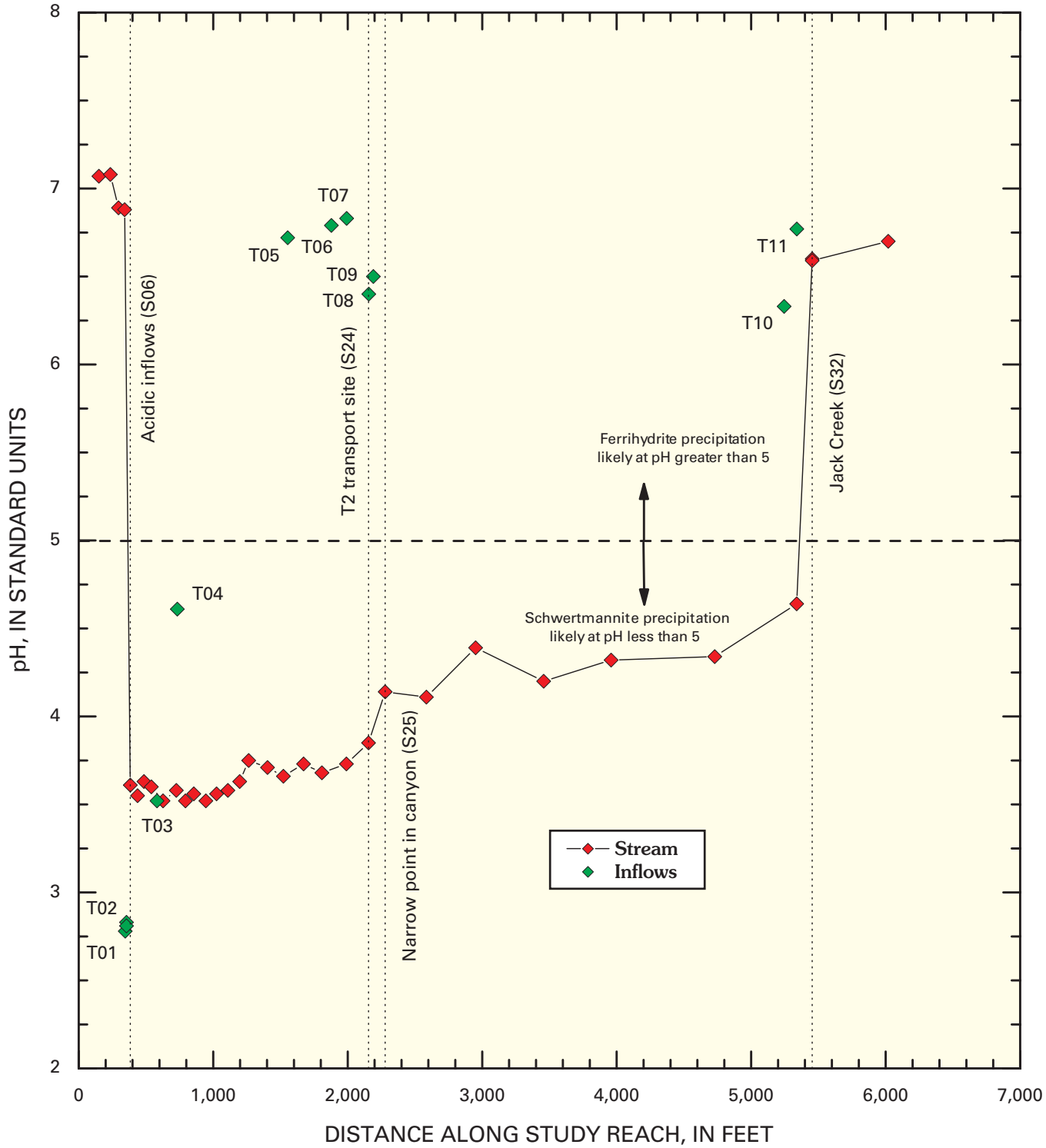

Figure 29. Variation of pH with distance, Bullion Mine tributary, September 1998.

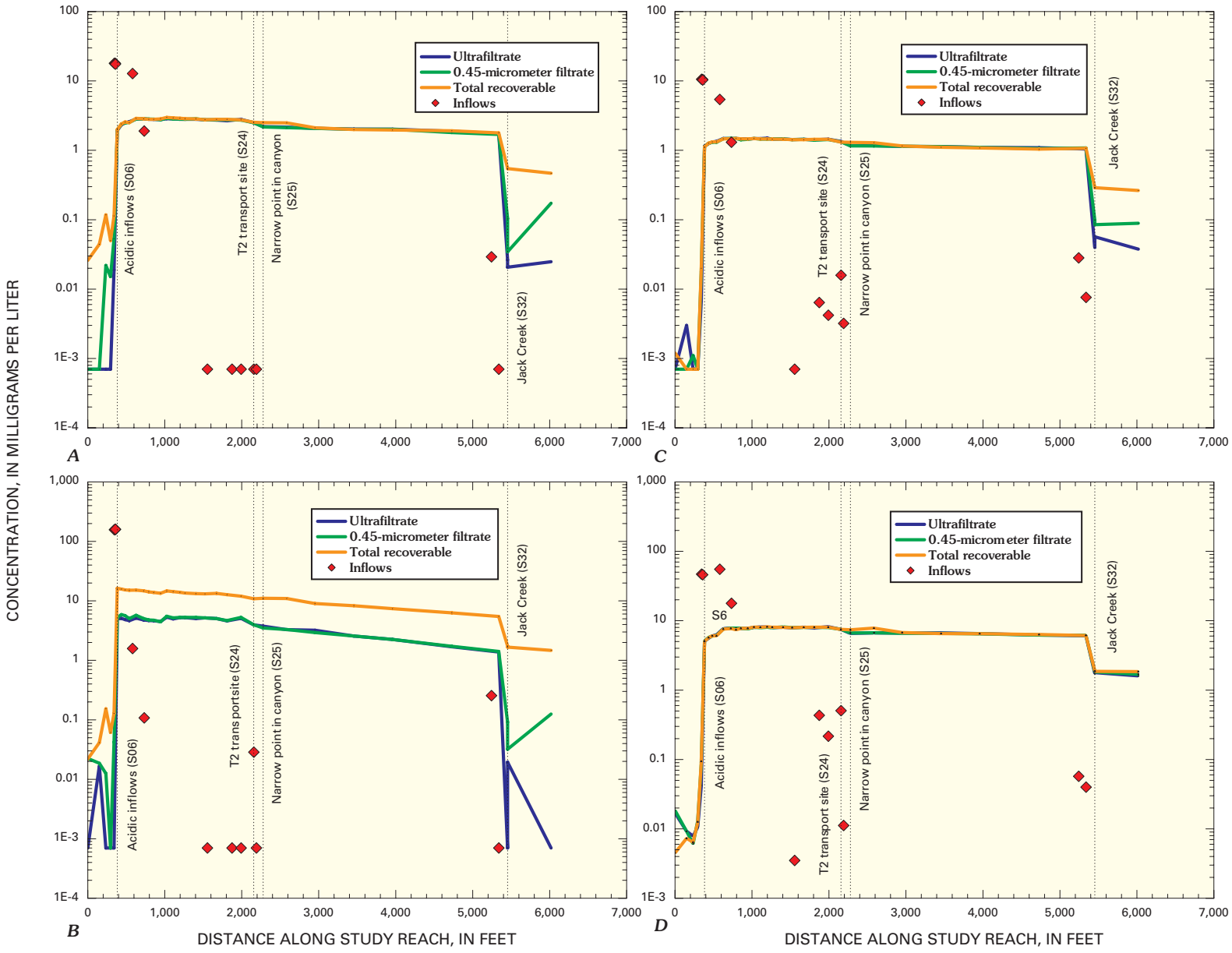

Figure 30. Variation of *A*, aluminum; *B*, iron; *C*, copper; and *D*, zinc concentrations with distance, Bullion Mine tributary, September 1998.

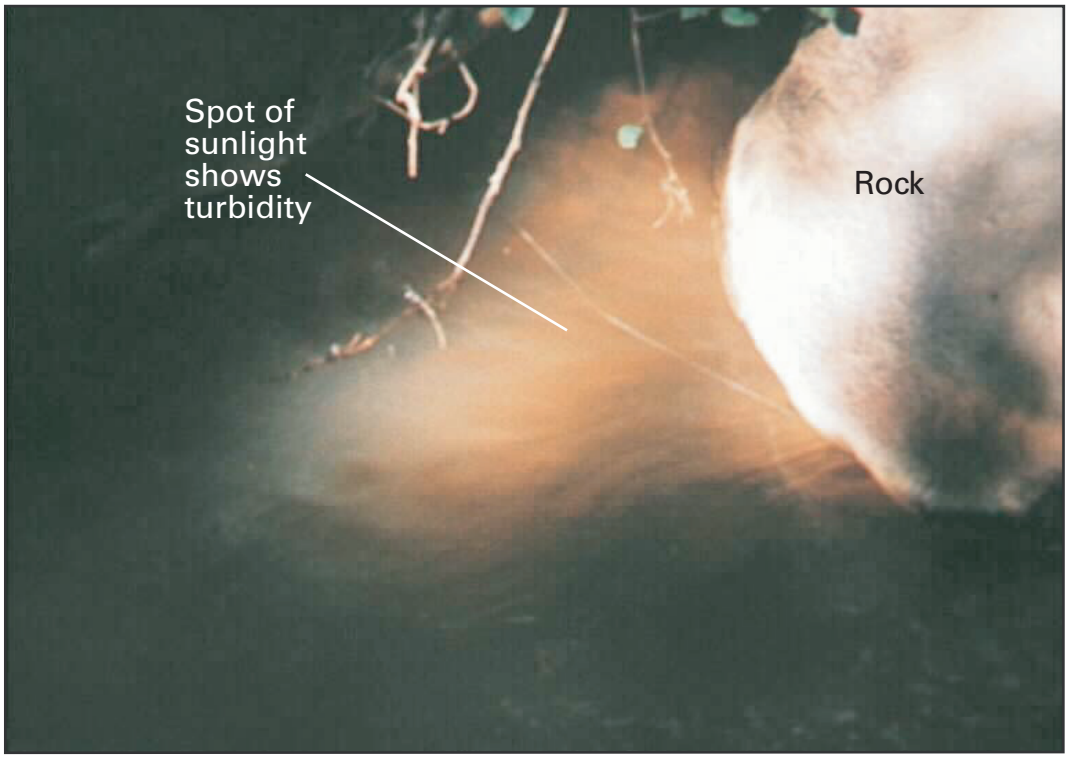

Figure 31. Bullion Mine tributary showing turbid nature of stream water owing to colloidal suspension of solids, September 1998. Length of photo area is about 1 m.

Table 8. Median composition of groups from principal components analysis for synoptic sampling sites, Bullion Mine tributary, September 1998.

[pH, in standard units; Dis, dissolved; LD, less than detection; Col, colloidal; all concentrations in milligrams per liter; -, no data]

Number of samples or solute	Phase	Group 1 Unaffected stream sites	Group 1 Unaffected inflows	Group 2 Stream after inflows T1 and T2	Group 3 Stream after inflow T3 to inflow T8	Group 3 Inflow T4, acidic, but higher pH	Group 4 Stream from S25 to S28	Group 5 Jack Creek samples	Group 6 Drainage from Bullion mine adit	Group 7 Inflows T6, T7, and T8 with higher pH
Number of samples		5	4	6	16	1	4	2	3	3
pH	Dis	6.89	6.61	3.62	3.65	4.61	4.17	6.65	2.82	6.79
Calcium	Dis	7.88	9.50	19.0	24.9	63.7	25.1	15.5	89.2	21.2
Magnesium	Dis	1.73	2.31	5.91	7.47	15.2	7.03	3.93	33.7	4.76
Sodium	Dis	21.2	2.72	17.9	15.8	4.23	12.8	4.91	5.27	2.76
Chloride	Dis	31.8	.210	26.2	22.4	0.730	16.4	4.08	2.94	0.360
Sulfate	Dis	7.43	5.11	131	160	273	136	41.4	1,100	36.1
Aluminum	Dis	LD	.013	2.18	2.80	1.89	2.12	.024	17.9	LD
	Col	.049	-	.048	.043	-	.177	.483	-	-
Cadmium	Dis	.002	.002	.068	.087	.151	.073	.019	.556	.007
	Col	LD	-	.001	LD	-	.004	.002	-	-
Copper	Dis	LD	.004	1.20	1.46	1.31	1.15	.043	10.6	.011
	Col	LD	-	.004	LD	-	.069	.235	-	-
Iron	Dis	LD	.005	4.74	5.01	.107	3.24	.005	158	.004
	Col	.061	-	10.4	8.48	-	6.56	1.58	-	-
Lead	Dis	LD	LD	.029	.042	.111	.031	LD	.382	LD
	Col	LD	-	LD	.007	-	.009	LD	-	-
Manganese	Dis	.001	.001	3.02	3.82	4.37	3.00	.645	25.1	.017
	Col	.002	-	.015	LD	-	.165	.016	-	-
Nickel	Dis	LD	LD	.014	.020	.049	.016	.002	.142	LD
	Col	LD	-	.002	.002	-	.005	.003	-	-
Strontium	Dis	.063	.068	.095	.115	.258	.119	.088	.310	.095
Zinc	Dis	.011	.022	6.06	7.90	17.7	6.66	1.68	47.4	.446
	Col	LD	-	LD	.004	-	.479	.181	-	-

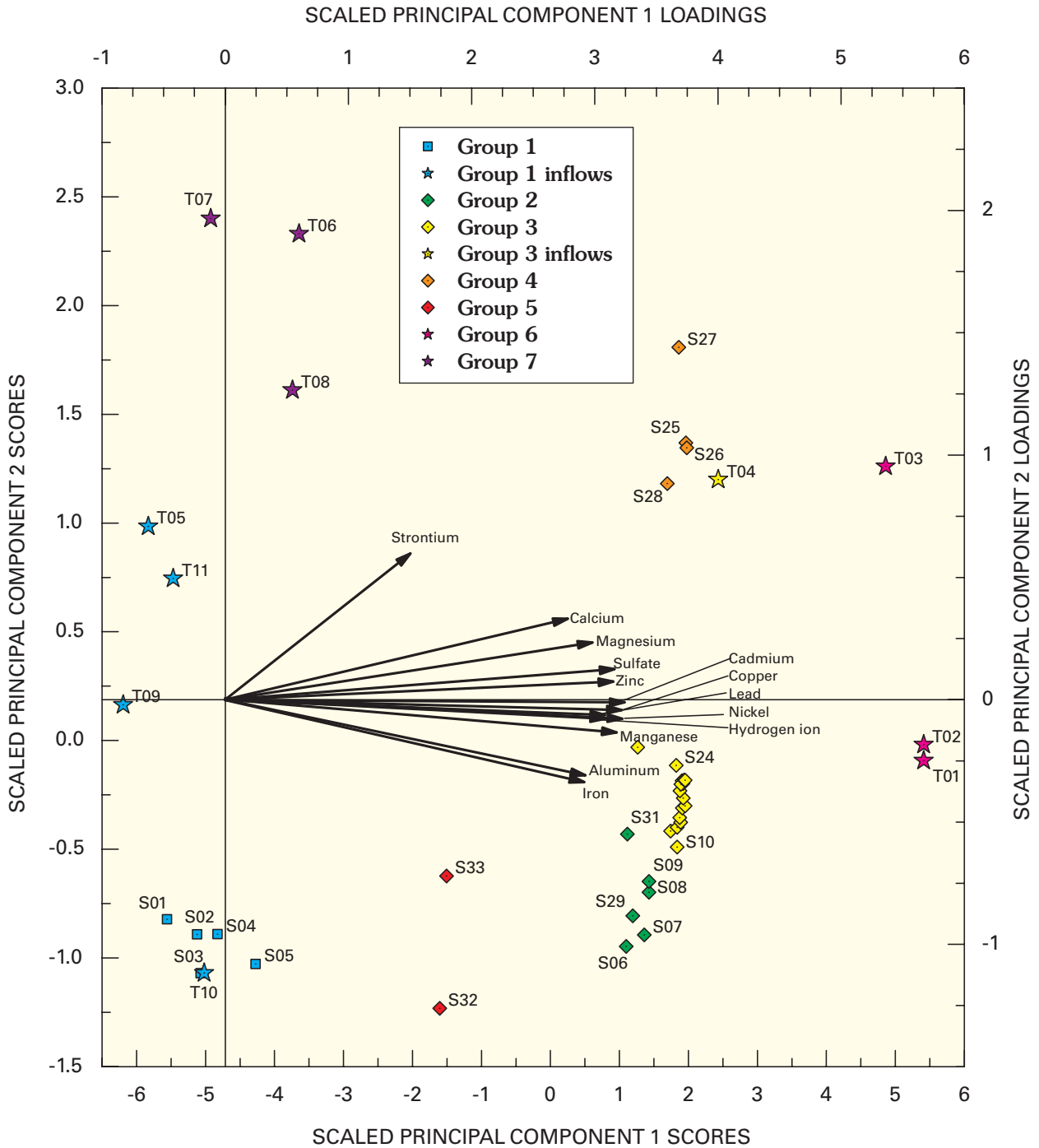

Figure 32. Biplot of principal component scores for synoptic samples and loadings for chemical constituents, Bullion Mine tributary, September 1998.

Load Profiles

Loading profiles of metals in the Bullion Mine tributary are comparable to those in Uncle Sam Gulch, mostly because of the distinct sources of metals and the chemical reactions that transformed metals downstream from neutral-pH inflows. Changes in the load for each individual stream segment are illustrated in figures 33 through 42; and a summary of load calculations is shown in table 9. There were three characteristic patterns of loading profiles among the solutes in the Bullion Mine tributary: (1) solutes that were conservative all along the study reach, (2) solutes that were conservative and then reactive transport downstream from Jack Creek, and (3) solutes that was reactive along the entire study reach.

Cadmium (fig. 33), manganese (fig. 34), zinc (fig. 35), and sulfate (fig. 36) were mostly conservative along the entire study reach. For each of these solutes, the greatest loading occurred downstream from the acidic inflows in segments S06 and S10, and for manganese and zinc additional loading occurred in segment S25 (table 9). Because this latter increase in load occurred as an increase of colloidal manganese and zinc (figs. 34*A* and 35*A*), it may have been caused by stirring up of the streambed colloids during sampling. However, a clear increase in strontium load was observed in that same stream segment (fig. 37), and strontium load would not likely increase from stirring up of the bottom. Downstream from segment S25, there was some loss of manganese load to the streambed in segment S27, and a similar small amount occurred downstream from the confluence with Jack Creek at segment S32.

Aluminum (fig. 38), copper (fig. 39), and nickel (fig. 40) loads were similar to cadmium, manganese, zinc, and sulfate except that downstream from the confluence with Jack Creek (S32), they were more reactive. Their loads changed from almost completely dissolved in the Bullion Mine tributary to almost completely colloidal in Jack Creek. This is consistent with the change in pH from less than 5.0 to greater than 6.0 that occurred as the two streams mixed (fig. 29).

Iron (fig. 41) and lead (fig. 42) were reactive along the entire study reach. Load profiles for dissolved and colloidal iron indicate the importance of the acidic inflow at T01 (fig. 41*A*). Because cadmium, copper, and iron reactions and loss to the streambed occurred on a time scale of transport within individual stream segments, their net instream load is less than the inflow load or is negative. Thus, the cumulative instream load is less than the cumulative inflow load (table 9). For example, the inflow load of iron increased 7.17 kg/day for segment S06, but instream load increased only 5.46 kg/day. The difference of 1.71 kg/day would be the amount of iron precipitation to the streambed. Travel time through the segment was less than 2 minutes, pointing out the rapid reaction of the iron precipitation and aggregation to form colloidal particles (Grundl and Delwiche, 1993; Kimball, Broshears, and others, 1994). Downstream from Jack Creek, a complete transformation of dissolved to colloidal iron occurred (fig. 41*A*); colloidal iron load increased by 0.72 kg/day and the dissolved load decreased by 0.81 kg/day; the difference was from additional loss to the streambed.

The lead profile (fig. 42) also indicated reactive transport through the study reach. Total load clearly increased at each of the acidic inflows. Some of the lead changed between dissolved and colloidal phases in response to increases in pH downstream from site S25. Downstream from Jack Creek, all the lead was removed from the water column to the streambed, sorbed to the iron colloids.

Locations of Major Loading

Similarities among the loading profiles indicate two principal locations of the metal loading along the Bullion Mine tributary. The greatest loading for all the constituents except strontium was in segment S06 (table 9). Segment S10 also received substantial loading. Inflows T01, T02, and T03, which are in segments S06 and S10, drain the Bullion mine adit, and their surface flow was traced back to the collapsed adit. From segment S15 to segment S25, metal loading was minimal. At segment S25, loads increased for several of the metals (table 9). This could be due to the narrowing of the canyon at that point (table 8), which may have forced some subsurface water into the stream channel.

Unsampled Inflow

Because the Bullion mine adit was the primary source of metals in the watershed, there was relatively little unsampled inflow in the Bullion Mine tributary (table 9). Unsampled inflow generally occurred at the same locations as the principal surface-water loadings, indicating that some of the flow from the adit had seeped into the ground but was still contributing to the load. Nickel and lead had the highest percentages of unsampled inflow (table 9).

Attenuation of Load

Downstream from the principal inflows of metals at T01, T02, and T03, attenuation of most of the metals was relatively slight. For cadmium, manganese, zinc, sulfate, copper, nickel, and iron, the inflow load exceeded the instream load at S06, which most likely means that there was some removal of these solutes that is not accounted for in the calculation of attenuation in table 9. At the low pH of Bullion Mine tributary, the removal of sulfate with iron could indicate the formation of schwertmannite as the streambed precipitate (Bigham and Nordstrom, 2000).

Colloidal iron was lost from the water column during transport downstream (fig. 41). The loss most likely involves a sequence of aggregation in the water column and then entrapment by biofilm on the streambed cobbles (Besser and others, 2001). Packman and others (2000) have proposed that colloids can be strained from the water column by the streambed as hyporheic exchange of water takes place during transport.

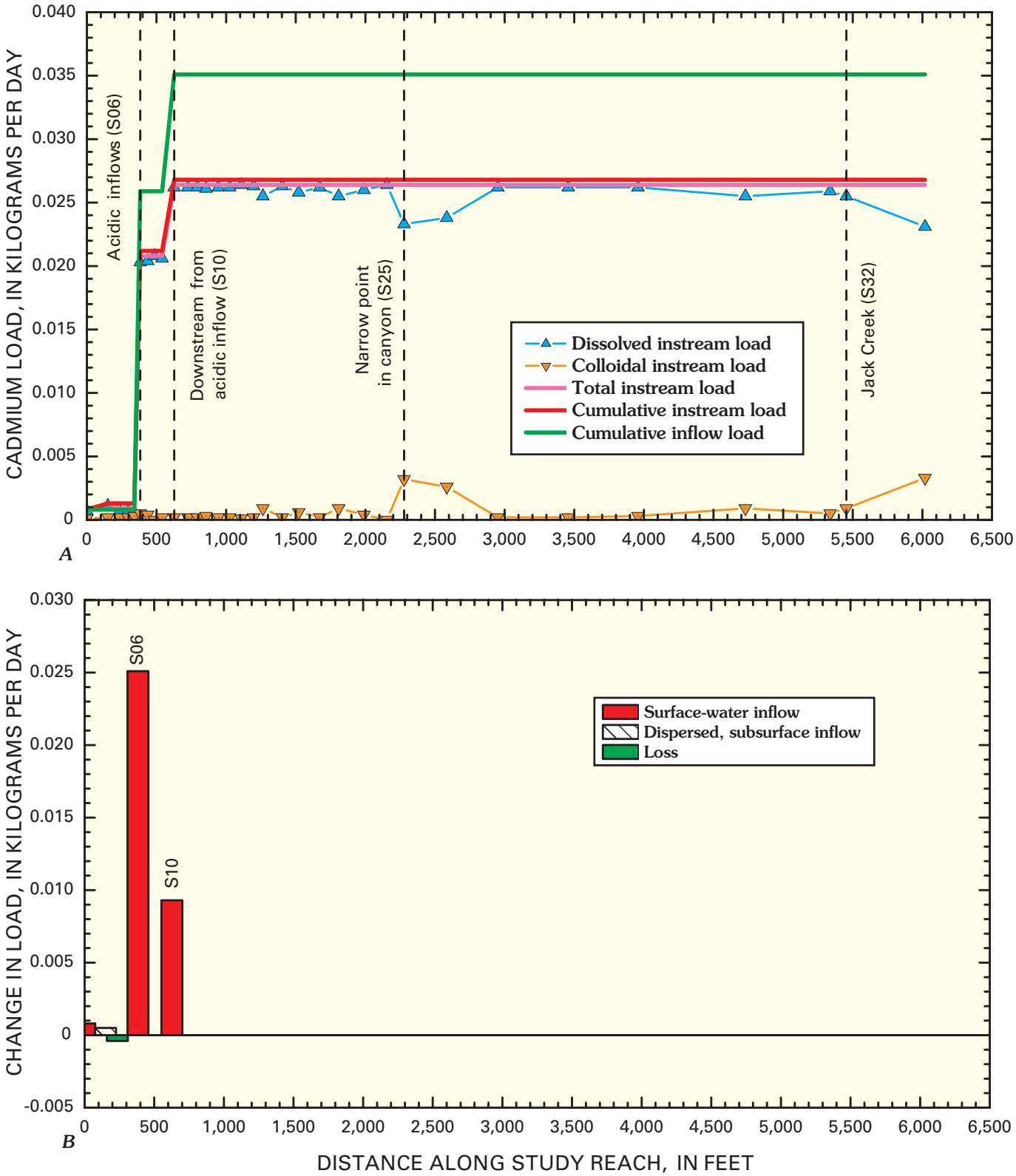

Figure 33. Variation of *A*, cadmium load with distance, and *B*, changes in load for individual stream segments, Bullion Mine tributary, September 1998.

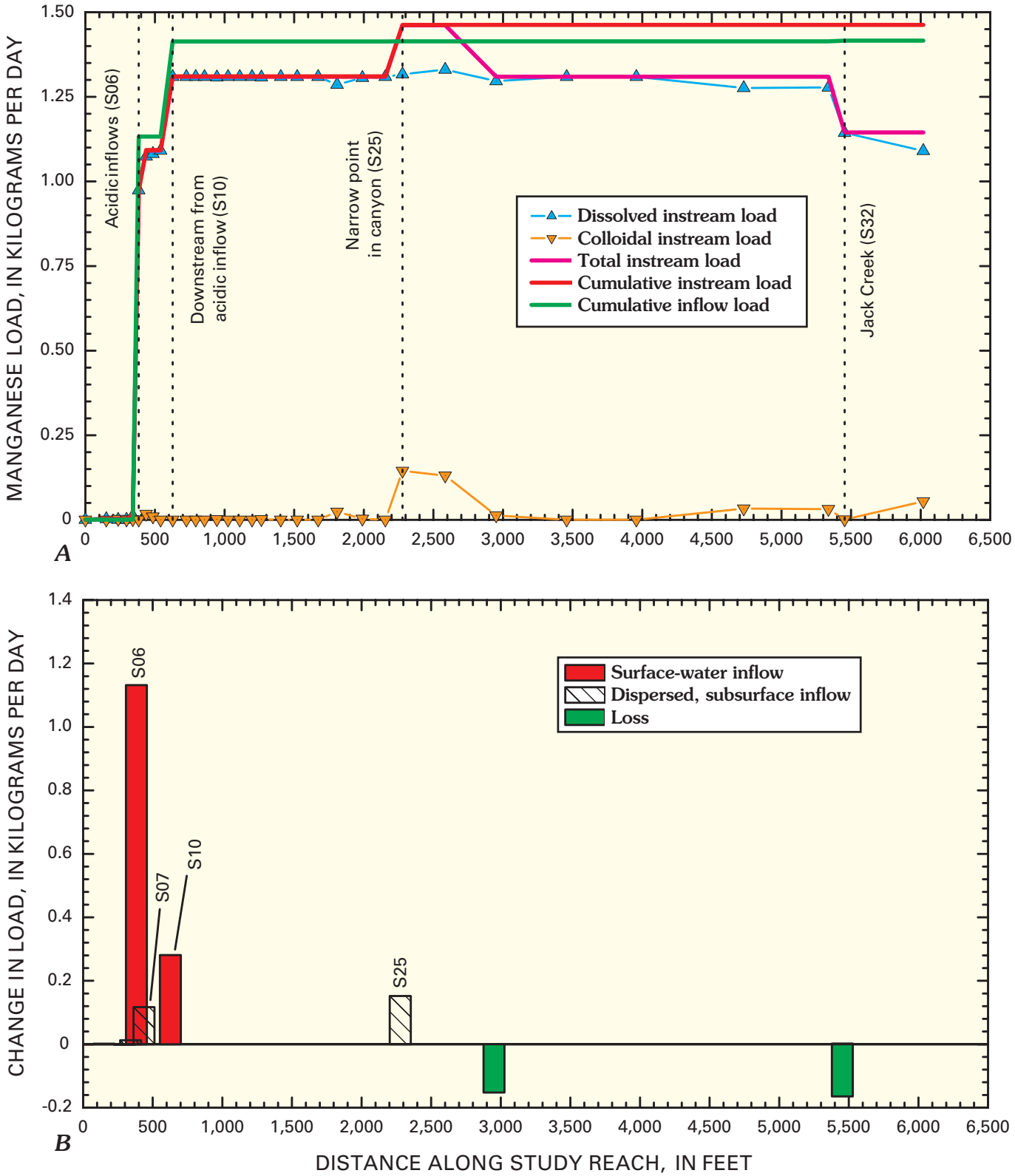

Figure 34. Variation of *A*, manganese load with distance, and *B*, changes in load for individual stream segments, Bullion Mine tributary, September 1998.

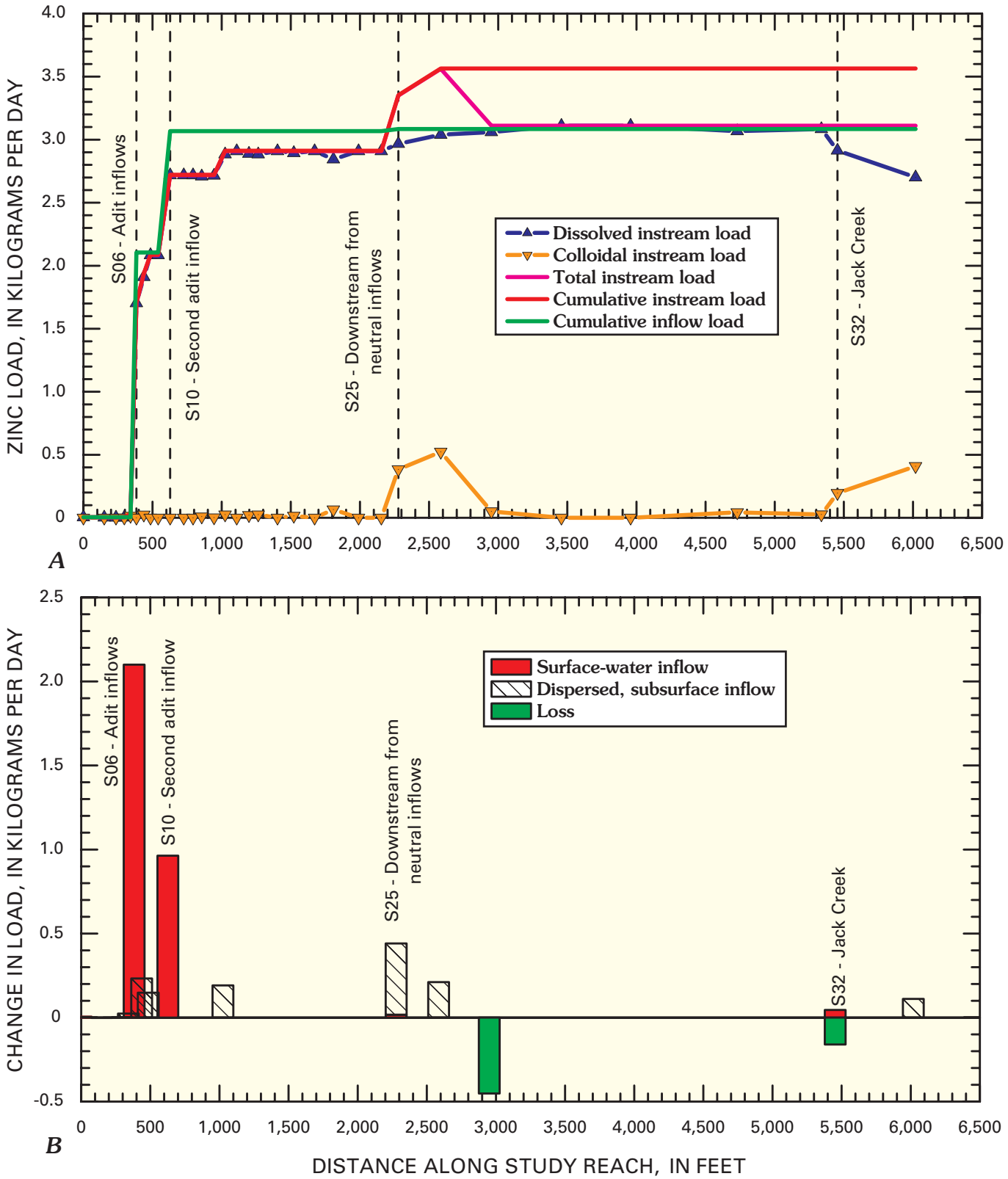

Figure 35. Variation of *A*, zinc load with distance, and *B*, changes in load for individual stream segments, Bullion Mine tributary, September 1998.

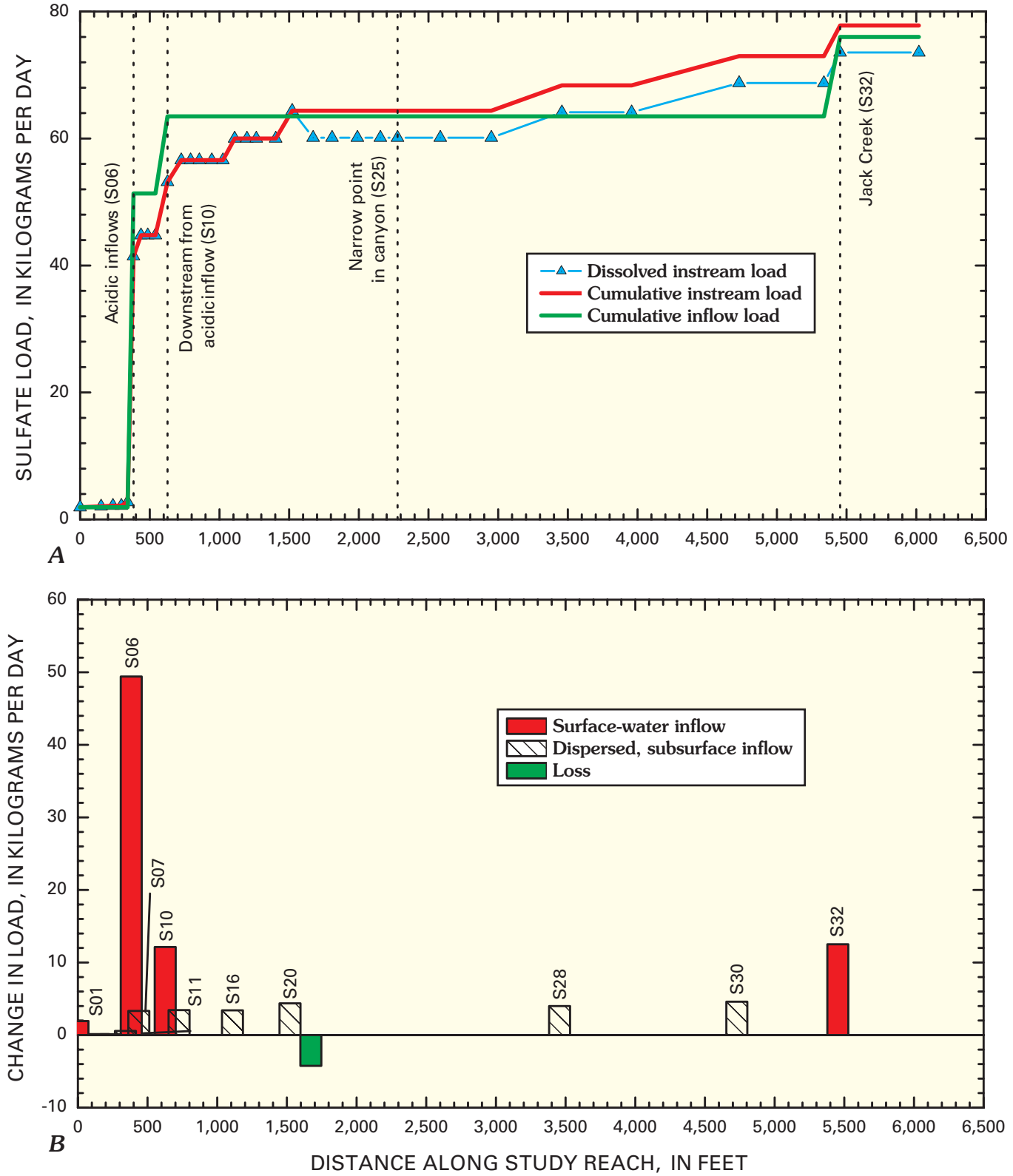

Figure 36. Variation of *A*, sulfate load with distance, and *B*, changes in load for individual stream segments, Bullion Mine tributary, September 1998.

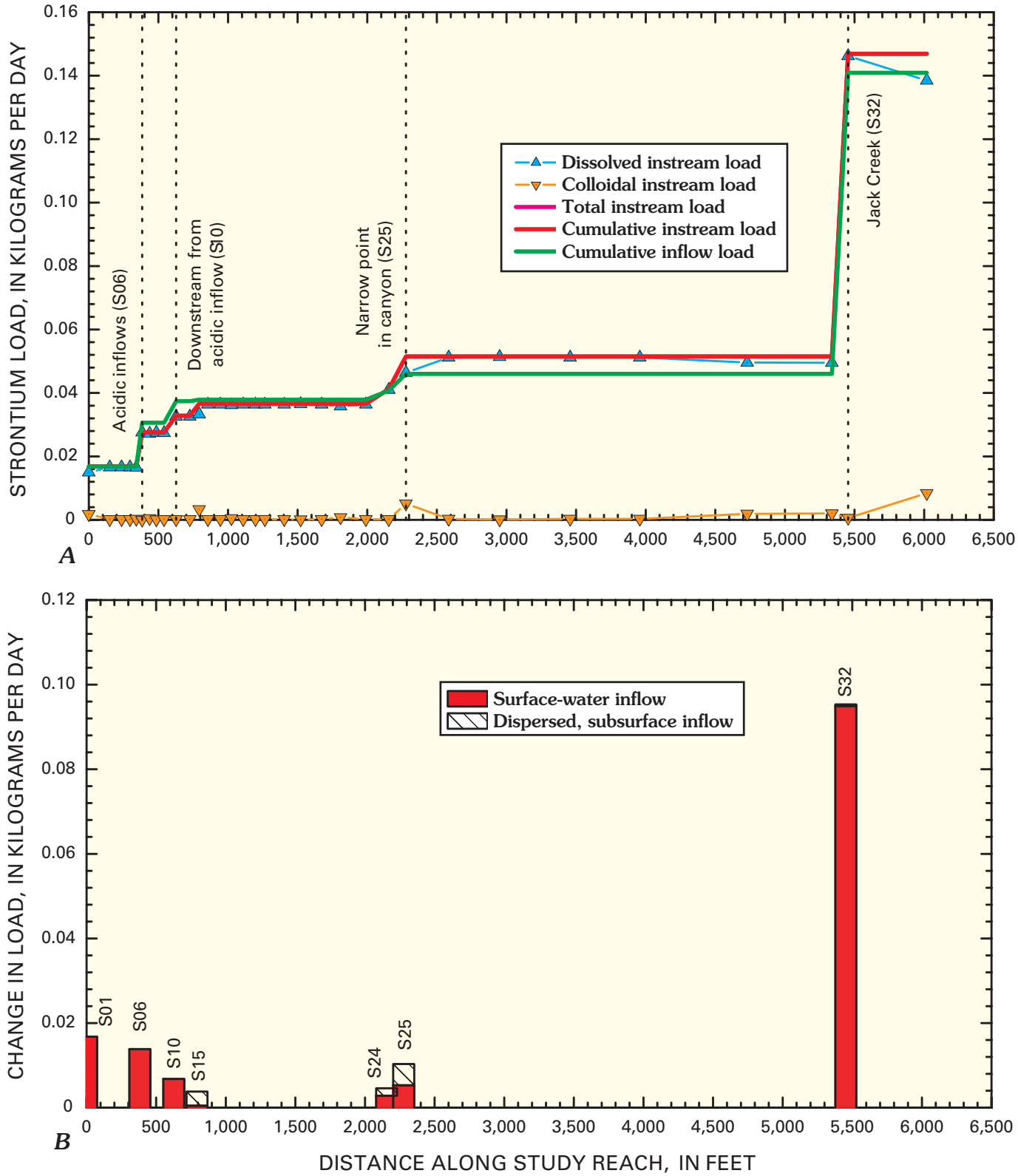

Figure 37. Variation of *A*, strontium load with distance, and *B*, changes in load for individual stream segments, Bullion Mine tributary, September 1998.

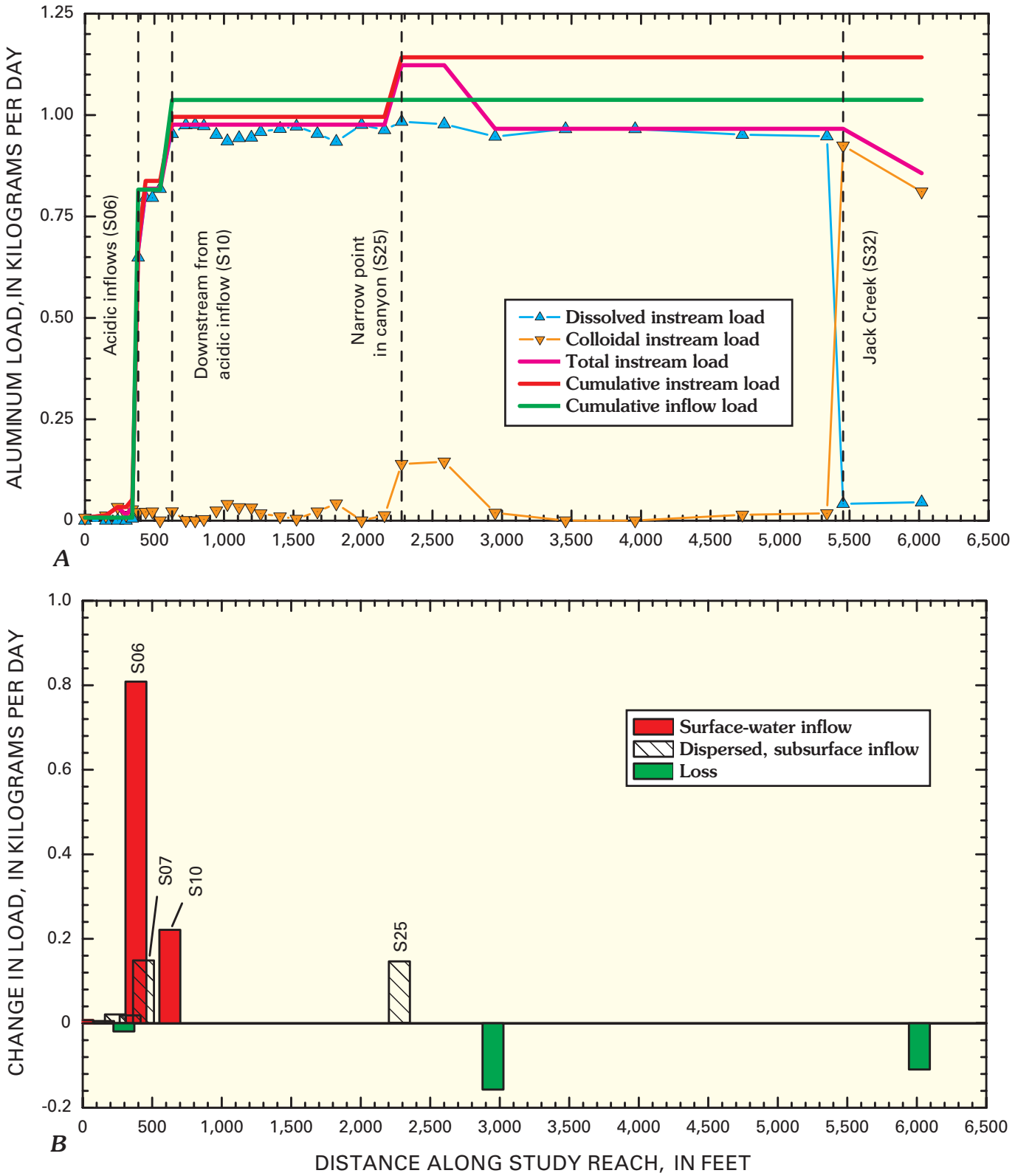

Figure 38. Variation of *A*, aluminum load with distance, and *B*, changes in load for individual stream segments, Bullion Mine tributary, September 1998.

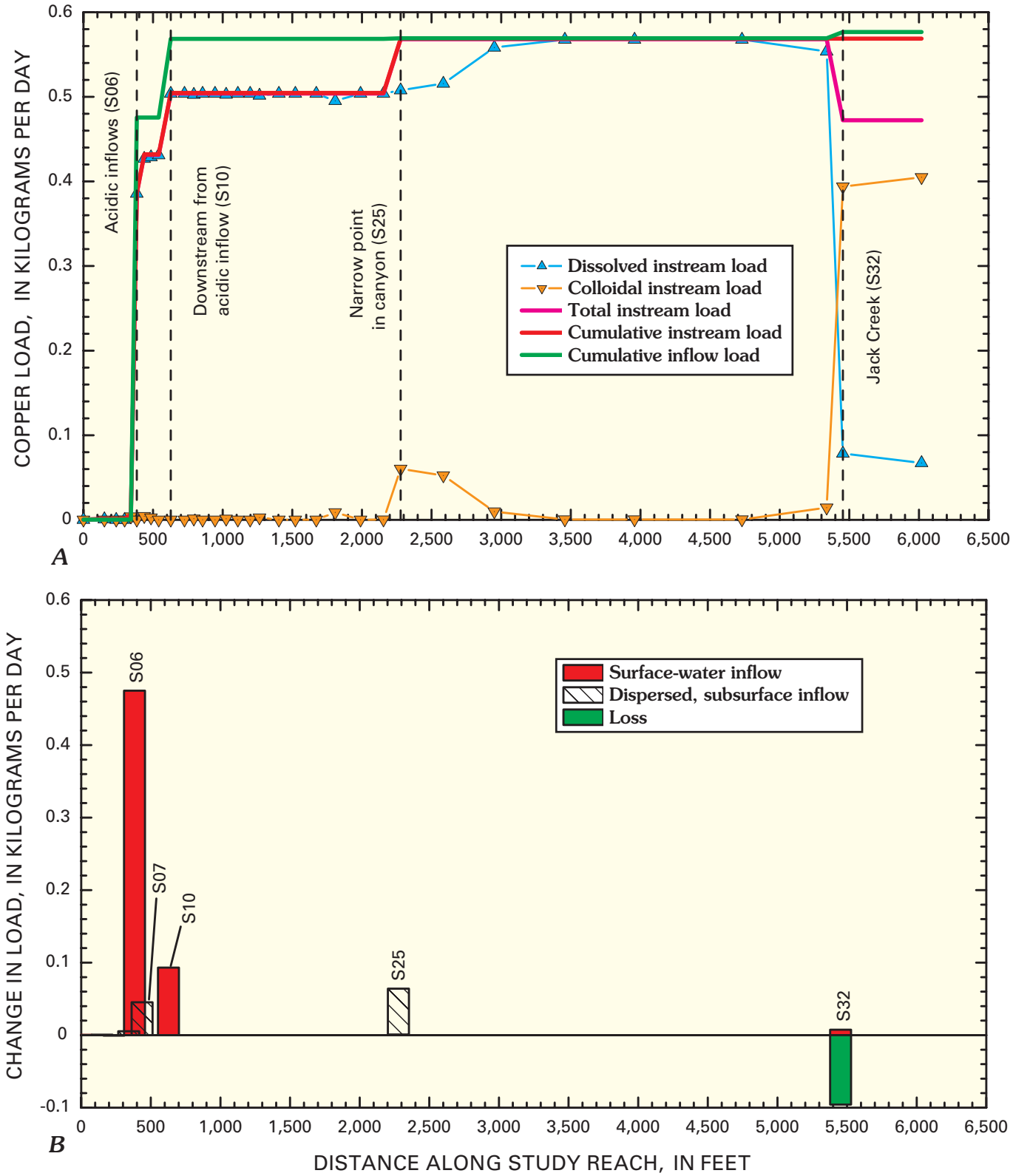

Figure 39. Variation of *A*, copper load with distance, and *B*, changes in load for individual stream segments, Bullion Mine tributary, September 1998.

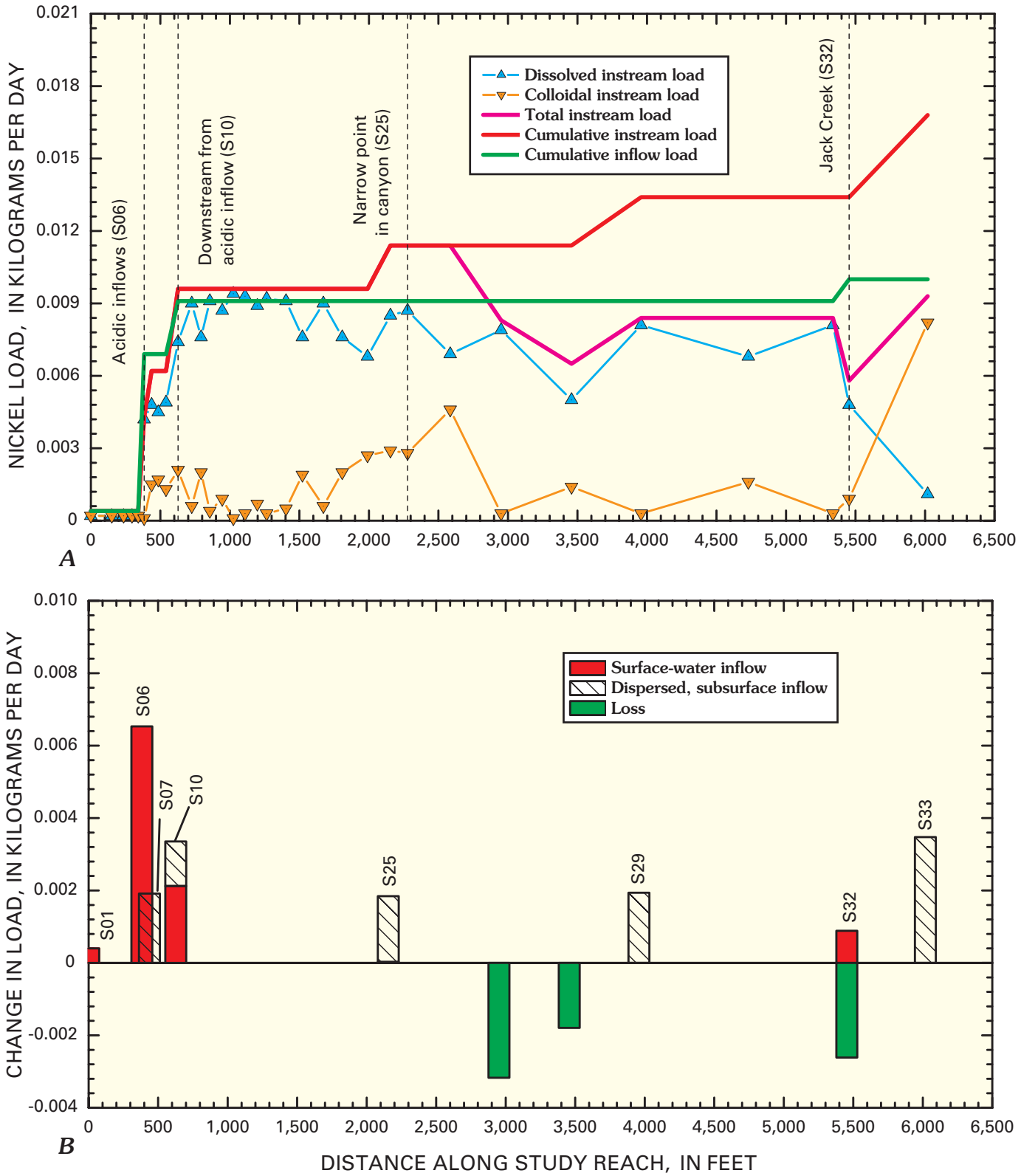

Figure 40. Variation of *A*, nickel load with distance, and *B*, changes in load for individual stream segments, Bullion Mine tributary, September 1998.

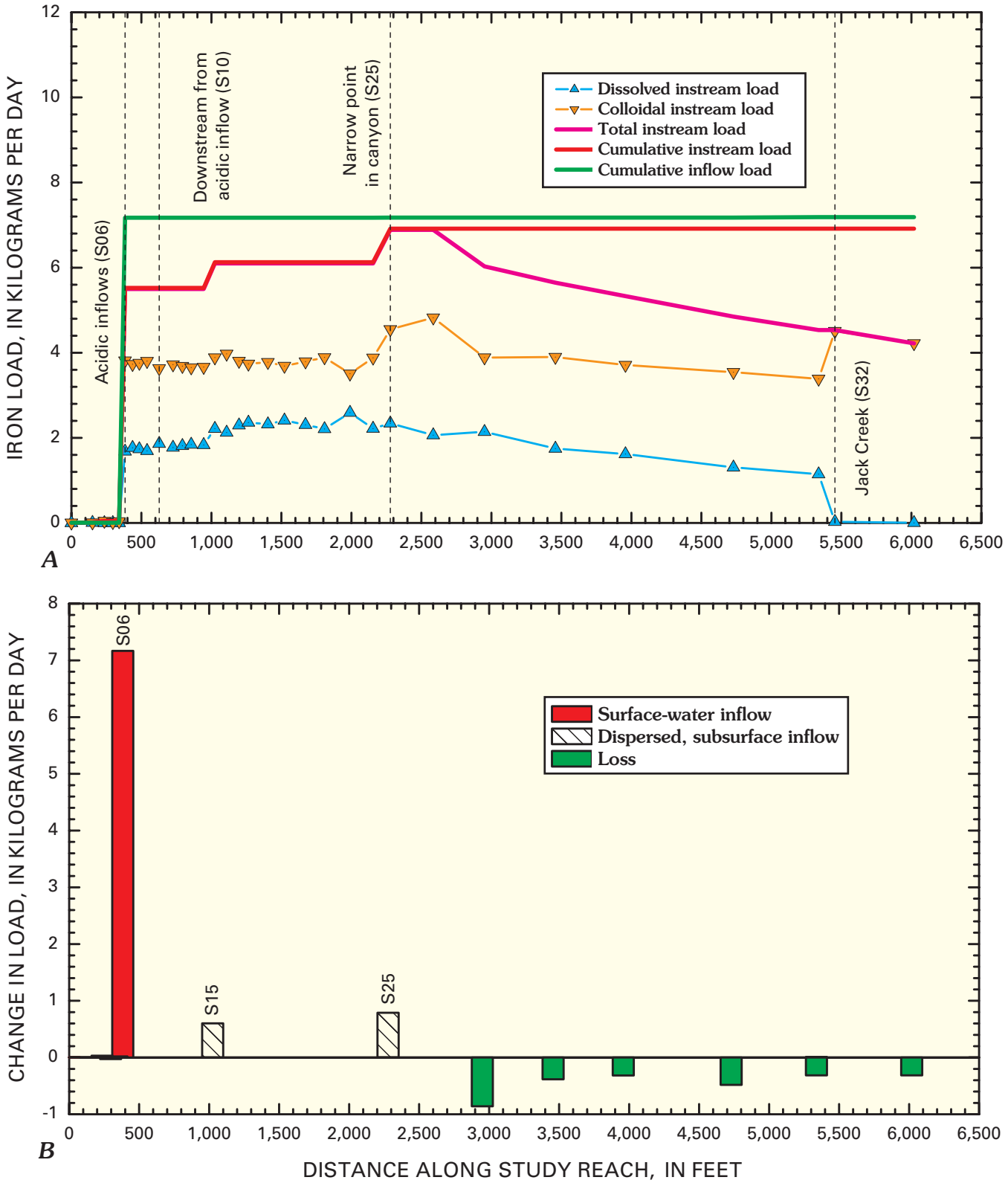

Figure 41. Variation of *A*, iron load with distance, and *B*, changes in load for individual stream segments, Bullion Mine tributary, September 1998.

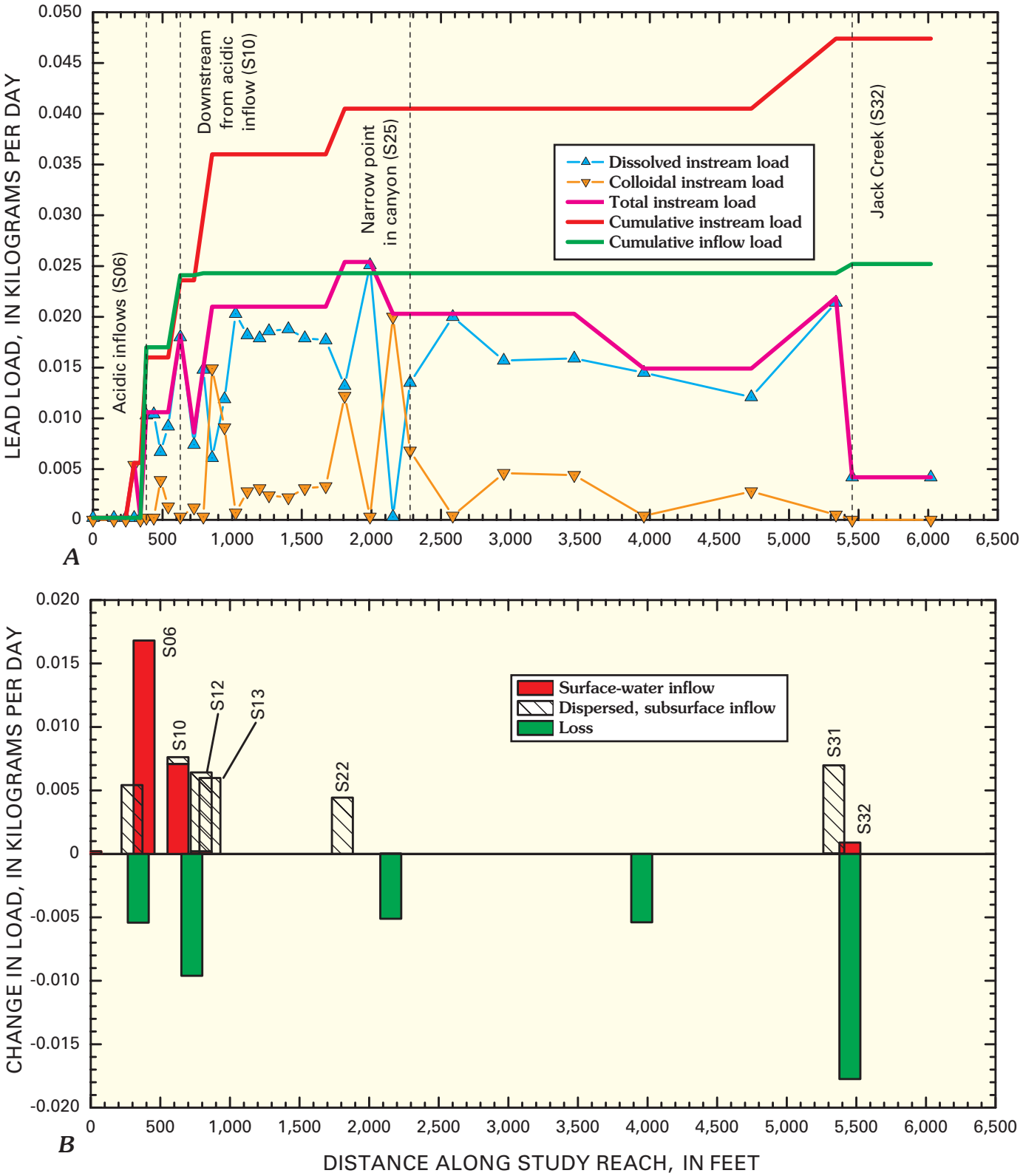

Figure 42. Variation of *A*, lead load with distance, and *B*, changes in load for individual stream segments, Bullion Mine tributary, September 1998.

Table 9. Change in load for individual stream segments and summary of load calculations for selected solutes, Bullion Mine tributary, September 1998.

[Distance, in feet along the study reach; Al, aluminum; Cu, copper; Fe, iron; Mn, manganese; Ni, nickel; Pb, lead; Sr, strontium; Zn, zinc; SO_4, sulfate; cumulative instream load, cumulative inflow load, unsampled load, and attenuation in kilograms per day; numbers in red with parentheses indicate a loss of load; cell color indicates the segments with the greatest load: red, largest load; orange, second largest; yellow, third; green, fourth; blue, fifth]

Segment number	Distance	Al	Cd	Cu	Fe	Mn	Ni	Pb	Sr	Zn	SO_4
S01	0	0.007	0.001	0.000	0.006	0.001	0.000	0.000	0.017	0.005	1.92
S02	150	.005	.000	.001	.006	.002				(.002)	.126
S03	235	.021	(.000)	(.001)	.032					(.000)	.112
S04	296	(.019)			(.026)	(.001)		.005		.001	
S05	341	.019		.005	.020	.013		(.005)		.024	.573
S06	383	.637	.020	.380	5.46	.961	.004	.010	.011	1.68	38.7
S07	437	.149		.045		.117	.002			.233	3.33
S08	485									.148	
S09	540										
S10	627	.158	.006	.073		.218	.003	.008	.005	.634	8.38
S11	726							(.010)			3.44
S12	793							.006	.004		
S13	856							.006			
S14	945										
S15	1,025				.603					.191	
S16	1,109										3.41
S17	1,197										
S18	1,264										
S19	1,404										
S20	1,522										4.37
S21	1,672										(4.24)
S22	1,808							.004			
S23	1,990										
S24	2,155						.002	(.005)	.005		
S25	2,278	.147		.064	.789	.152			.010	.441	
S26	2,585									.211	
S27	2,951	(.157)			(.859)	(.152)	(.003)			(.451)	
S28	3,457				(.383)		(.002)				4.00
S29	3,958				(.316)		.002	(.005)			
S30	4,729				(.482)						4.61
S31	5,338				(.315)			0.007			
S32	5,454			(.096)		(.165)	(.003)	(.018)	.095		4.81
S33	6,019	(.109)			(.313)		.003				
Cumulative instream load		1.14	.027	.569	6.92	1.46	.017	.047	.147	3.56	77.8
Cumulative inflow load		1.04	.035	.577	7.19	1.42	.010	.025	.141	3.08	76.0
Percent inflow load		91	131	101	104	97	59	53	96	87	98
Unsampled inflow		.105	(.008)	(.008)	(.270)	.047	.007	.022	.006	.480	1.80
Percent unsampled load		9.2	(31)	(1.4)	(3.9)	3.2	41	47	4.0	13	2.3
Attenuation		.286	.000	.096	2.69	.318	.008	.043	.000	.454	4.24
Percent attenuation		25	1.4	17	39	22	45	91	.0	13	5

Downstream from the inflow of Jack Creek, substantial attenuation occurred for copper, manganese, nickel, and lead (figs. 39, 34, 40, and 42). These metals most likely sorbed to iron and aluminum colloids. As the colloidal material was removed, the metal loads decreased. Cadmium, zinc, aluminum, and iron (figs. 33, 35, 38, and 41) were transformed from dissolved to colloidal phases but were not substantially removed from the water column; their total-recoverable concentrations remained nearly constant.

Discussion

On the basis of the three tracer-injection studies, we can make some generalizations about sources of metals within the Boulder River watershed and discuss the major processes that affect the metal transport. Because copper and zinc adversely affect the aquatic life, this discussion will focus on those two metals.

Sources of Metals

Surface-water inflows were the principal source of the copper and zinc loads. Unsampled inflow of copper was 23 percent of the total cumulative load in Cataract Creek, but only 8 percent in Uncle Sam Gulch, and less than detection in the Bullion Mine tributary (tables 3, 6, and 9). Unsampled inflow of copper in Cataract Creek occurred only in the last large stream segment between Big Limber Creek and the mouth (fig. 10*B*). Because access for sampling was not given, we do not know if a source in that segment could have been sampled. Unsampled inflow for zinc load ranged from 12 to 26 percent in the three study reaches, indicating that most of the zinc loads also were surface-water inflows.

This surface-water inflow is dominated by drainage from the Crystal and Bullion mine adits in both Basin and Cataract Creeks at low flow (tables 3, 6, and 9). Nimick and Cleasby (this volume) had a similar conclusion, based on more widespread watershed sampling. Other sources of metals in these watersheds are minimal in comparison to these adit drainages. The tracer-injection studies were conducted at different times and under slightly different conditions, but they provide a picture of loading during base-flow conditions that can be compared among the streams. Loading of copper and zinc from the Bullion Mine adit was 0.50 and 2.69 kg/day, respectively. By comparison, loading from the Crystal Mine adit was 3.05 and 13.9 kg/day for copper and zinc; or about five times greater. Loadings of copper and zinc reaching the Boulder River from Cataract Creek are greater than loads from Basin Creek (Nimick and Cleasby, this volume), which is consistent with these differences in loading.

Processes Affecting Metals

Metal attenuation, particularly in Uncle Sam Gulch and the Bullion Mine tributary, resulted from inflows of near-neutral pH water downstream from the principal metal sources. Those elements that are more reactive in the streams, principally aluminum, copper, iron, and lead, were lost to the streambed in Uncle Sam Gulch. Although they were not lost to the same extent in the study reach of the Bullion Mine tributary, they were affected by attenuation downstream from the confluence with Jack Creek. Attenuation may continue in Basin Creek (Nimick and Cleasby, this volume). A substantial amount of the manganese and zinc that entered the streams from both mine adits was transported all the way to the Boulder River and likely affects aquatic health there.

Metals that are lost to the streambed can be flushed downstream during periods of snowmelt runoff or storms (Church and others, 1997). Thus, attenuation of the metals does not mean that the metals are no longer a concern for aquatic health. As part of the streambed material, these metals can enter food pathways to aquatic organisms (Farag and others, this volume, Chapter D10). This has also been documented in other streams affected by mine drainage (Clements, 1994; Besser and others, 2001).

Implications

Loading profiles that have been documented from the tracer-injection studies have important implications for possible remediation. When metal loading in a watershed is dominated by several discrete sources, and those sources contribute a high percentage of the total loads, the most effective approach to remediation would obviously be to focus on those identified sources. Remediation efforts of the many smaller sources of metals would have only limited impact on stream recovery. The lack of regional alteration that can produce widespread metal loading also simplifies remediation options.

Summary

Tracer-injection and synoptic sampling methods were used to quantify the locations and magnitude of loading to selected reaches of three streams in the Boulder River watershed study area in Montana. Tracer studies helped identify the location of major sources of metal loading to the streams, the extent of loading from subsurface sources, and the extent of attenuation downstream from the sources. Along the 40,905-ft study reach of Cataract Creek, 21.2 kg/day of zinc were added to the stream. About 75 percent of this load came from Uncle Sam Gulch, a principal tributary. The major source of metal loading to Uncle Sam Gulch was the Crystal mine adit discharge. The Bullion Mine adit discharge was the principal source to the Bullion Mine tributary of Jack Creek. Other sources were small in comparison to these two. The adit

discharge from the Bullion mine accounted for 2.8 kg/day of zinc, which was only about 20 percent of the zinc load coming from the Crystal mine adit in Uncle Sam Gulch. Both adit discharges drain the same mineral deposit and contribute acidic, metal-rich water to the receiving streams. Most of the loading was from identifiable surface inflows, but part of the total load of each metal was contributed by subsurface inflow. During transport in Uncle Sam Gulch and the Bullion Mine tributary, much of the iron and aluminum was transformed from dissolved to colloidal phases downstream from the inflows of neutral-pH tributaries. This colloidal material affects the transport of other metals that sorb to the colloids. Deposition of this material on the streambeds provides a route for metals to enter the food web and create a condition of chronic toxicity for fish downstream. These two mine-adit sources likely have the most impact on the aquatic health of the Boulder River watershed.

References Cited

Baes, C.F., Jr., and Mesmer, R.E., 1976, The hydrolysis of cations: New York, John Wiley, 489 p.

Bencala, K.E., and McKnight, D.M., 1987, Identifying in-stream variability—Sampling iron in an acidic stream, *in* Averett, R.C., and McKnight, D.M., eds., Chemical quality of water and the hydrologic cycle: Chelsea, Mich., Lewis Publishers, Inc., p. 255–269.

Bencala, K.E., McKnight, D.M., and Zellweger, G.W., 1990, Characterization of transport in an acidic and metal-rich mountain stream based on a lithium tracer injection and simulations of transient storage: Water Resources Research, v. 26, p. 989–1000.

Besser, J.M., Brumbaugh, W.G., May, T.W., Church, S.E., and Kimball, B.A., 2001, Bioavailability of metals in stream food webs and hazards to brook trout (*Salvelinus fontinalis*) in the Upper Animas River watershed, Colorado: Archive of Environmental Contamination and Toxicology, v. 40, p. 48–59.

Besser, J.M., and Leib, K.J., 1999, Modeling frequency of occurrence of toxic concentrations of zinc and copper in the Upper Animas River, *in* Morganwalp, D.W., and Buxton, H.T., eds., U.S. Geological Survey Toxic Substances Hydrology Program—Proceedings of the Technical Meeting, Charleston, S.C., March 8–12, 1999, Volume 1, Contamination from hardrock mining: U.S. Geological Survey Water-Resources Investigations Report 99–4018A, p. 75–81.

Bigham, J.M., and Nordstrom, D.K., 2000, Iron and aluminum hydroxysulfates from acid sulfate waters, *in* Alpers, C.N., Jambor, J.L., and Nordstrom, D.K., eds., Sulfate minerals—Crystallography, geochemistry, and environmental significance: Mineralogical Society of America, Reviews in Mineralogy and Geochemistry, v. 40, p. 351–403.

Broshears, R.E., Bencala, K.E., Kimball, B.A., and McKnight, D.M., 1993, Tracer-dilution experiments and solute-transport simulations for a mountain stream, Saint Kevin Gulch, Colorado: U.S. Geological Survey Water-Resources Investigations Report 92–4081, 18 p.

Church, S.E., Kimball, B.A., Fey, D.L., Ferderer, D.A., Yager, T.J., and Vaughn, R.B., 1997, Source, transport, and partitioning of metals between water, colloids, and bed sediments of the Animas River, Colorado: U.S. Geological Survey Open-File Report 97–151, 135 p.

Cleasby, T.E., Nimick, D.A., and Kimball, B.A., 2000, Quantification of metal loads by tracer-injection and synoptic sampling methods in Cataract Creek, Jefferson County, Montana, August 1997: U.S. Geological Survey Water-Resources Investigations Report 00–4237, 39 p.

Clements, W.H., 1994, Benthic invertebrate community responses to heavy metals in the Upper Arkansas River basin, Colorado: Journal of the North American Benthological Society, v. 13, no. 1, p. 30–44.

Davis, J.C., 1986, Statistics and data analysis in geology, Second Edition: New York, John Wiley, 646 p.

Daultrey, S., 1976, Principal components analysis: Concepts and Techniques in Modern Geography 8, Institute of British Geographers, 50 p.

Desborough, G.A., Leinz, R.W., Sutley, S.J., Briggs, P.H., Swayze, G.A., Smith, K.S., and Breit, George, 2000, Leaching studies of schwertmannite-rich precipitates from the Animas River headwaters, Colorado, and Boulder River headwaters, Montana: U.S. Geological Survey Open-File Report 00–004, 16 p.

Fey, D.L., Church, S.E., and Finney, C.A., 2000, Analytical results for Bullion Mine and Crystal mine waste samples and bed sediments from a small tributary to Jack Creek and from Uncle Sam Gulch, Boulder River watershed, Montana: U.S. Geological Survey Open-File Report 00–031, 63 p.

Fulghum, J.E., Bryan, S.R., Linton, R.W., Bauer, C.F., and Griffis, D.P., 1988, Discrimination between adsorption and coprecipitation in aquatic particle standards by surface analysis techniques—Lead distributions in calcium carbonates: Environmental Science & Technology, v. 22, p. 463–467.

Grundl, T., and Delwiche, J., 1993, Kinetics of ferric oxyhydroxide precipitation: Journal of Contaminant Hydrology, v. 14, p. 71–97.

Grundy, W.D., and Miesch, A.T., 1987, Brief descriptions of STATPAC and related statistical programs for the IBM personal computer—Documentation: U.S. Geological Survey Open-File Report 87–411–A, 34 p.

Jarrett, R.D., 1992, Hydraulics of mountain rivers, *in* Yen, B.C., ed., Channel flow resistance centennial of Manning's formula: International Conference of the Centennial of Manning's and Kuichling's Rational Formula, Littleton, Colo., Water Resources Publications, p. 287–298.

Kilpatrick, F.A., and Cobb, E.D., 1985, Measurement of discharge using tracers: U.S. Geological Survey Techniques of Water-Resources Investigations, book 3, chapter A16.

Kimball, B.A., 1997, Use of tracer injections and synoptic sampling to measure metal loading from acid mine drainage: U.S. Geological Survey Fact Sheet FS–245–96.

Kimball, B.A., Bencala, K.E., and Broshears, R.E., 1994, Geochemical processes in the context of hydrologic transport—Reactions of metals in St. Kevin Gulch, Colorado, *in* Dutton, A., ed., Toxic substances in the hydrologic sciences: Minneapolis, Minn., American Institute of Hydrology, p. 80–94.

Kimball, B.A., Broshears, R.E., Bencala, K.E., and McKnight, D.M., 1994, Coupling of hydrologic transport and chemical reactions in a stream affected by acid mine drainage: Environmental Science & Technology, v. 28, p. 2065–2073.

Kimball, B.A., Callender, Edward, and Axtmann, E.V., 1995, Effects of colloids on metal transport in a river receiving acid mine drainage, Upper Arkansas River, Colorado, U.S.A.: Applied Geochemistry, v. 10, p. 285–306.

Kimball, B.A., McKnight, D.M., Wetherbee, G.A., and Harnish, R.A., 1992, Mechanisms of iron photoreduction in a metal-rich, acidic stream, St. Kevin Gulch, Colorado, U.S.A.: Chemical Geology, v. 96, p. 227–239.

Kimball, B.A., Nimick, D.A., Gerner, L.J., and Runkel, R.L., 1999, Quantification of metal loading in Fisher Creek by tracer injection and synoptic sampling, Park County, Montana, August 1997: U.S. Geological Survey Water-Resources Investigations Report 99–4119, 40 p.

Kimball, B.A., Runkel, R.L., and Gerner, L.J., 2001, Quantification of mine-drainage inflows to Little Cottonwood Creek, Utah, using a tracer-injection and synoptic-sampling study: Environmental Geology, v. 40, p. 1390–1404.

Kimball, B.A., Runkel, R.L., Walton-Day, K., and Bencala, K.E., 2002, Assessment of metal loads in watersheds affected by acid mine drainage by using tracer injection and synoptic sampling—Cement Creek, Colorado, U.S.A.: Applied Geochemistry, v. 17, p. 1183–1207.

Lichte, F.E., Golightly, D.W., and Lamothe, P.J., 1987, Inductively coupled plasma–atomic emission spectrometry, Chapter B *in* Baedecker, P.A., ed., Methods for geochemical analysis: U.S. Geological Survey Bulletin 1770, p. B1–B10.

Metesh, J.J., Lonn, J.D., Duaime, T.E., and Wintergerst, Robert, 1994, Abandoned-inactive mines program, Deerlodge National Forest—Volume I, Basin Creek drainage: Montana Bureau of Mines and Geology Open-File Report 321, 131 p.

Nordstrom, D.K., and Ball, J.W., 1986, The geochemical behavior of aluminum in acidified surface waters: Science, v. 232, p. 54–56.

Packman, A.I., Brooks, N.H., and Morgan, J.J., 2000, A physicochemical model for colloid exchange between a stream and a sand streambed with bed forms: Water Resources Research, v. 36, no. 8, p. 2351–2361.

Rantz, S.E., and others, 1982, Measurement and computation of streamflow—Volume 1, Measurement of stage and discharge: U.S. Geological Survey Water-Supply Paper 2175, 2 vols., 631 p.

Runkel, R.L., Kimball, B.A., McKnight, D.M., and Bencala, K.E., 1999, Reactive solute transport in streams—A surface complexation approach for trace metal sorption: Water Resources Research, v. 35, no. 12, p. 3829–3840.

Smith, K.S., 1999, Metal sorption on mineral surfaces—An overview with examples relating to mineral deposits, *in* Plumlee, G.S., and Logsdon, M.J., eds., The environmental geochemistry of mineral deposits—Part A, Processes, techniques, and health issues: Littleton, Colo., Society of Economic Geologists, Reviews in Economic Geology, v. 6A, p. 161–162.

Ward, J.R., and Harr, C.A., 1990, Methods for collection and processing of surface-water and bed-material samples for physical and chemical analyses: U.S. Geological Survey Open-File Report 90–140, 71 p.

Webster, J.G., Swedlund, P.J., and Webster, K.S., 1998, Trace metal adsorption onto an acid mine drainage iron (III) oxy hydroxy sulfate: Environmental Science & Technology, v. 32, no. 10, p. 1361–1368.

Zellweger, G.W., 1994, Testing and comparison of four ionic tracers to measure stream flow loss by multiple tracer injection: Hydrological Processes, v. 8, p. 155–165.

Zellweger, G.W., Avanzino, R.J., and Bencala, K.E., 1989, Comparison of tracer-dilution and current-meter discharge measurements in a small gravel-bed stream, Little Lost Man Creek, California: U.S. Geological Survey Water-Resources Investigations Report 89-4150, 20 p.